3-D LIQUID CRYSTAL DISPLAY FOR MINE DETECTING RADAR

GENERAL ELECTRIC CO SYRACUSE N Y HEAVY MILITARY ELECTRONIC SYSTEMS

APR 1974

DVI 000203

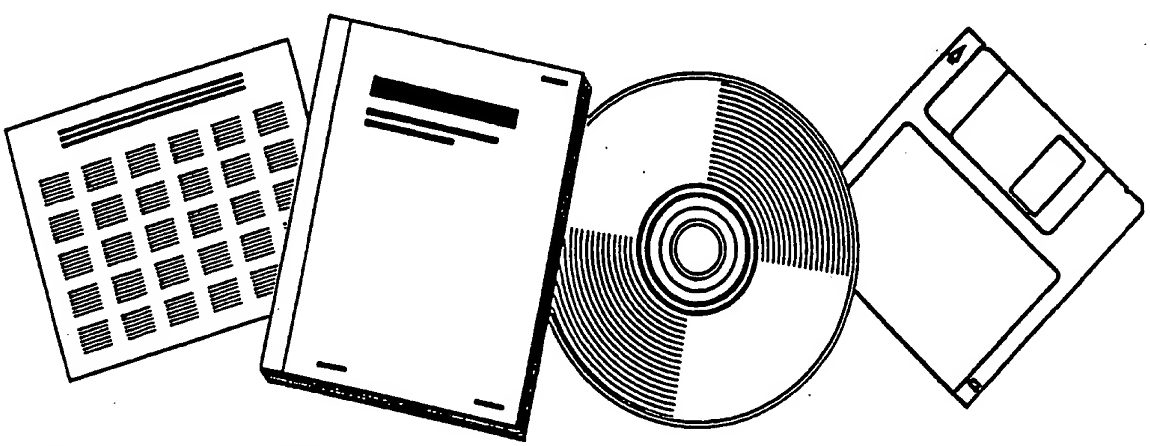

U.S. DEPARTMENT OF COMMERCE
Nati nal Technical Information Service

Tailored to Your Needs!

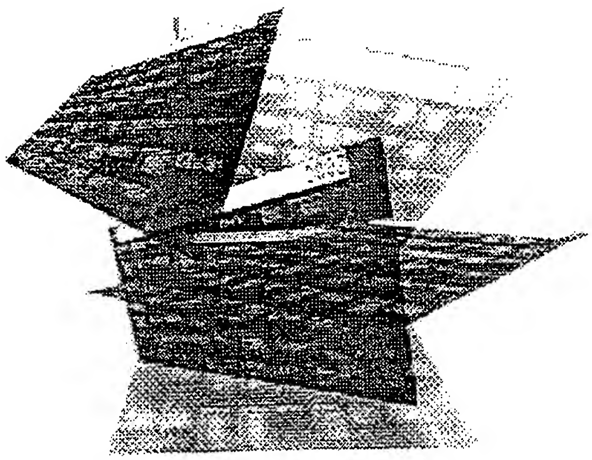

Selected Research In Microfiche

SRIM® is a tailored information service that delivers complete microfiche copies of government publications based on your needs, automatically, within a few weeks of announcement by NTIS.

SRIM® Saves You Time, Money, and Space!

Automatically, every two weeks, your SRIM® profile is run against all *new* publications received by NTIS and the publications microfiched for your order. Instead of paying approximately $15-30 for each publication, you pay only $2.50 for the microfiche version. Corporate and special libraries love the space-saving convenience of microfiche.

NTIS offers two options for SRIM® selection criteria:

Standard SRIM®–Choose from among 350 pre-chosen subject topics.

Custom SRIM®–For a one-time additional fee, an NTIS analyst can help you develop a keyword strategy to design your Custom SRIM® requirements. Custom SRIM® allows your SRIM® selection to be based upon *specific subject keywords*, not just broad subject topics. Call an NTIS subject specialist at (703) 605-6655 to help you create a profile that will retrieve only those technical reports of interest to you.

SRIM® requires an NTIS Deposit Account. The NTIS employee you speak to will help you set up this account if you don't already have one.

For additional information, call the NTIS Subscriptions Department at 1-800-363-2068 or (703) 605-6060. Or visit the NTIS Web site at *http://www.ntis.gov* and select SRIM® from the pull-down menu.

U.S. DEPARTMENT OF COMMERCE
Technology Administration
National Technical Information Service
Springfield, VA 22161 (703) 605-6000
http://www.ntis.gov

3-D LIQUID CRYSTAL DISPLAY

FOR

MINE DETECTION RADAR

FINAL TECHNICAL REPORT

EDITOR JOHN C. REICHE, HMES

APRIL 1974

PREPARED FOR

UNITED STATES ARMY MOBILITY EQUIPMENT RESEARCH

AND DEVELOPMENT CENTER

FORT BELVOIR, VIRGINIA 22060

UNDER CONTRACT DAAK02-72-C-0521

PREPARED BY

GENERAL ELECTRIC

HEAVY MILITARY ELECTRONIC SYSTEMS
SYRACUSE, NEW YORK

DISTRIBUTION UNLIMITED

UNCLASSIFIED

SECURITY CLASSIFICATION OF THIS PAGE (When Data Entered)

AD-783 509

REPORT DOCUMENTATION PAGE		READ INSTRUCTIONS BEFORE COMPLETING FORM
1. REPORT NUMBER	2. GOVT ACCESSION NO.	3. RECIPIENT'S CATALOG NUMBER
4. TITLE (and Subtitle) 3-D Liquid Crystal Display for Mine Detecting Radar		5. TYPE OF REPORT & PERIOD COVERED Final - July 1972-June 1974
		6. PERFORMING ORG. REPORT NUMBER
7. AUTHOR(s) Editor: John C. Reiche Contributors: J. E. Bigelow, R. A. Krashrow, H. S. Cole, Jr., S. Aftergut		8. CONTRACT OR GRANT NUMBER(s) DAAK02-72-C-0521
9. PERFORMING ORGANIZATION NAME AND ADDRESS General Electric Co. Heavy Military Electronic Systems Syracuse, New York		10. PROGRAM ELEMENT, PROJECT, TASK AREA & WORK UNIT NUMBERS
11. CONTROLLING OFFICE NAME AND ADDRESS Technical Research Support Office U.S.A. Mobility Equipment Research & Dev. Center Washington, D.C.		12. REPORT DATE April 1974
		13. NUMBER OF PAGES 134
14. MONITORING AGENCY NAME & ADDRESS(if different from Controlling Office)		15. SECURITY CLASS. (of this report) Unclassified
		15a. DECLASSIFICATION/DOWNGRADING SCHEDULE

16. DISTRIBUTION STATEMENT (of this Report)

Unlimited Distribution

PRICES SUBJECT TO CHANGE

17. DISTRIBUTION STATEMENT (of the abstract entered in Block 20, if different from Report)

18. SUPPLEMENTARY NOTES

A paper based on information contained herein was presented at the Society for Information Display symposium on 21 March 1974, in San Diego, California

19. KEY WORDS (Continue on reverse side if necessary and identify by block number)

3-D Display, Liquid Crystals, Cholesteric Nematic Liquid Crystals, Field Effect, Half Select Matrix Address Scheme, Gray Scale

DVI 000206

20. ABSTRACT (Continue on reverse side if necessary and identify by block number)

This report describes the development of a Liquid Crystal 3-D Display. The display consists of a stack of ten cholesteric-nematic liquid crystal cells. Each cell consists of a matrix of 20 x 40 addressable elements, 0.15 x 0.15 inches per element, with a total active display area of 3 x 6 inches. The modified half select matrix addressing scheme provides for up to four levels of gray scale. Display electronics is designed to accept information formatted by a minicomputer to refresh the display at a 2.5 to 10 hertz rate.

-continued-

20. ABSTRACT (continued)

Physical and chemical characteristics of the cholesteric nematic liquid crystal are described in detail.

DVI 000207

SUMMARY

This report describes the development of a Liquid Crystal 3-D Display. The display consists of a stack of ten cholesteric-nematic liquid crystal cells. Each cell consists of a matrix of 20 x 40 addressable elements, 0.15 x 0.15 inches per element, with a total active display area of 3 x 6 inches. The modified half select matrix addressing scheme provides for up to four levels of gray scale. Display electronics is designed to accept information formatted by a minicomputer to refresh the display at a 2.5 to 10 hertz rate. Physical and chemical characteristics of the cholesteric nematic liquid crystal are described in detail.

Up

DVI 000208

FORWARD

In accordance with the tasks of U. S. Army Mobility Equipment Research and Development Center Contract DAAK02-72-C-0521, the General Electric Company has developed, designed, and fabricated a 3D display module with drive electronics. This display has been demonstrated using simulated data and data supplied under the contract. The development of the liquid crystal material, fabrication of the cells and display module was done under the direction of J. E. Bigelow at Corporate Research and Development, Schenectady, New York. The design and construction of the interface electronics and system engineering was under the direction of J. C. Reiche at Heavy Military Electronics Systems, Syracuse, New York. The contributions of the following individuals must be acknowledged:

PROGRAM MANAGER	P. G. BRAUNSCHWEIGER	HMES
CELL FABRICATION	DR. S. AFTERGUT	CR & D
	DR. D. W. SKELLY	CR & D
	G. T. SEWELL	CR & D
	B. C. WAGNER	CR & D
DISPLAY MODULE DEVELOPMENT	J. E. BIGELOW	CR & D
DRIVE ELECTRONICS	C. R. STEIN	CR & D
INTERFACE ELECTRONICS	J. C. REICHE	HMES
LIQUID CRYSTAL MATERIAL DEVELOPMENT	DR. S. AFTERGUT	CR & D
	H. S. COLE JR.	CR & D
	R. A. KASHNOW	CR & D
SOFTWARE PROGRAMMING	L. W. CONKLIN	HMES

TABLE OF CONTENTS

DVI 000210

TABLE OF CONTENTS (CONTINUED)

DVI 000211

LIST OF FIGURES

DVI 000212

FIGURE		PAGE

LIST OF TABLES

THIS PAGE INTENTIONALLY BLANK

DVI 000215

I. INTRODUCTION

The effort described in this report has been accomplished by two General Electric units; Heavy Military Electronics Systems (HMES), Syracuse, New York and Corporate Research and Development (CRAD) Schenectady, New York. HMES performed the Study of 3-D Display techniques and provided the interface electronics between the display drivers and a digital input. CRAD developed the liquid crystal cells and drive electronics.

The choice of a liquid crystal display technique was based on general considerations of the kind of presentation that should be possible and the probable success in view of the state of development, as will be explained in the section on the study of 3-D techniques. However, there are still many questions left unanswered at that stage for there are many different liquid crystal techniques that might be considered, all of which could give a controlled visual effect of scattering or absorption within a clear region so a larger study effort, which is described, addresses the question of which liquid crystal effect to use. Considerations now are based on the probable quality of the optical effect with a stack of cells, the addressability of a matrix, and the prospects of achieving high speed of response and gray scale.

The next major portion of the effort is of a design nature to define in detail the cell construction, the construction of the cell assembly in the display device and the design of the circuits for formating the data, addressing the cells and driving them.

DVI 000216

II. STUDY OF 3-D DISPLAY TECHNIQUES

Various techniques for achieving a true volumetric 3-D display were investigated. A large number of the 3-D displays in the literature are stereoscopic which cause viewer eye fatigue and they lack the dimension cues reguired for true depth determination. Further since a real time display was required, the Holographic approach was not pursued.

Initially the following approaches were considered as good contenders: Liquid crystals, Gas Discharge display panels, a Gas Volume excited by two crossed laser beams, Moving Vanes with supports mounted perpendicular to the viewing surface, Electrostactic particles suspended in a liquid, and Ferroelectric Ceramic display. The salient qualities of each display mechanism are summarized in Appendix A.

III. SELECTION OF LIQUID CRYSTAL EFFECT

Three liquid crystal effects were considered theoretically for possible applications to this display. These were the dynamic scattering mode (DSM), the twisted nematic type of display (TN) , and the cholesteric to nematic transition (CN). DSM is the most commonly encountered liquid crystal display effect at the present time, owing largely to the simplicity of making a working cell. The optical effect lends itself to this application, for in the absence of excitation the cell is clear and with excitation it becomes highly scattering. The visual effect of excited regions in a stack of cells would be that of a cloud floating in a clear region with good prospects for high transmission through the clear regions. There are many limitations to this scheme; however, the most serious of which is the difficulty of addressing a matrix as large as 20 by 40 elements. The only successful matrix addressing technique for DSM

DVI 000217

known to date is the two frequency technique[1] which has been applied to developmental terminal devices by General Electric[2]. By this technique, as many as 16 elements have been scanned, but better selectivity and lower voltages make 8 a preferable number. One could have scanned through the 20 element axis in this application with two sets of 10 elements simultaneously scanned, such that data could come in on intersecting leads from the two sides of the cell, but it would be undesirable to have that many leads. When pushing a scanning technique towards the maximum number of addressable elements for a given flicker rate, there is no prospect for gray scale control, since the limiting address condition exists for on off control.

The twisted nematic technique makes use of an orientation pattern in the unexcited regions of a cell which causes 90° rotation of the plane of polarization of light. With a field applied the molecules re-orient so that there is no change of polarization of light transmitted through the cell. Thus, such a cell between crossed polarizers would go from transmissive to opaque when a field is applied, and with parallel polarizers would go from opaque to transmissive. The addressing capability has been reported to be good enough for a 5 x 7 dot matrix character representation and may be good enough for the present application, but this has not been established. In any event, it would be necessary to stack cells between a single pair of polarizers to avoid cumulative losses of many polarizers. Thus, rotational effects would add up to give a very confusing result so that even on to off control without cross talk from layer to layer

DVI 000218

would be impossible to achieve. Finally, prospects for gray scale seem very poor and the likelihood of discerning 3-dimensional shape with opaque layers stacked one above the other would be very difficult unless one could see the opaque region from practically every vantage point.

The cholesteric to nematic transition makes use of an electrically controlled orientation pattern change from a twisted up helical structure, which scatters light strongly in the field-free condition, to an aligned state with molecules perpendicualr to the cell walls when a field is applied. The applied field produces a very clear cell. The physical nature of liquid crystals and particularly, those liquid crystals formulated to enable the CN transition is discussed in Appendix B. In that Appendix there is also a theoretical discussion of the basic limitations to optical behavior and speed of response of this display effect, which served as a guide to the experimental program aimed at optimizing the effect for this application. One may summarize that lengthy technical discussion by saying that this effect seems to be the best choice for this application because it has prospects for achieving a desirable optical effect and a capability for addressability of the required matrix size, even with gray scale. The optical effect would be similar to that of DSM, namely, a scattering cloud but of controlled scattering power within a very clear volume. The large matrix address capability for the CN material derives from the much greater speed of decay to the scattering state (as during a brief address period) than the time to return to clear state. This is

further augmented by the sharpness of the static characteristics curve of scattering versus voltage.

IV. DISPLAY SYSTEM CONFIGURATION

The final design configuration of cells, supports, illumination, and various circuit sections was governed to a large degree by the give and take interaction of basic display requirements and estimation of human factors and the state of the art of cell component fabrication. The basic display requirements are summarized in Figure 1 in the form of a 3-dimensional matrix. There are 20 display elements in the x direction representing position horizontally across the direction of travel of the sensing antenna array. With interpolation 10 antennas will give 20 elements of data in this dimension. The y axis represents position along the direction of travel, such that, with a moving antenna array a set of data on the x axis will be generated successively for new values of y. Thus, any structure detected will appear to move through the display along the y direction. To give adequate time to perceive a shape moving through the display, 40 display elements were selected for this axis such that the proportions of each display element will be square with an element of x representing the same true ground dimension as an element of y. The z direction represents depth into the ground and is presented in the display by 10 intervals along the z axis at which are located 10 separate display cells. Electronic changes could permit a change in the scale factor in the z dimention, so the primary consideration in the display was given to the relative magnitude of the span of z with respect to the span of x in order that depth could most easily be perceived. If z were too small with respect to x, the observer could not easily distinguish one depth from another, yet if it were too great the effect

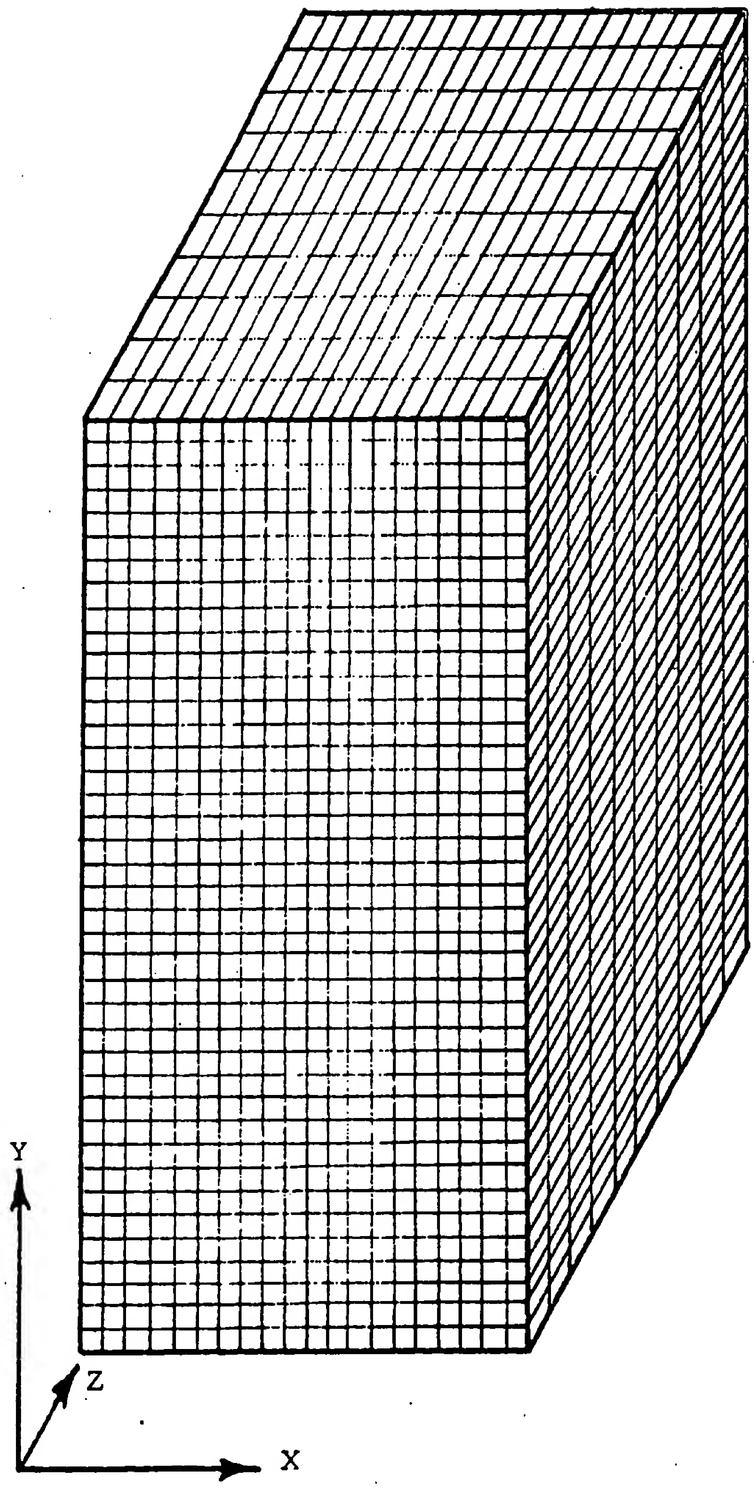

FIGURE 1 DISPLAY MATRIX

would be like looking into a mailing tube. This becomes a human factors consideration which was not settled in a scientific way, but by common sense opinion that the span of x should be approximately the same as the span of z. Another human factors consideration relates to the overall size of the display and the consequences of perceiving the individual resolution elements. Obviously, with the number of elements present, if one were unable to see individual resolution elements by virtue of their small spacing, the total display would subtend about 1° of arc to the observer. Since there is no resolution to spare, it is therefore necessary that resolution elements be perceived. Another consideration, which may be more practical to apply, is that the total subtended angle of the display approximate that of other displays which the observer is used to using, such as a CRT. For radar type information, this might dictate that a diagonal of the display for viewing at a comfortable distance be about 5 to 12 inches.

Finally, we look at the influence of the state of the art of making the cell components. The cholesteric to nematic transition is a field effect with a sharp threshold, so uniform operation at a given voltage, as needed for gray scale presentation, demands that the thickness of the liquid crystal film be uniform within about 5%. To achieve such uniformity in a gap of only about 1/2 mil (12 microns) requires a flatness of the individual pieces of glass to the order of a micron. The difficulty of achieving this goes up at an extremely high rate as the size of the plates is made larger. Not only does the quality of a polishing operation tend to approach a certain error per unit of size, but errors due to flexibility of the glass and the holder during the polishing operation increase as a steep function of size. Plates approximately 10 inches on the

diagonal seem to be at about the upper limit practical for the precision needed. For such a size a minimum thickness giving adequate rigidity would be about 3/8 inch. The final size chosen was 7 x 7 1/2 inches so that they could be assembled to provide access to etched conductors by alternate, over-hanging of one plate past the other. Allowing for the width of gaskets and space needed for filling the holes, the display area could be a 6 inch square, but for the proportions needed as shown in Figure 1 the display area for each plate would be 3 x 6 inches. A stack of 10 cells with two pieces of glass each would have a thickness of 7.5 inches, but with a refractive index of 1.5 would appear to be 5.0 inches. This seemed close enough to the range of x so that the human factors criterion discussed earlier would be satisfied. The size of an individual resolution element would be 6/40 or 0.15 inches. This was adjusted slightly to 0.156 inches to enable a commercial connector to be used without fanning out the etched connectors on the cells.

To mount such as assembly of cells, properly illuminated, so that it can be seen easily by an observer it was considered desirable that the actual display assembly be made separate from the electronics to keep the size and weight of the package to a minimum. Even with the electronics separate, this display subsystem is a substantial package as indicated by the sketch of Figure 2. The weight of glass is approximately 32 pounds; the weight of the housing and support, approximately 15 pounds, and the weight of an index matching oil to fill the space between and around the cells to eliminate air to

DVI 000223

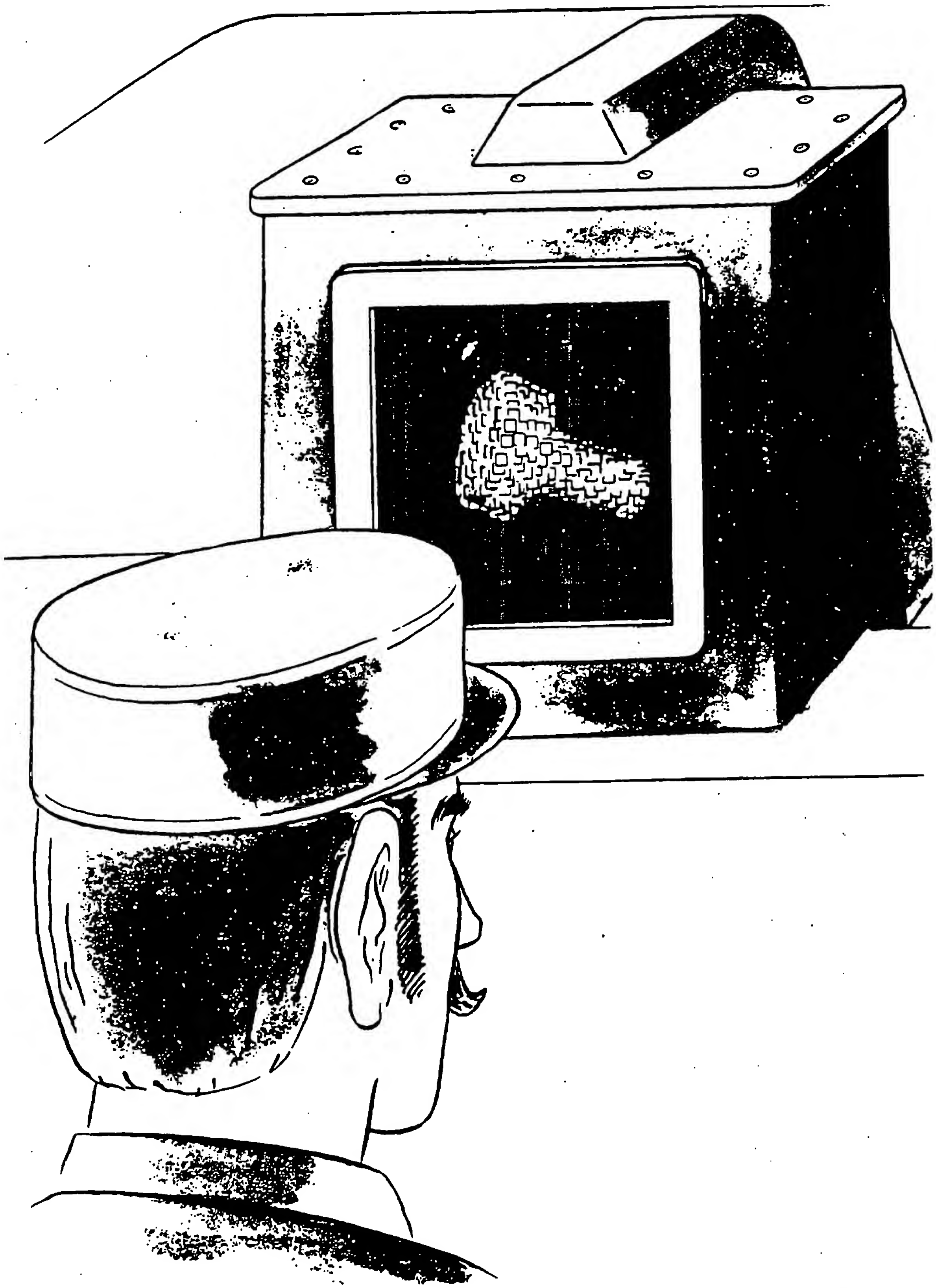

DVI 000224

FIGURE 2 ARTISTS SKETCH OF DISPLAY MODULE

glass surface reflections is about 13 pounds, giving a total weight of about 60 pounds. Dimensionally it is approximately a 10 inch cube. Appendix I contains layouts for the display assembly.

As will be described more in the section on cell construction, the overall transmission of the stack of cells will be about 14%, so some means of artificial illumination must be provided to supplement natural light that could be available to illuminate the back side of the stack. The assembly in its tank-like enclosure would thus have the fluid-tight windows in front and back with lamps extending beyond the 10 inch dimension behind to direct light into the back. The light from the lamps will be at an angle such that rays would not come directly out the front window to the observer when all cells are clear.

V. CIRCUIT DESIGN AND CONSTRUCTION

A. Addressing Scheme Chosen

The addressing scheme chosen for this application is a variation of the "conventional" half select system in that time constant differences in the display medium play a more important part in the success of the system than in the more conventional half select system. It is a half select system in the sense that numerically equal quantities of excitation are applied to intersecting elements of the display. The temporal coincidence of these waveforms determines the state of the display. The details of this addressing system should be made clear by the following discussion.

Figure 3 shows the transfer characteristic of the liquid crystal material chosen. At low voltages, the material is in a scattering state. At high voltages the material is in a perfectly transparent state. Between these two states is a

DVI 000225

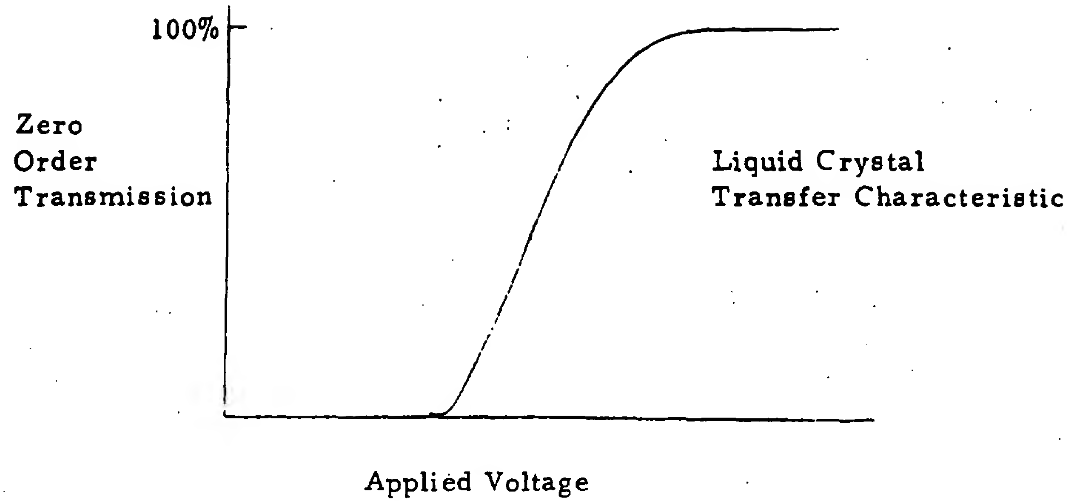

FIGURE 3 TRANSFER CHARACTERISTIC OF LIQUID CRYSTAL MATERIAL

critical voltage which divides the two regions. The speed with which the material assumes a new state is determined by the difference of the squares of the applied voltage and this critical voltage. It is this wide variation in time constant that makes a "holding" voltage scheme work. The addressed site is put in the decided state quickly during address time by a voltage far from the critical voltage. It is held in that state for the rest of the scan cycle by a holding voltage near the critical voltage. In the implementation chosen, this holding voltage is provided by the "data" waveform which carries data to all cells on that row.

Figure 4 shows some of these waveforms and the resulting composite waveforms at a few sample intersections. All signals applied to the display have a net zero DC value to minimize any degradation of the liquid crystal material which may be related to electrolysis.

DVI 000226

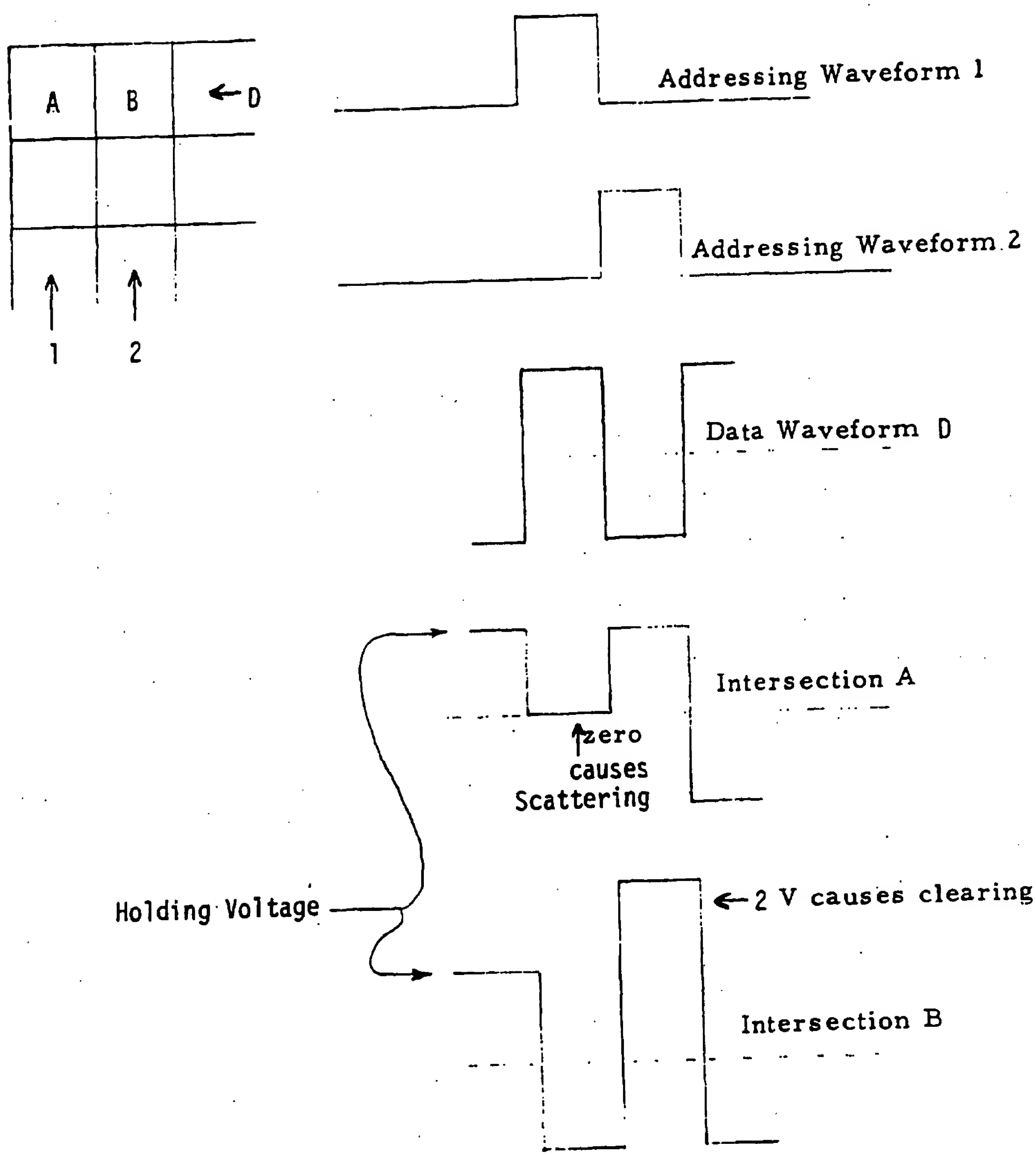

Figure 4. WAVEFORM DIAGRAM MATRIX ADDRESSING

One set of these intersecting waveforms contain only timing information and is called the addressing waveform. The second set contains the data to be displayed in appropriate time synchronization with the addressing waveforms. Data are presented in the form of phase modulation of this data waveform. This arrangement results in a system which exhibits zero cross talk.

Waveforms actually applied to clear a cell element are shown in Figure 5 (a). The upper waveform is the address or column waveform that is applied in a two-to-one interlace scheme. Column one in each of the ten cells is addressed in parallel, then column three in each of the ten cells, five, seven, ..., nineteen, two, four, six, ..., and twenty; thus completing one display frame, and then process starts all over again. The address or column waveform consists of three square wave pulses. The total period of these three pulses is the time one cell element is addressed. The center trace is the data waveform that is always present but the data waveform is 180^0 out of phase with the column waveform to place about 200VPP on the addressed cell element producing the clear state. The bottom waveform is the voltage seen by the addressed cell element. After a cell element is addressed the data waveform and the cell waveform may change phase as other cell elements are addressed.

Figure 5 (b) shows the data waveform shifted 180^0 from figure 5 (a); thus producing zero volts across the cell element during address time producing a cloudy cell element state. Figure 6 shows the phase of the data waveform shifted during address time to be in phase with one or two column pulses placing the cell element in a partially cloudy state.

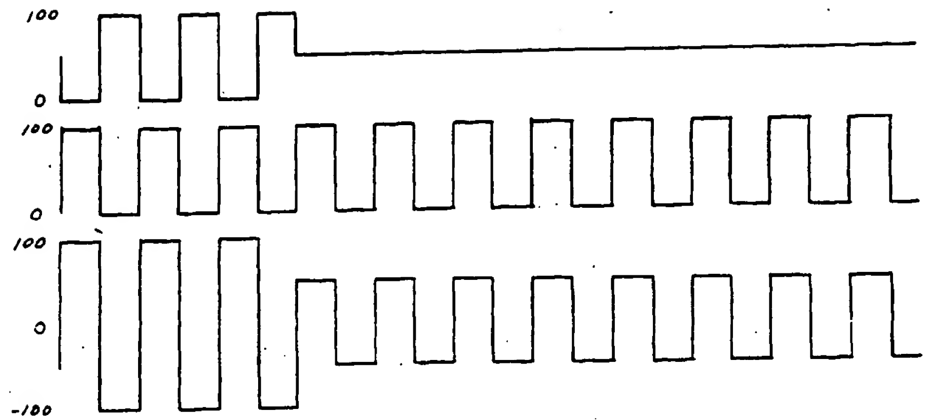

a) Column, data, and cell waveforms for clear cell state.

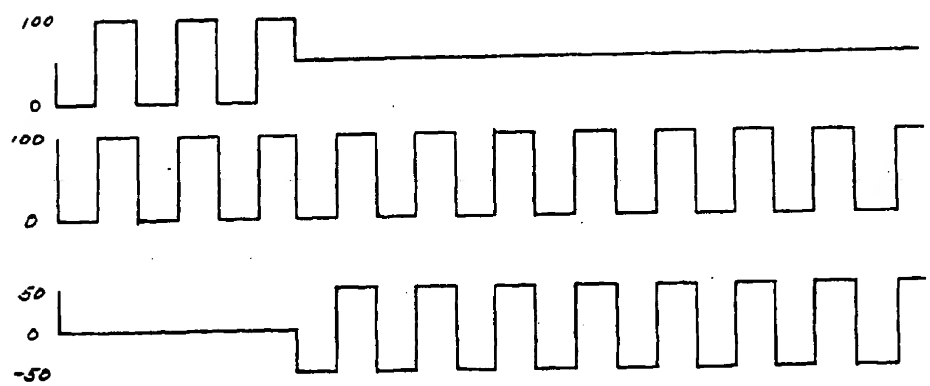

b) Column, data, and cell waveforms for cloudy cell state.

FIGURE 5

MATRIX ADDRESS WAVEFORMS
FOR CLEAR AND CLOUDY CELL STATES

DVI 000229

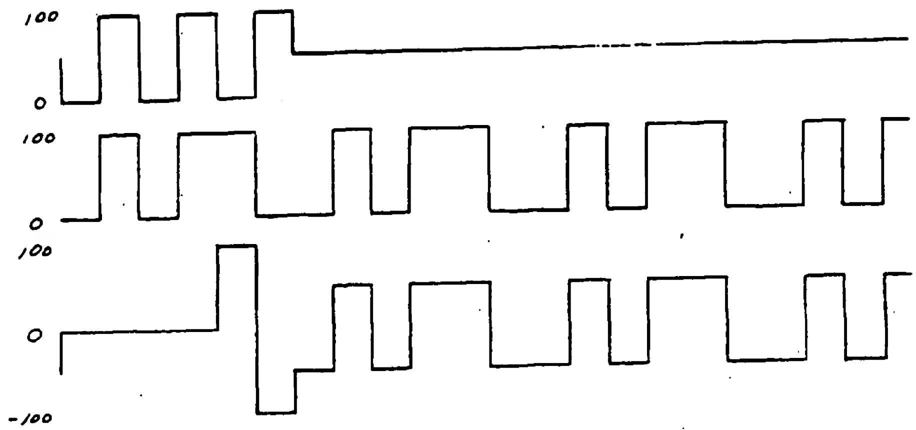

a) Column, data, and cell waveforms for 1/3 cloudy cell state.

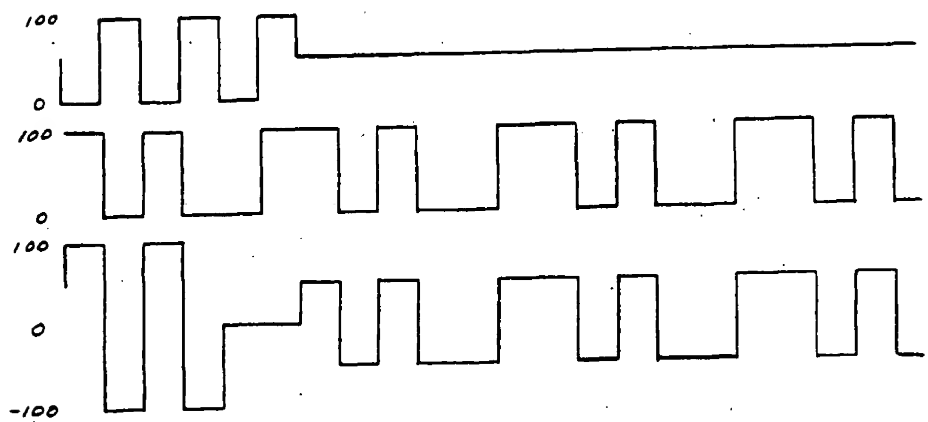

b) Column, data, and cell waveforms for 2/3 cloudy cell state.

FIGURE 6

MATRIX ADDRESS WAVEFORMS

FOR TWO PARTIALLY CLOUDY STATES

DVI 000230

As a result of current flowing in the indium oxide leads on the glass, there will be a voltage drop along the conductor with the result that the inner elements of the cell will experience less excitation than the outer elements. The following analysis of the situation pertains.

The cell may be characterized by the following parameters. Values are given for a single square element along the conductor with a linear dimension of 0.156". (This is the basis cell size of the display).

Conductance of the LC Material	2.7×10^{-7} MHOS
Susceptance of the LC Cell (at 1 KHz)	2.7×10^{-7} MHOS
Resistance of the indium oxide lead	200 Ω/□.

Inasmuch as the current entering on one plate will be brought out through orthogonal leads on the other plate, an exact analysis which pertains uniformly over the cell is more calculation than the situation requires. The assumptions for which this calculation is made are:

1. Plate will be driven from both edges (thus the maximum path length is 20 squares), and
2. All the cell's capacitance and conductance is located half way along the servicing lead.

Thus there are 20 squares of series resistance and 20 squares of capacitance and conductance.

RS, the series resistance, = 20 R = 4K ohms

Gt, the total conductance, = 20 G = 5.4×10^{-6} MHOS

BT, the total susceptance, = 20 B = 5.4×10^{-6} MHOS and

Y, the admittance, = Gt + j Bt = 7.6×10^{-6} 45^{o}

The Z, the series equivalent of this admittance,

$$= \frac{1}{Y} = 131.5K < -45^0 = 93K - j\,93K \text{ ohms.}$$

Now the attenuation can be calculated from the series circuit

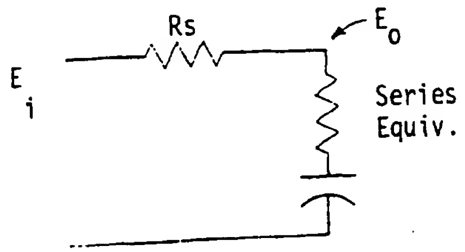

$$\frac{E_o}{E_i} = \frac{93K - j\,93K}{97K - j\,93K} = 0.979.$$

For these conditions the voltage loss is 2.1% and should not present a problem.

B. Circuit Design

Specifications on the cells indicate that RMS value of the required waveforms will be less than 100 volts. The circuit boards have been designed to meet cell voltage requirements. Detailed construction of the boards is covered in Section D. Changes in voltage can be accomplished simply by turning the power supply voltage up or down.

The display matrix, consisting of 10 cells each 20 x 40 elements in extent, sets the quantity of electronic drivers which must be provided. In order to maximize cell element address time the cells are scanned through the 20 element side, and thus 20 line drivers are required. Then 10 cells x 40 elements per cell sets the requirement for four hundred data line drivers.

(It would have been more economic of electronics to try to scan through the 40 element side, but this would mandate a slower frame rate with more flicker.)

1. General Timing Generator

The display timing generator is a single card unit which controls timing of the display. An external master oscillator is used as the frequency source (an AC "carrier" to provide the DC-free waveforms spoken of above). Counting down the master oscillator frequency, then, provides appropriate signal outputs at the element and frame rates, and when decoded, signals indicating the current address. Synchronization with the data inputs via the computer is accomplished by monitoring these decoded address signals. Specific scan rates are adjustable from 2.5 Hz to 12 Hz by varying the master oscillator from 2.4KHz to 11.5KHz.

The schematic and timing diagram in Figure 7 show how the timing of the display system is generated. Integrated circuit A contains an RC oscillator which can be thought of as a phase shift device. Three sections of the IC are used as the oscillator and two follow as signal amplifiers and shapers. Integrated circuit A may be used as the master oscillator by adding appropriate capacitors shown in the dotted lines and connecting output of the last inverter to the input of the 16 state counter.

Circuit 1B is a 16 state counter which has outputs at 1/2, 1/4, 1/8, and 1/16 the input frequency. These are subsequently referred to as P, R, S, and T, respectively, and are used in the following ways.

DVI 000233

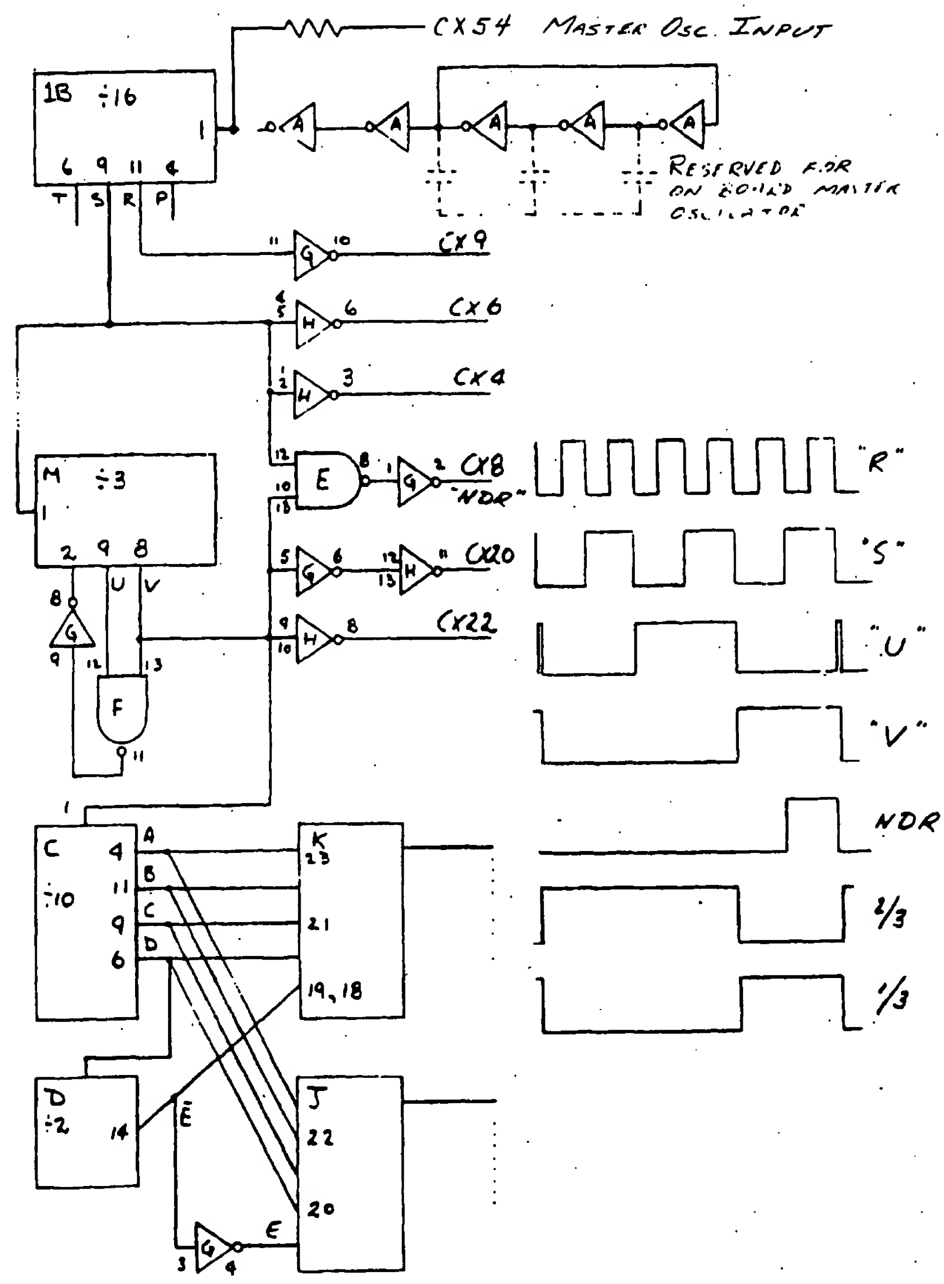

FIGURE 7 LOGIC & TIMING DIAGRAM

DVI 000234

The "S" waveform is used as the basic carrier frequency of the data and addressing waveforms to the cell. Circuit M, with the aid of a gate from F, counts cycles of the carrier and advances the address counter, C, one count for every three cycles of "S". This column time (3 cycles of "S") is divided into 1/3 and 2/3 segments for gray scale modulation. Circuits C and D count 20 sets of these intervals to scan through the 20 columns.

The unit has been assembled in such a way as to cause an interlaced scan through the display. That is, the odd numbered columns are addressed in sequence (1, 3, 5, etc.) and then the even numbered ones are addressed sequentially to complete the scan. Should it become desireable to try other scanning sequences, there are a number of ways in which alternate scan cycles could be made. One way would be to rewire some of the backplane.

2. Data Line Driver

A typical data line driver is shown in diagram of Figure 8. It is a "totem pole" arrangement, implemented with suitable high voltage transistors as mentioned, and driven by a logic level input from an exclusive-or gate. The exclusive-or gate provides the phase modulation of the carrier according to data provided to it by the computer. In the construction of circuit boards, there are provided 20 of these data amplifiers on each board.

3. Address Line Driver

A typical address line driver is shown in Figure 9. It, too, is a totem pole araangement, but with a third stable output state. The totem, of course, connects the output line either to ground or to power supply - - states 1 and 2. The third state disconnects both ends of the totem (as in popular tri-state logic) and connects the output lead to a voltage half that of the main power supply in such a way that current can flow either way in the connection. This

DVI 000235

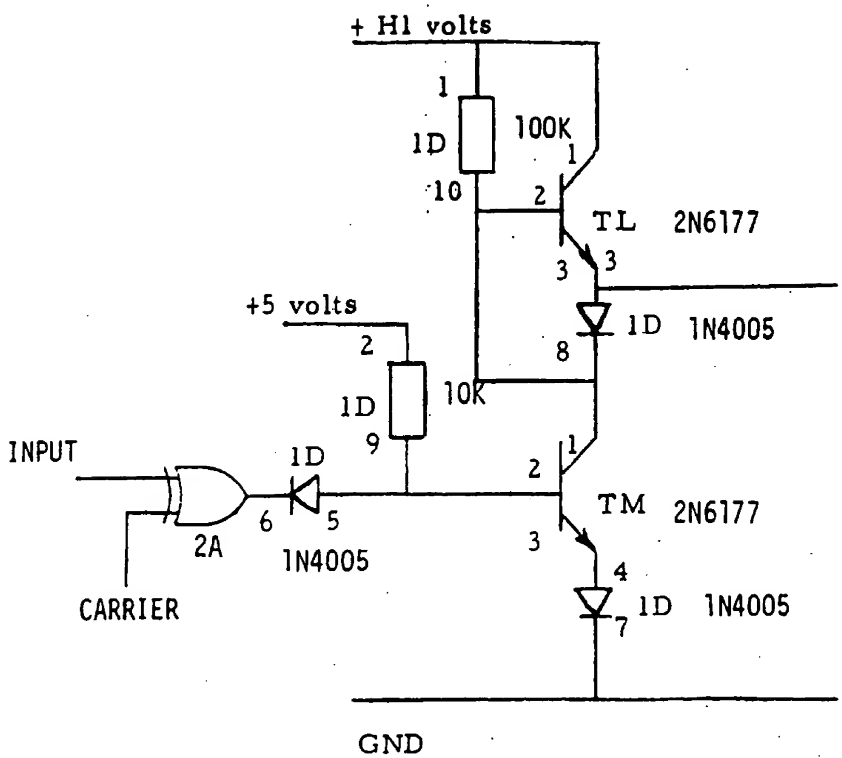

FIGURE 8 DATA LINE DRIVER

EXPANSION TABLE FOR FIGURE 8

Circuit Number	Input Pin Number	Transistor Numbers		IC NUMBER	IC In	IC Out	Component Number	Output Pin Number
1	11	TL	TM	2A	2	3	1D	33
2	12	TN	TP	2A	6	4	1E	34
3	13	TQ	TR	2A	9	10	1F	35
4	14	TS	TT	2A	13	11	1G	36
5	15	TU	TV	2B	2	3	1H	37
6	16	TW	TX	2B	6	4	1J	38
7	17	TY	TZ	2B	9	10	1K	39
8	18	QA	QB	2B	13	11	1L	40
9	19	QC	QD	2C	2	3	1M	41
10	20	QE	QF	2C	6	4	1N	42
11	21	QL	QM	2C	9	10	3D	43
12	22	QN	QP	2C	13	11	3E	44
13	23	QQ	QR	2D	2	3	3F	45
14	24	QS	QT	2D	6	4	3G	46
15	25	QU	QV	2D	9	10	3H	47
16	26	QW	QX	2D	13	11	3J	48
17	27	QY	QZ	2E	2	3	3K	49
18	28	VA	VB	2E	6	4	3L	50
19	29	VC	VD	2E	9	10	3M	51
20	30	VE	VF	2E	13	11	3N	52

DVI 000236

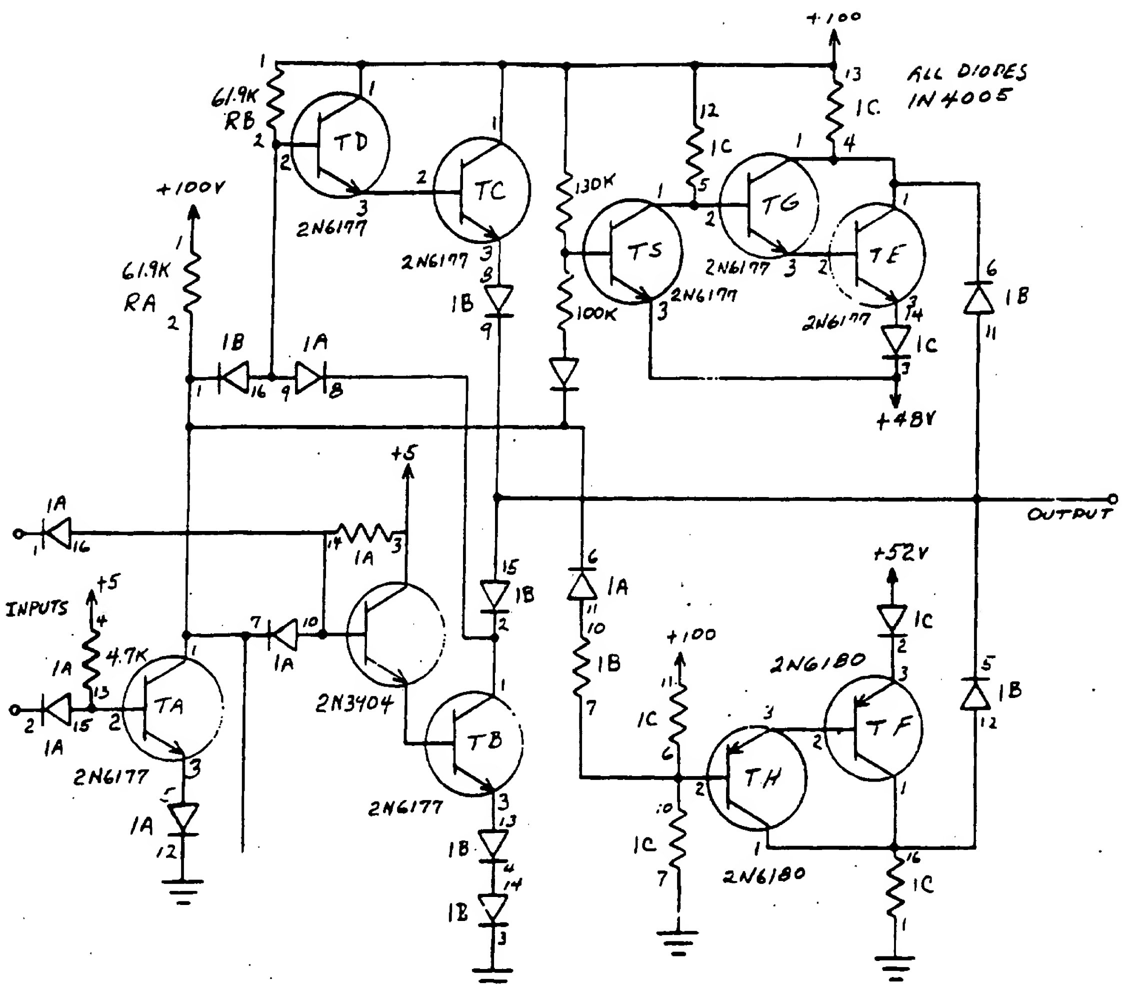

FIGURE 9 ADDRESS LINE DRIVER

low output impedance is required so that there will be a sink for the data lead current at all times. In order that this output impedance be as low as possible, the emitter diodes of both darlingtons in the clamp are returned to offset voltages in such a way as to keep diodes 1B11-6 and 1B5-12 conducting regardless of the direction of current in the external lead. Such additional power supply voltages are obtained from the divider shown below.

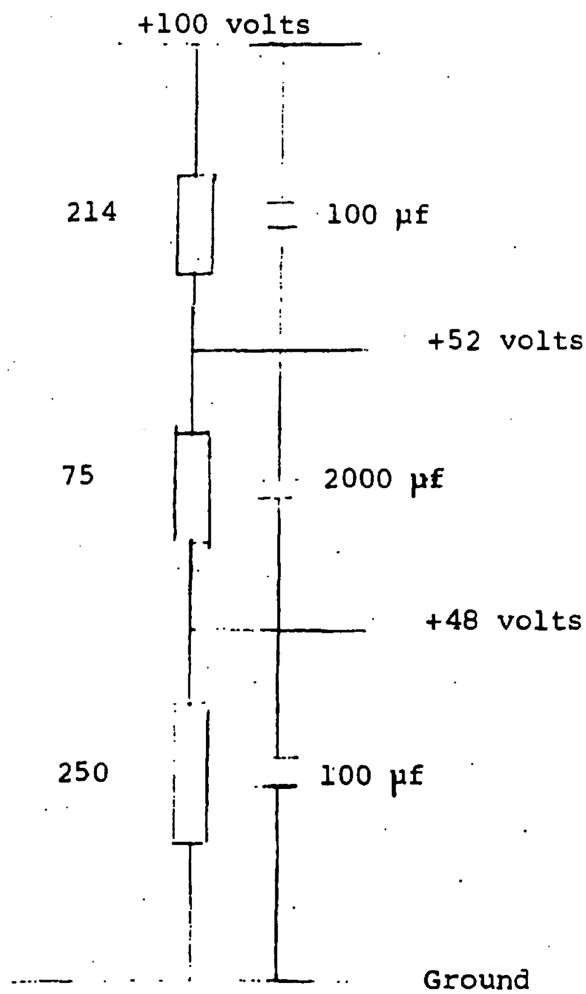

Power Supply Divider

DVI 000238

Each circuit board has one address line driver and twenty data line drivers on it. Twenty of these circuit boards, then, provide for all of the display drivers.

4. Logic Latch Circuit

The Logic latch circuit provides data storage and interfaces with the Data Line Driver. Sixteen bit words are serially loaded into the input buffer and then transferred into the output buffer in parallel. A logic diagram for two input bits is shown below.

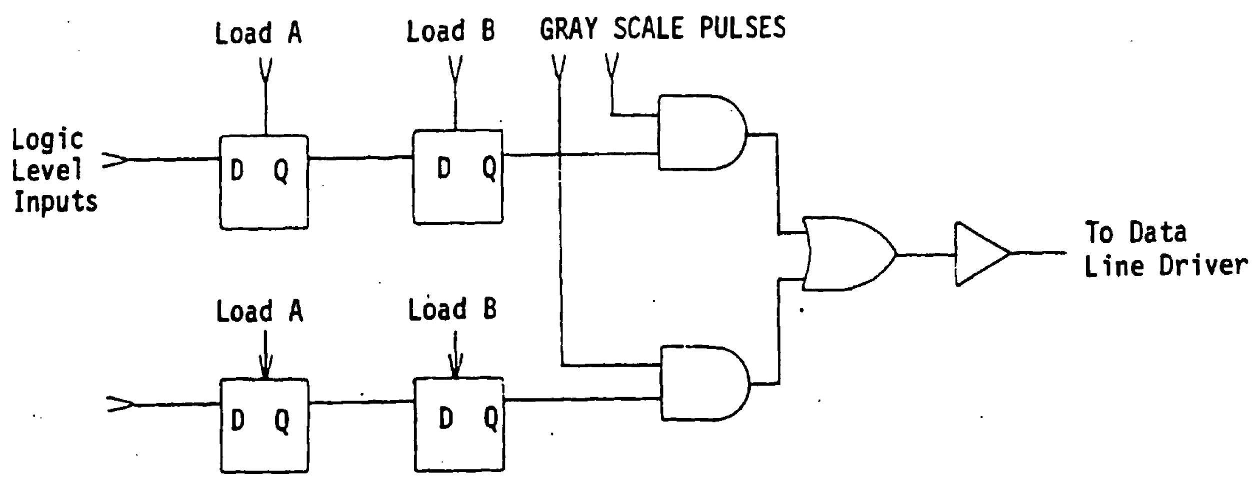

LOGIC LATCH DIAGRAM

The input and output buffers are D type flip flops. The data buffers feed into standard and-or logic with an output to feed the Data Line Driver.

DVI 000239

CMOS Integrated Circuits are used to implement the required logic functions as follows:

D-Type Flip Flop	CD 4042AE
And-or Select Gate	CD 4019AE
Buffer	CD 4050AE

Inasmuch as there are 400 Data Line Drivers, 400 of these circuits are provided. A total of 20 boards are required, with 20 Ckts. per board. A complete schematic of the Logic Latch Board is shown in Appendix C Figure 27.

5. Termination and Driver Board

The termination and driver board, with schematic shown in Appendix C Figure 28, provides 100Ω termination of the 16 data lines from the computer, and buffers these lines with or without logic inversion depending on the setting of S1 TRUE/COMPLEMENT SWITCH. Also included on this board are a 50Ω TTL drivers used to request new data, and terminate plot mode in the computer. Other circuits on this board are used to widen the data input strobe, and take care of word transfer start through use of frame sync from the computer. Board construction is plug in IC's with wire wrap connections. The use of wire wrap construction provides an easy method of adapting to the requirements of the computer interface.

DVI 000240

6. Counter Board

The counter board schematic shown in Appendix C Figure 29 is also a wire wrap board. After frame sync is received from the computer and while the display is addressing the last column a counter on this board is advanced one count for each data strobe. Further in connection with each data strobe one of the fifty output pulses is activated and used to sequentially load 50 words into the Logic Latch Boards.

Appendix F is a timing diagram indicating this action for two out of the twenty 50 word transfers that constitute a complete frame. Software programs used to demonstrate and organize the data for the display are included in Appendix G.

7. Edge Clearing Amplifier

Because the liquid crystal material requires voltage on it to be clear, the two bands of 10 outside vertical columns on each cell need to be driven. A frequency twice that of the carrier frequency on the horizontal leads is chosen so that the RMS voltage at these intersections will be constant regardless of the phase of the signal to the horizontal leads. Such a signal is the "R" waveform of the Timing Generator. Rather larger power transistors have been chosen for this driver so as to be able to drive all 200 leads with one driver. It, too, is a totem pole arrangement, and its diagram is shown in figure 10.

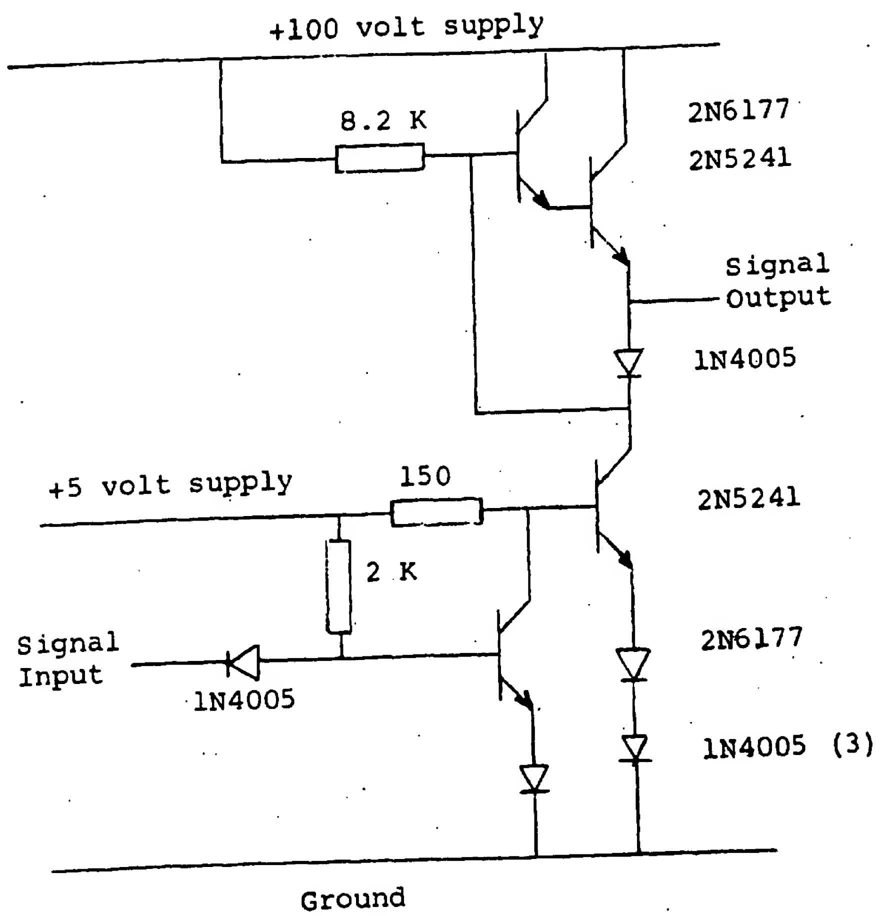

FIGURE 10 EDGE CLEARING AMP

DVI 000242

C. Debugging

While 'standard' electronic debugging techniques are all that should be required in the maintenance of this equipment, the following conditions are noted as a guide to the solution of problems which might develop.

1. Shorts in the cell: Should a short between the front and back of a cell develop, unusual amounts of current will flow in the affected leads. Such currents will be limited by the circuit output impedance (in which case the voltage applied to the horizontal lead in question will be different from its neighbors) or by the impedance of the indium oxide strip on the glass (in which case a gradation in the front level along the lead will be noted). In either case, both the offending leads in the cell are likely to be frosty due to reduced voltage. If so, it will be necessary to sacrifice one of the leads by open circuiting it somewhere. It has seemed advantageous to open circuit the horizontal lead so that the vertical lead again becomes active.

2. Inoperative leads: A possible cause of inoperative leads is the lack of electrical contact at the connector. Redundant connections to the cell have been made (for another reason, as explained elsewhere in this report) and the likelyhood of a complete open has been lowered significantly by that technique.

DVI 000243

3. Catastrophic transistor failures: The transistors are subjected to very low stress in comparison to their ratings and all failures seen thus far have been traceable to operator misintervention. The output impedances are necessarily low to drive the capacitive loads of the cells and the amplifiers might not stand prolonged shorts to either power supply or ground. In such cases, the transistor loading becomes about half that published as the maximum free air value. Unusually large pulsations of the DC current meter in the 100 volt supply often accompany a shorted transistor.

4. Electrical characterization of the LC cells. The following electrical parameters of the LC cell may be used as comparison against which future readings may be more meaningful:

a. Threshold voltage - - all the cells were in the range of 46 to 49 volts rms at their threshold. An easy way to measure threshold voltage is use a variable 60 Hz source (such as variac). As voltage is increased just before the liquid crystal material begins to unwind (at the threshold) it goes through its most intense scattering (cloudy) condition.

b. Indium oxide lead resistance - - measured from one edge of the cell to the other, the lead resistance averages 7 to 8 K ohms.

c. LC material shunt resistance - - the shunt resistance of one element of the display is about 24 Megohms. Care must be taken in the measurement of this value, however, since the number of spurious conduction paths through the cell is very high. Perhaps the easiest

DVI 000244

way to measure this value, is to measure the parallel combination of the resistances of all 40 elements in one row or column.

d. LC material shunt capacitance - - the shunt capacitance of one element of the display is about 93 picofarads. Again, the number of spurious capacitances in the cell make the measurement of the capacitance of one single element impossible. The easiest measurement is the parallel combination of all 40 elements in one row or column.

D. Circuit Board Construction

The circuit board construction technique chosen for this application is a echanized wire placement process provided by Photocircuits Division of Kollmargan Corporation (Glen Cove, N. Y.). In small quantity lots, the price of this process is much below that of preparation of photoetching masks. Working from a list of wires and rough component layout sketch, their machinery places wire physically on the board in accordance with the customers plan. Where components are to be connected to the wire, a hole is drilled through the board and wire, laying bare the end of the wire. Then the hole is plated through by an electrodeless plating technique.

Cost considerations are such that even at a quantity of 20, as are required in this application, some saving can be made over regular mask layout and photoetching.

DVI 000245

The wirelists and layout sketches for circuit boards are shown in Appendix D and Appendix E.

The notation used in Appendix D Tables III, IV follows these rules:

1. A rectangular grouping of holes in a Dual-In-Line configuration will have a group number consisting of a number and a letter, e.g., 3A, 1A, 2B.
2. An individual pin in that group will be noted by the group number followed by the pin number, e.g., 3A1, 1A14, 2B10.
3. The connector pin numbers begin with CX.
4. Transistors have 2 letter group names beginning with T, Q, or V.
5. A wire on the board is designed as from 1A1 to 3A14 to 2B11 in the form 1A1/3A14/2B11.

VI. FABRICATION OF LIQUID CRYSTAL CELLS

The display is an array of ten cells stacked in parallel like a deck of cards. Each cell consists of two glass plates, 7.5 x 7 x 0.375 in., coated on one side with electrodes of transparent indium oxide. The cells are assembled with electrodes facing each other and separated by a gap of 0.0005 in. which is filled with liquid crystal. The overall dimension of the assembled cell is 7.5 x 7.5 x 0.75 in. The active area of 6.25 in. square has a matrix of 40 x 40 display elements but only a matrix of 20 x 40 elements in the central 3.1 x 6.2 in. area is designed to be multiplexed. The elements are formed by intersection of parallel electrode strips etched in the indium oxide and oriented at right angles. The strips are located along the entire 7.5 in. length of the glass plates and electrical contact is made by connectors attached to the edges of the plates.

The liquid crystal material is a combination of nematic and cholesteric liquid crystals of positive dielectric anisotropy. A layer of this material is transparent when energized by an electric field and becomes opaque when the field is removed. The electro-optic effect is due to a field-induced transformation of the geometric arrangement of the molecules. The clear state corresponds to the nematic state with homeotropic alignment, and the opacity is due to light scattering of the focal conic configuration in the cholesteric state. Application of voltage produces a transition between the cholesteric and nematic phases.

DVI 000247

The threshold voltage for the cholesteric-nematic transition is inversely proportional to the thickness of the liquid crystal layer. To minimize the potentials required to drive the display, it is desirable to employ a very thin layer of the order of 0.0005 in. The thickness has to be controlled to better than 10% in all the cells for proper operation of the display. The extremely critical liquid crystal thickness tolerance demanded for this application turned out to be the most difficult task in the fabrication of the cells and required the development of special materials and assembly techniques. The completed cells had uniform gaps and liquid crystal layer thicknesses of 0.0005 in. as well as uniform threshold potentials. Four of the ten cells were free of defects and permitted the activation of every one of the 40 x 40 matrix elements. The other six cells had sundry imperfections mostly outside the operational 20 x 40 element area. These imperfections were due to a few breaks or high resistance regions in the strip electrodes and shorts between between opposite electrodes, in addition to some "noisy" regions in the liquid crystal layer. The electrical defects affect all or part of the row or column in which they occur.

Glass Substrates

Special requirements for the glass substrates were high light transmission and flatness. Maximum light transmission was necessary to keep absorption losses to a minimum in a 10-cell display made with 20 glass plates and conductive coatings. As the greenish tint in ordinary soda-lime glass is objectionable in a 7.5 in. stack of 20 plates, crown glass was selected because it is essentially colorless.

The requirement for flatness arises from the need for critical control of liquid crystal thickness. The display area had originally been specified as 6 x 6 in. Allowing for space for sealing the cell with a gasket and making contact to edge connectors, plate size had to be 7 x 7.5 in. To control the designed 12 μm liquid crystal thickness to within 5%, the variation over a 10 in. diagonal of plate surface must not exceed 0.3 μm or 0.03 μm per in. Specially selected pieces of float glass or superior quality plate glass, both noted for their flatness, have variations of 1-2 μm per in. It was therefore necessary to have the crown glass polished to flatness specifications, but it was not economically feasible to specify flatness to within 0.03 μm per in. A best-effort offer by Planar Optics Company to polish 7 x 7.5 in. crown glass to within 0.1 μm per in. was accepted, and a test sample furnished by that company was within this tolerance. To attain this result, the glass had to be 0.375 in. thick.

To expedite contract performance, glass plates were shipped directly from the polisher to Optical Coatings Laboratory, Inc. for deposition of conductive coatings of indium oxide without our inspection of the glass for flatness. Deposition of indium oxide by sputtering is not expected to distort flatness as may occur when tin oxide, the other common conductive coating, is coated by pyrolysis at temperatures as high as 400^{0} C. Since high light transmission must be traded off against electrical resistivity, the resistivity was allowed to be as high as 200 ohms per square.

DVI 000249

The first shipment of ten indium oxide coated plates had a transmission of 80% to white light. Ten cells of this substrate filled with liquid crystal would have a total transmission of about 10% when immersed in a fluid of matching refractive index to reduce glass-to-air reflection losses. Subsequently received coated plates had a higher transmission of about 82.5% which should have given about 15% transmission under the same conditions. Not all of these could be used, and the final display is made with glass from both shipments.

Flatness of the indium oxide coated plates was measured with a planometer manufactured by Towne Laboratories. Some plates were flat to within 0.1 μm per inch but some had variations of up to 0.3 to 0.4 μm per in., and these included both concave and convex shapes.

Four holes, one for filling with liquid crystal and three for venting, were drilled with an ultrasonic drill near the corners of one plate for each cell.

Preparation of Strip Electrodes

The electrodes are parallel strips with 0.156 in. center-to-center spacing and the gap between strips is 0.005 in. wide. Strip width was selected to interface with commercial edge connectors of 0.156 in. spacing. The strips were etched into the indium oxide by photolithographic methods commonly employed in microcircuit fabrication. The appropriate photomask was supplied by Towne Laboratories. Plates were coated with photoresist (Shipley Axo 111) and exposed to ultraviolet light through

DVI 000250

the photomask. The resist was solvent-developed to dissolve the exposed resist and bare narrow strips of indium oxide which was removed by etching with zinc-hydrochloric acid. The remaining photoresist was then stripped off. The electrode bearing surfaces were then overcoated with a thin (< 1 μm) layer of an organic silicon-containing surfactant (Dow Z-2-2300) deposited from aqueous solution. This coating helps control the alignment of liquid crystal molecules at the surface and reduces noise in the display.

The etched plates were tested for electrical continuity and absence of shorts between adjacent strips. Shorts were present in some of the plates and these were opened by applying a voltage between adjacent strips to cause electrical breakdown in the narrow regions constituting the shorts. It was not possible to open these shorts by scratching with a sharp instrument because the indium oxide coating is extremely hard. The resistance of the strips was typically 8,000 to 10,000 ohms. Some of the strips had higher resistance, possibly due to defects in the indium oxide coating. It is conceivable that attack of the surface by compounds used in polishing the plates to flatness or, more likely, the presence of residues of polishing compounds would interfere with the deposition of the oxide coating.

Cell Assembly

To assemble a cell, two plates are oriented with their electrode strips at right angles and facing each other. Before sealing the edges with a gasket, provision must be made to control the gap between the plates.

DVI 000251

Several approaches to seal cells with gaskets of various kinds proved to be unsuccessful. The thickness of the gasket was to determine the gap and liquid crystal thickness. Gasketing materials tried were polyester, polycarbonate and epoxy impregnated paper. The gaskets were clamped between the plates, and the assembly was heated to the appropriate temperature for softening the plastics and effecting a bond. In every instance the resulting cell had a nonuniform gap and was occasionally shorted by contact between electrodes. To prevent shorting, tiny plastic spacers were introduced inside the cell but these also contributed to nonuniformity. Variation of clamping pressure and heating and cooling rates did not lead to improved results. Even sealing without clamping pressure produced distorted spacing profiles. It was concluded that the distortions occur during cooling, possibly due to uneven contraction of the glass and plastic sealing materials.

A novel technique eventually yielded cells with uniform and reproducible gaps. Small spacers (about 0.02 in. square), cut from 0.0005 in. thick polyester sheet, were sandwiched between the glass plates to provide a 0.0005 in. separation. Inspection of the cell in monochromatic light revealed a number of fringes corresponding to variations in gap height. One or more C-clamps were attached to edges of the cell, and the clamp pressure and distribution of spacers were manipulated until a minimum number of fringes, usually 3 to 6 was obtained. The glass plates had to be reasonably well matched to achieve this result. While in the

DVI 000252

clamped position, epoxy resin was applied to the plate edges and was drawn into the spacing between the plates by capillary action. To control the viscosity of the resin, the assembly was maintained at about 35°C. The epoxy was allowed to cure at 35°C for 24-48 hours. The fringe pattern was substantially unchanged after the epoxy had set up and the clamps had been removed. In experiments to determine the effects of post-cure above 35°C, it was noted that the fringe pattern changed on heating the cell. When cooled after keeping for one hour at 60°C, the room temperature pattern appeared to be the same as before heating. Some permanent changes were, however, observed at room temperature when cooled from 100°C. Provided that the substrates are reasonably flat, with flatness variation no greater than about 2 μm over the entire area, it appears that the present method of assembly is capable of controlling gaps as small as about 10 μm within 5%.

<u>Liquid Crystal Material</u>

The liquid crystal formulation was specially developed for this application as described in Appendix B.

The formulation is:

23% N-(p-Methoxybenzylidene)-p-(n-butyl)-aniline (MBBA),

23% N-(p-Butoxybenzylidene)-p-aminobenzonitrile (BuBAB)

23% N-(p-Octyloxybenzylidene)-p-aminobenzonitrile (OctylBAB)

23% Cholesteryl nonanoate

8% Dodecane

DVI 000253

This formulation represented the best compromise for fast response time and low threshold voltage. It has a mesophase of 12-80 C, threshold potential for the cholesteric-nematic transition of 4.3 per μm thickness, resistivity of 3.4×10^{10} ohm-cm at room temperature and dielectric constant of 8.03 in the unactivated focal conic state.

MBBA (high purity grade), cholesteryl nonanoate and dodecane, purchased from Eastman Organic Chemicals, were used as received. BuBAB and OctylBAB were synthesized and purified by multiple recrystallizations. BuBAB was further purified by vacuum sublimation.

The liquid crystal formulation was introduced into the cells heated to $60^{\circ}C$ to reduce the viscosity of the liquid crystal and facilitate its flow. Fill and vent holes were capped with glass discs which were overcoated with an epoxy button.

DVI 000254

VII. CONCLUSIONS AND RECOMMENDATIONS

A. ADDRESSING WAVEFORMS

When viewing the display in one of the partially cloudy states, considerable flicker is observed during address time. So the effectiveness of the addressing waveform was evaluated by focusing the output of one display element onto a photo transistor (Fairchild FPT100). The output of the photo transistor, as displayed on an oscilloscope, was proportional to incident illumination. During the evaluation, the display was illuminated by a 150 W reflector flood lamp located about two inches from the rear of the display module. In order to prevent 120Hz flicker, that was observed when using a 60Hz excitation; the lamp was connected to a 400Hz source.

The voltage waveform applied to a display element was also presented on the oscilloscope using the chopped mode, and taking the difference between the column signal and the data signal. Photographs of the oscilloscope traces are shown in figures 11 and 12. The upper trace is the voltage applied to a cell element, and the lower trace is the relative light transmission of one cell element. The phase of the voltage applied to the cell element during non-address time is the same for all data taken in figures 11 and 12. This uniformity in phase is derived from the fact that all other cell elements in the same row as the element under observation are being driven to the clear state. In figure 11 the first three cycles is the time that the display element under observation is addressed. In figure 12 the oscilloscope sweep started three cycles

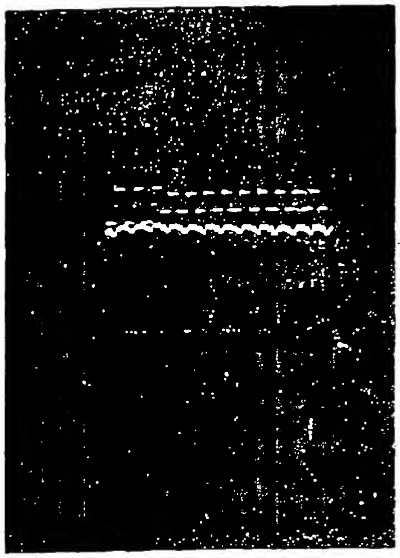

a

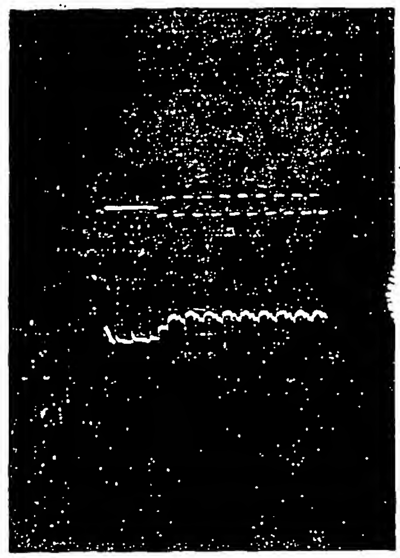

b

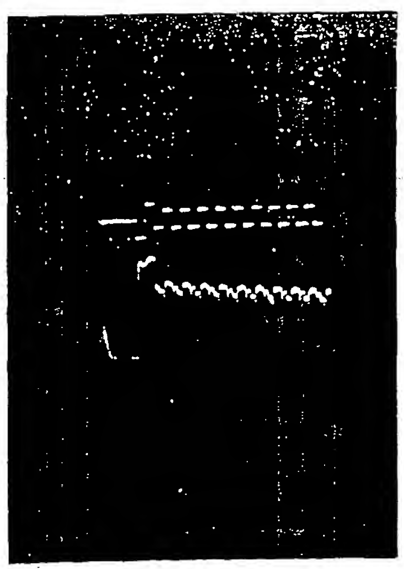

c

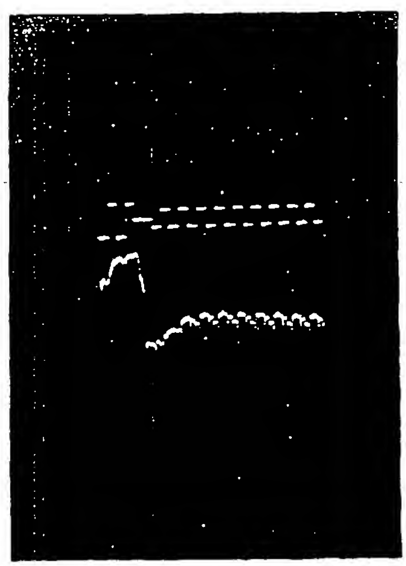

d

Figure 11 Liquid crystal response compared to applied voltage. The upper trace shows voltage applied to cell element, and the lower trace shows relative amount of light transmitted through the cell element for the various liquid crystal states: a) clear, b) cloudy, c) one third cloudy, d) two thirds cloudy.

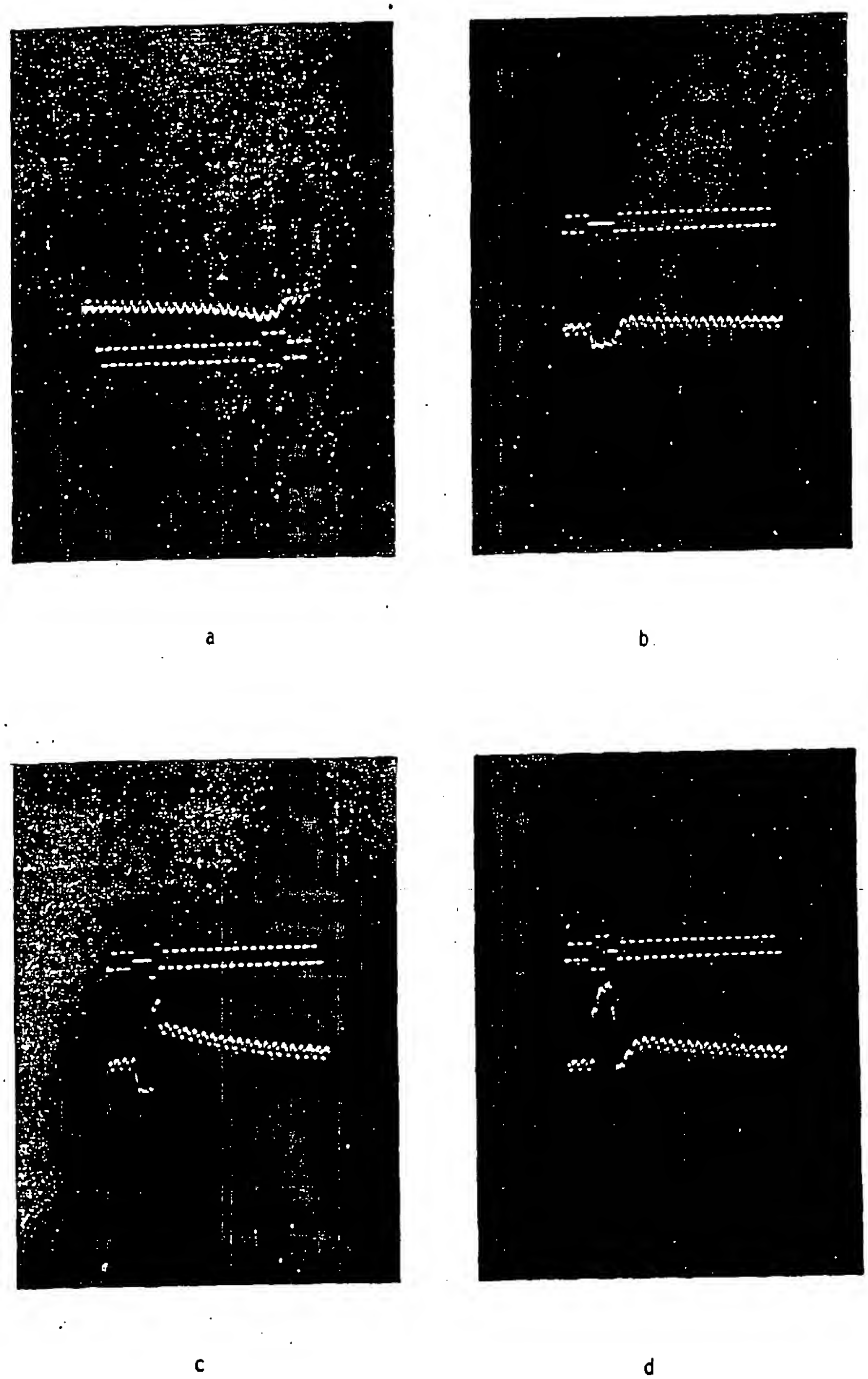

Figure 12 Liquid crystal response compared to applied voltage. Same as Figure 19 except trigger is one column sooner and oscilloscope sweep speed is cut in half.

before address time and the sweep was changed from 5 msec/cm used in figure 11 to 10 msec/cm. The above adjustments allow the total change in light transmittance over one display frame to be observed.

The highest light transmittance is for a clear cell, as in figure 11 A. The cloudy state shown in figure 11 B has the lowest light transmittance. In figures 11 C and D the average light transmittance is in between the clear and cloudy state. As is apparent from figures 11 C, and 12 C, a very large change in light transmittance takes place during address time. It is recommended that instead of applying zero volts for the first two cycle of address time that the 100 volt square wave sustaining voltage be applied in order to eliminate the large dip in light transmittance. Thus the amount of observed flicker should be greatly reduced. Similarly the voltage waveforms of figures 11 d, and 12 d could be modified to reduce the first two cycles from a peak to peak of 200 volts down to the holding voltage of 100 volts. This reduction in voltage would eliminate the high light transmittance during the first two cycles of address time. Here again the amount of observed flicker would be reduced.

B. EDGE CLEARING AMPLIFIER

The two non-active areas ten elements wide on each side of the display could be driven clearer if a higher supply voltage was used for the edge clearing amplifier. This voltage increase would have to be independent of the voltage supplied to data and column drivers, in order to maintain control of the active display area. The voltage would also have to be expanded symmetrically in order to keep a DC bias from des-

troying cell electrodes. For example, making the present positive source +125 volts and the present ground -25 volts. The symmetrical expansion outlined above would drive the inactive edges of the display to the clear state regardless of the phase of the signals on the data lines.

C. LIGHTING

Various methods for lighting the display were investigated. Initial testing of the display module pinpointed a heating problem. Heat from the illumination source caused the rear cells in the display module to heat up; thus changing their threshold voltage. A fluorescent light source was tried, but the color of the display changed at a beat rate from yellow to blue. The beat rate depended on display refresh rate.

In order to solve the heating effect of incandescent illumination; the effects of two dichroic mirrors obtained from Liberty Mirror Co. were evaluated. One dichroic mirror with coating 901 reflected light in the yellow portion of the visible spectrum and transmitted other portions of the visible spectrum as well as infrared. The other dichroic mirror coating 90-500 transmitted the upper half of the visible spectrum and reflected the lower half of visible spectrum as well as infrared. The objective in using the dichroic mirrors is to keep the infrared rays out of the display to prevent heating.

The blue light transmitted by the 90-500 mirror was not desirable because the liquid crystal material used in the display cells

strongly scatters blue light. The scattering reduces contrast and makes the display less transparent.

The best lighting for the display was obtained using the 901 mirror. The mirror was placed in a vertical plane 45^{o} from the back of the display module. A 150 Watt reflector flood lamp was located such that its rays were horizontal, centered on the mirror and parallel to the back of the display module. This arrangement gave the cloudy elements in the display a bright yellow color and kept the infrared rays out of the display module.

D. The threshold voltage was observed to be very temperature dependent. When displaying gray scale, the temperature dependence of threshold voltage was extremely critical. It is recommended that the remote programming feature of the 100 Volt power supply be exploited by sensing display module temperature and controlling power supply output voltage. A more sophisticated approach would be to periodically put up a gray scale pattern for part of one frame and compare cell transmittance to a standard. The comparison output would then be used to control power supply voltage, in order to optimize gray scale capability.

APPENDIX A- A SUMMARY OF 3-D DISPLAY TYPES

DISPLAY TYPE	APPROX % LIGHT TRANSMISSION ONE LAYER	APPROX % LIGHT TRANSMISSION TEN LAYERS	VARIABLE INTENSITY	CONTRAST UNDER HIGH/LOW AMBIENT	SMALLEST CELL SIZE INCHES	MAXIMUM ARRAY SIZE	PROB-ABILITY OF SUCCESS	REMARKS	COMPANY	REFERENCE
Liquid Crystals Light Scatter-ing	94	50	Yes	Excellent	<.002	30x30	Good	Light Scattering Valve	G.E. Company Schenectady	Applied Physics Letters Vol 19 No. 9 1 Nov 71 Pg. 343
Liquid Crystals Field Effect	94	50	Yes	Excellent	<.002	30x30	Excellent	Light Valve	G.E. Company Schenectady	J. E. Bigelow
Liquid Crystals Photoconductive	90	35	Yes	Excellent	<.002	Image Source Depend-ent	Poor	Difficult to optically couple image to each layer	G.E.Company Schenectady	J. E. Bigelow
Liquid Crystals Field Effect Perpendicular			Yes	Good		100x100	Poor	Brightness & Color depend-ent on angle of view	Telefunken Ulm, Ger.	SID Digest 1972 Pg. 98
Electrostatic Marks	Some Scattering Each	Light Cell					Poor	Small Particles Controlled by Electrostatic Field	A.M. Marks	Patents 3,512,876 3,257,903
Gas Discharge Digivue	70	2.8	Diffi-cult	Low	.017	512x512	Poor	Light Emitting	Owens, Ill. Toledo,Ohio	Tech Bulletin DU-140 7/1/71
Gas Discharge Self Scan	0-pa-que	0	Diffi-cult	Low	.030		None	Light Emitting	Burroughs, Plainfield NJ	Burroughs Corp Plainfield,NJ
Gas Discharge Crossed Laser Beams	≈100	≈100	Limited	Low	<.08		Under Develop-ment	Light Emitting	Battelle Ins Columbus Ohio	IEEE Trans Vol ED-18 No. 9 9/71 Page 724
Solid State Ferroelectric Ceramic	21	5	Yes	Good	<.25		Poor	Light Valve Uses Polarizers	Sandia Labs Albuquerque, NM	SID Digest '72 Page 14, Aviation Week 3 July 1973 P43
Moving Vanes Distec System (Electrostatic)	≈100	≈100	No	Excellent	.063		Good	Light Scattering Some Obstruction due to electrode & vane supports	Display Tech Cupertino, Cal.	SID Digest '72 Pg. 108
Moving Vanes Distec System	95	60	No	Excellent	.063		Good	Light Scattering Clear Plastic support each layer.	Display Tech Cupertino, Cal.	

DVI 000261

APPENDIX B

Physical and Chemical Studies of the Cholesteric-Nematic Transition

by

R. A. Kashnow, H. S. Cole, Jr., and S. Aftergut

I. PHYSICAL STUDIES

INTRODUCTION

A nematic liquid crystal is an ordered fluid with uniaxial optical properties.[3] It is a suitable electro-optic medium principally because of two attributes: (1) the optical anisotropy (i.e. the birefringence) is of sufficient magnitude to effect visible changes in light-scattering or absorption; (2) the local direction of the optic axis can be altered by the application of electric fields of reasonable magnitudes. An interesting and useful variant of the nematic molecular ordering is the "chiral nematic," more commonly called the cholesteric state. In this state, which can be achieved by adding an appropriate optically-active substance to a nematic, and which occurs naturally in a large number of cholesterol derivatives, the optic axis exhibits helical ordering.

For flat-panel display applications, the liquid crystal material must be contained between closely-spaced planar substrates. For such configuration, a variety of molecular configurations can be assumed by the chiral nematic substance, depending primarily upon the influences of the boundaries and the application of an external field. We shall consider in some detail below several important configuration which can be achieved, and we shall discuss the transitions between them.

QUIESCENT STATE

The simplest arrangement is known as the "Grandjean planar" texture,[4] and is sketched in Fig. 13. The helical axis is normal to the bounding plates; symmetry therefore allows the preparation of monodomain samples of arbitrary size. The Grandjean structure is achieved by preparing samples with "parallel" boundary condition; i.e., the optic axis at the bounding planes must be rendered unidirectional and constrained to lie parallel to the substrates. For such samples, the Grandjean state is the quiescent one with respect to electric field perturbation; it is the steady-state configuration adopted in the absence of an applied field.

Optically a sample in the Grandjean planar state does not scatter light strongly.[5] The transmissive properties depend, however on the ratio p_0/λ, where p_0 is the undisturbed helical pitch and λ is the wavelength of incident light. For example, for visible light wavelengths, samples with p_0 greater than about one micron appear clear (transmissive) and exhibit very little dispersion. For values of p_0/λ closer to unity, however, dispersive reflective effects dominate and an irridescent appearance results.

Chiral nematics with homeotropic boundary conditions (optic axis normal to the substrate planes) have not been widely studied. Our recent observations indicate that such samples may adopt a rather complex spiral structure in the quiescent state. Figure 14a shows a micrograph of a sample in such a state; Figure 14b shows a possible molecular arrangement consistent with the observations. This state is, like the Grandjean texture, not a strong light-scattering one.

DVI 000264

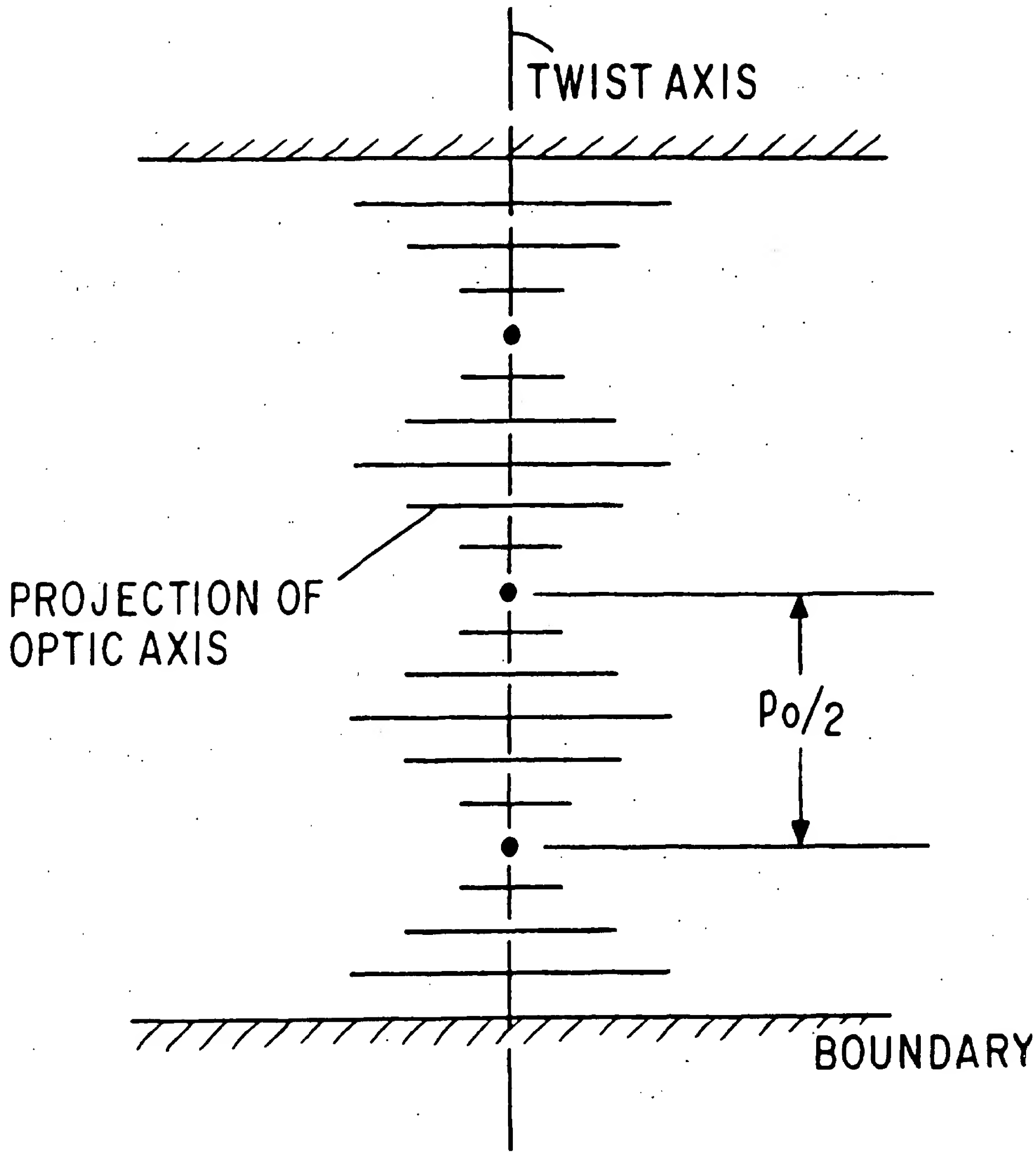

Figure 13-Grandjean planar texture. Helical twist axis is normal to substrate planes. $p_o/2$ denotes the half-pitch of the twisted distribution of the optic axis.

DVI 000265

PERTURBATION BY AN ELECTRIC FIELD

Consider next the application of an electric field across a chiral nematic layer which is initially in either of the quiescent states described above. For the electro-optic effect considered in this report -- the cholesteric-nematic transition[6,7] -- we require liquid crystal materials of positive dielectric anisotropy (PDA): Here the subscripts p and t distinguish the principal, low-frequency dielectric constants parallel and transverse, respectively, to the nematic "director," which is the (averaged) direction of the long molecular axis. In PDA substances, the director tends toward alignment with the applied field direction (since this minimizes free energy).

The initial effect of an applied electric field on a sample in either the Grandjean or spiral states is, effectively, a reorientation of the helical axis. This leads to a strong light-scattering state which has been widely referred to in the literature as a "focal-conic" state, or the "storage mode."[8] The latter term reflects the persistence of this configuration upon removal of the field. We shall refer to this light-scattering state as the "domain" texture.[9] Figure 15a shows a microphotograph of a sample in this state, and Figure 15b a sketch of the corresponding modecular alignment pattern. Note that an array of disclination lines (the liquid-crystal analogues of dislocations in solids) is required to accommodate the "bulk" alignment pattern with the fixed alignment at the boundaries. This array has the same periodicity as the intrinsic pitch of the helical structure.

DVI 000266

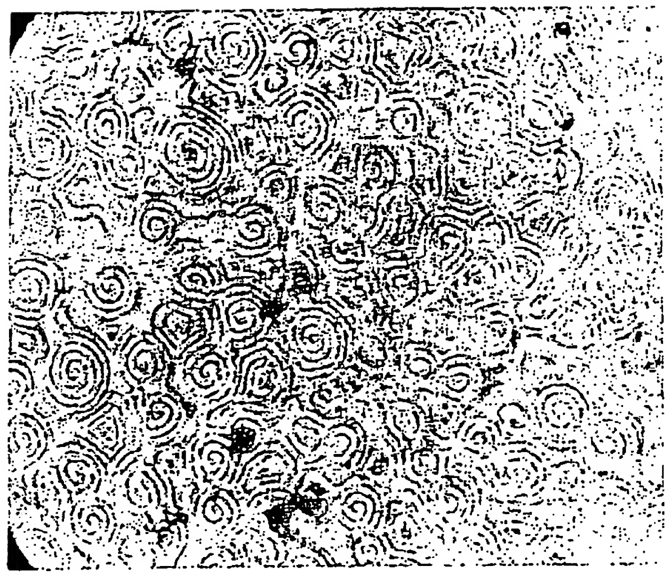

This page is reproduced at the back of the report by a different reproduction method to provide better detail.

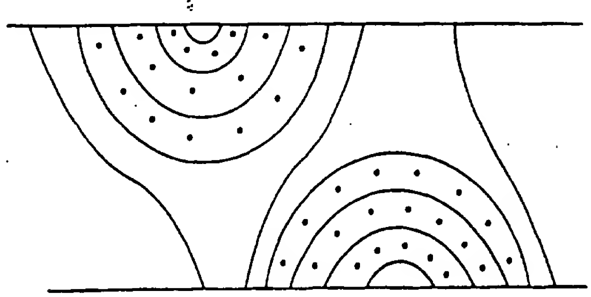

DVI 000267

Figure 14

a) Microphotograph (446X, parallel polarizers)of quiescent state of a cholesteric sample (5% COC) with homeotropic boundaries, showing the spiral polygonal structure;

b) A cross-sectional view of a possible director distribution underlying the spiral structure in (a) (after Ref. 20).

Increasing the electric field strength across a layer in this domain state causes first a dilation of the pitch and eventually a discontinuous transition to an aligned, quasi-nematic state[10,11] (Figure 16). The transition occurs at a critical field strength,[11]

$$E_c = q_0 \, (4\pi k_{22}/\Delta\varepsilon)^{1/2} \tag{1}$$

where $q_0 = \pi/p_0$ is the undisturbed wavenumber, k_{22} is an elastic constant for twist deformations, and $\Delta\varepsilon$ is the aforementioned dielectric anisotropy. The dependence of the dilation and subsequent divergence of the pitch on the applied field can be described by the following equation:[10]

$$p/p_0 = 4\pi^{-2} K(k)\varepsilon(k) \tag{2}$$

$$E/E_c = k/\varepsilon(k)$$

where $K(k)$ and $\varepsilon(k)$ are complete elliptic integrals of the first and second kind, respectively. By allowing the argument, k, to very between 0 and 1, we have generated some values of reduced pitch vs. reduced field strength; these values are plotted in Figure 17.

Experimental confirmation of the theoretical predictions of Eq. (2) have been published for the cases of applied magnetic[12] and electric[13] fields. Since we are directly concerned with the light-scattering properties of these structures, we have measured the (steady-state) zero-order-transmission (ZOT) as a function of applied field. Typical data are shown in Figure 18 and are in qualitative agreement with calculations which assume that the ZOT varies as $(p/p_0)^n$ with $n = 4$.

DVI 000268

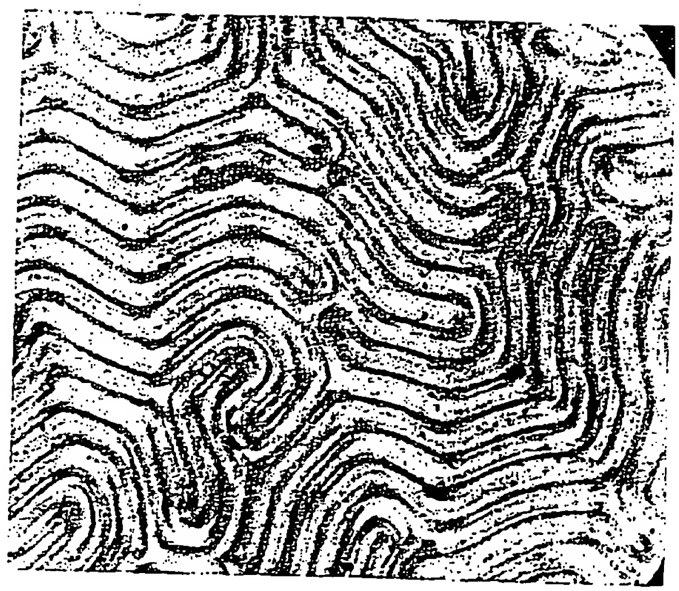

This page is reproduced at the back of the report by a different reproduction method to provide better detail.

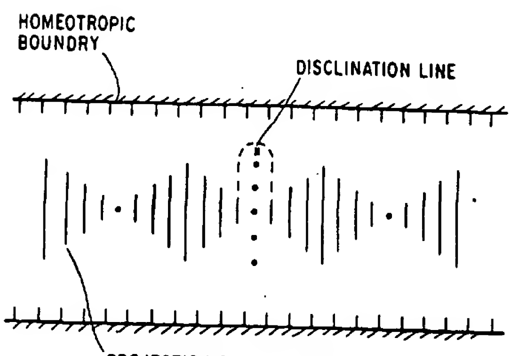

DVI 000269

Figure 15

a) Microphotograph (446X, parallel polarizers) of the light-scattering domain structure in a sample containing 3% COC;

b) A cross-sectional view of the director distribution in the domain structure (after Ref. 9).

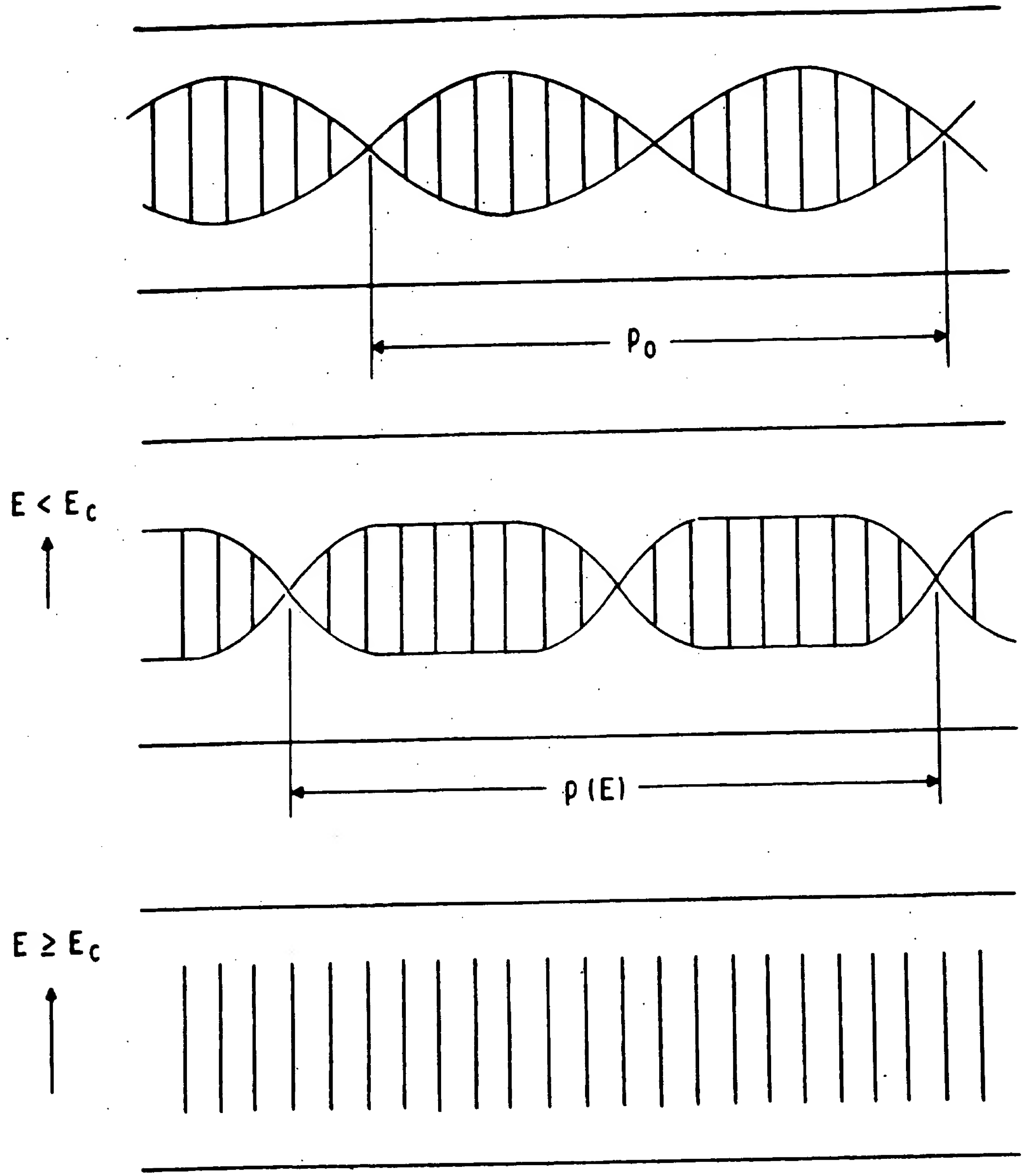

DVI 000270

Figure 16

Cross-sectional sketch of the director distribution, starting with a pitch p_0 in the domain structure, showing the dilation ($p(E)$)as a field is applied, and the subsequent transition to a nematic state for $E > E_c$(after Ref. 10).

DEPENDENCE OF THE PITCH ON CHOLESTERIC CONCENTRATION

The undisturbed pitch p_0 is known to depend inversely on the concentration of optically-active solute in a nematic solvent.[14] For example, Figure 19 shows a plot of the reciprocal half-pitch vs. concentration (in weight percent) for a system in which the solute is cholesteryl oleyl carbonate (COC) and the solvent a binary mixture of four parts by weight p-methoxybenzylidene-p-n-butylaniline (MBBA) to one part by weight p-ethoxybenzylidene-aminobenzonitrile (PEBAB). The values of pitch were measured from microphotographs of the domain structure, such as Figure 15A.

These measurements were relatively insensitive to temperature. For example, a sample containing 1.25 percent by weight COC with $p_0(T = 33.0^oC)/2 = 8.4\mu m$ showed an increase in $p_0/2$ of about 0.3 percent per deg. C between 33 and 53^oC.

THRESHOLD FIELD

In the cholesteric-nematic transition, the wavenumber of the dominant perturbation, q_0, is independent of sample thickness. As a consequence, the threshold voltage increases with sample thickness, in contradistinction to most liquid crystal electro-optic effects (such as dynamic scattering) for which the threshold voltage is independent of sample thickness. An experimental verification of this feature is shown in Figure 20, in which data are shown for a wedge-shaped sample containint 3.9% COC. The temperature dependence of the threshold for this composition is shown in Figure 21.

DVI 000271

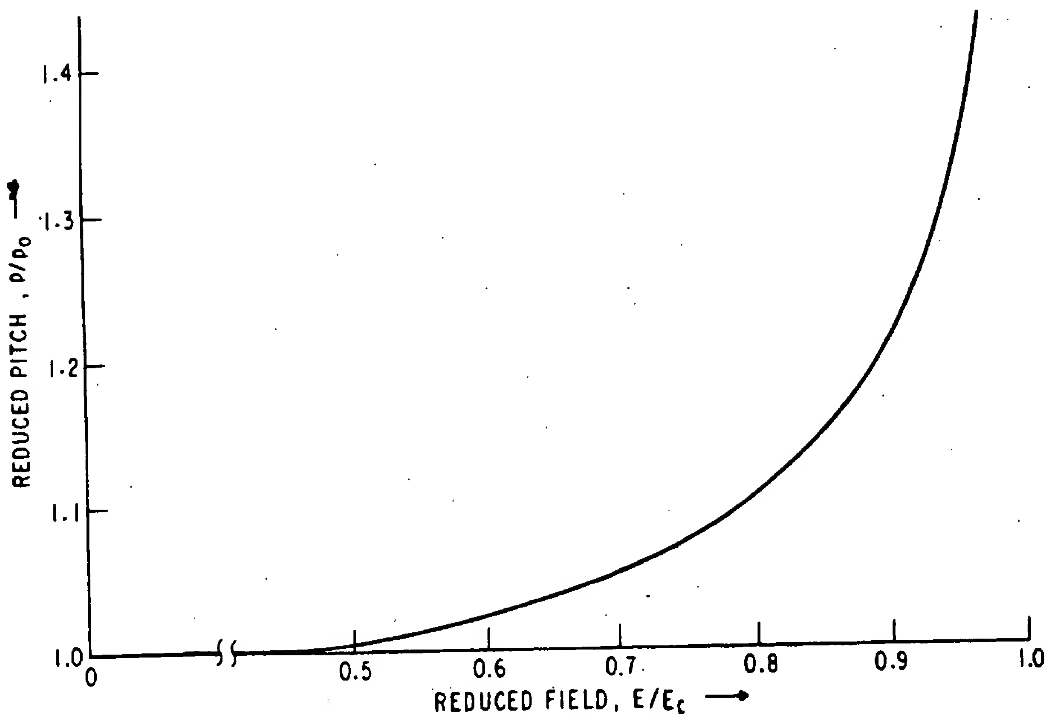

Figure 17

Theoretical plot of the reduced pitch vs. reduced field for the dilation process sketched in Fig. 16.

DVI 000272

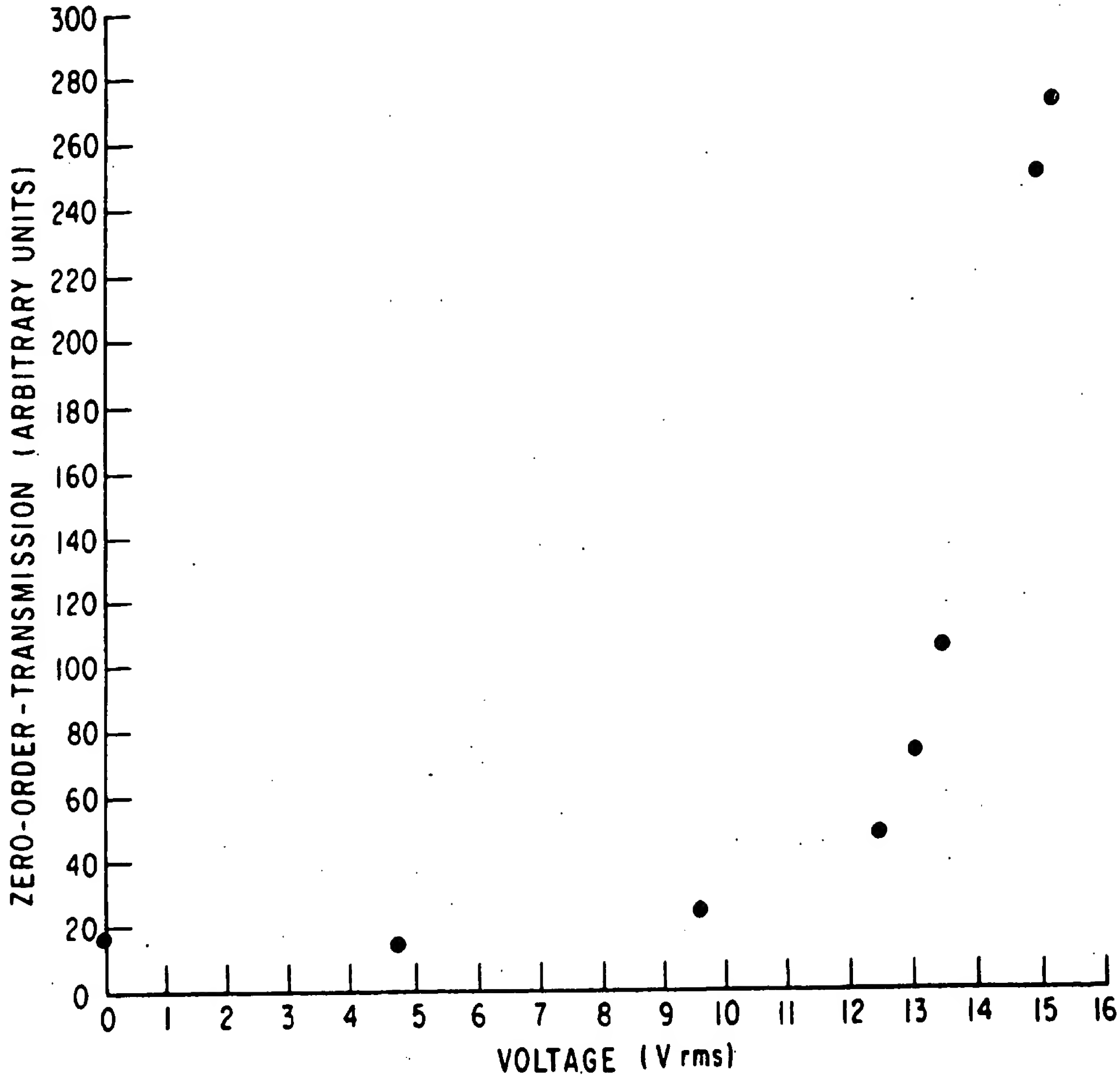

Figure 18

Zero-order-transmission vs. applied voltage for a cholesteric sample containing 3% COC.

DVI 000273

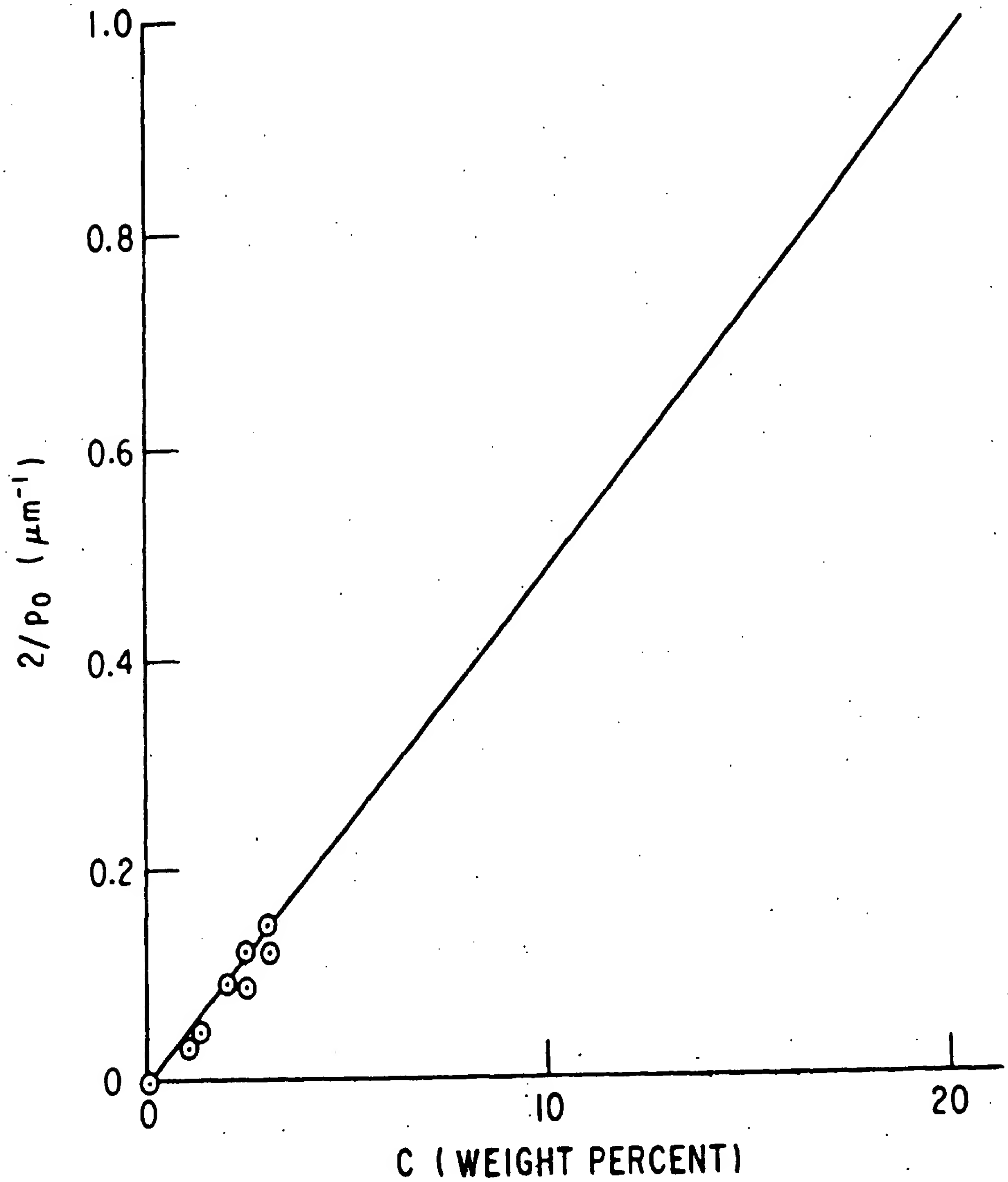

Figure 19

Recicprocal half-pitch vs. concentrationof COC in a 4:1 (MBBA : PEBAB) binary mixture.

DVI 000274

RESPONSE TIMES

We denote as the rise time the response time for transition to the (optically clear) quasi-nematic state when a field of strength E is applied to a sample in the (light-scattering) domain state. τ_R can be expressed as

$$\tau_R = \eta \left\{ \frac{\Delta\varepsilon}{4\pi} \left(E^2 - E_c^{\ 2}\right) \right\}^{-1} \tag{3}$$

where E_c is given by Eq. (1) and η denotes the twist viscosity. As Eq. (3) indicates, this response time can be made as slow as desired by applying a field just slightly in excess of threshold. Typically, for fields about twice threshold, τ_R is of order tens of milliseconds, although the relevant material constants are amenable to considerable variation, as discussed further below.

The decay time which characterizes the relaxation process is considerably more complex. We must distinguish two cases: (1) the field strength is reduced slowly, or set to a nonzero value in excess of a minimum value required to maintain the helical axis parallel to the substrates (i.e. to prevent the domain structure from relaxing to the quiescent state); (2) the field is suddenly reduced to zero.

For case (1), the relaxation process can be described as the growth of a defect structure[9,15] which fills space to form the (light-scattering) domain texture shown in Figure 16. The time scale for the relaxation under these circumstances depends upon the value to which the field is reduced.

DVI 000275

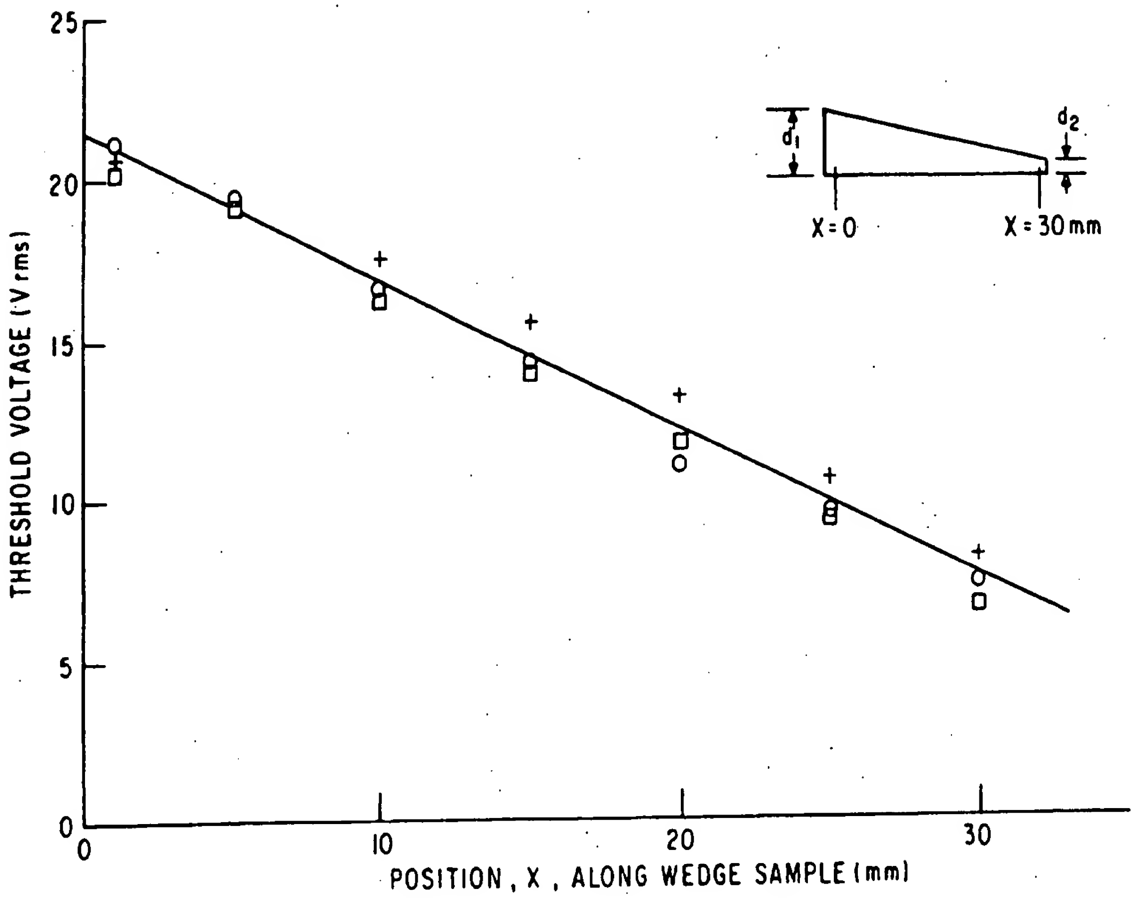

Figure 20

Threshold voltage vs. sample thickness measured in a wedge-shaped sample containing 3% COC.

DVI 000276

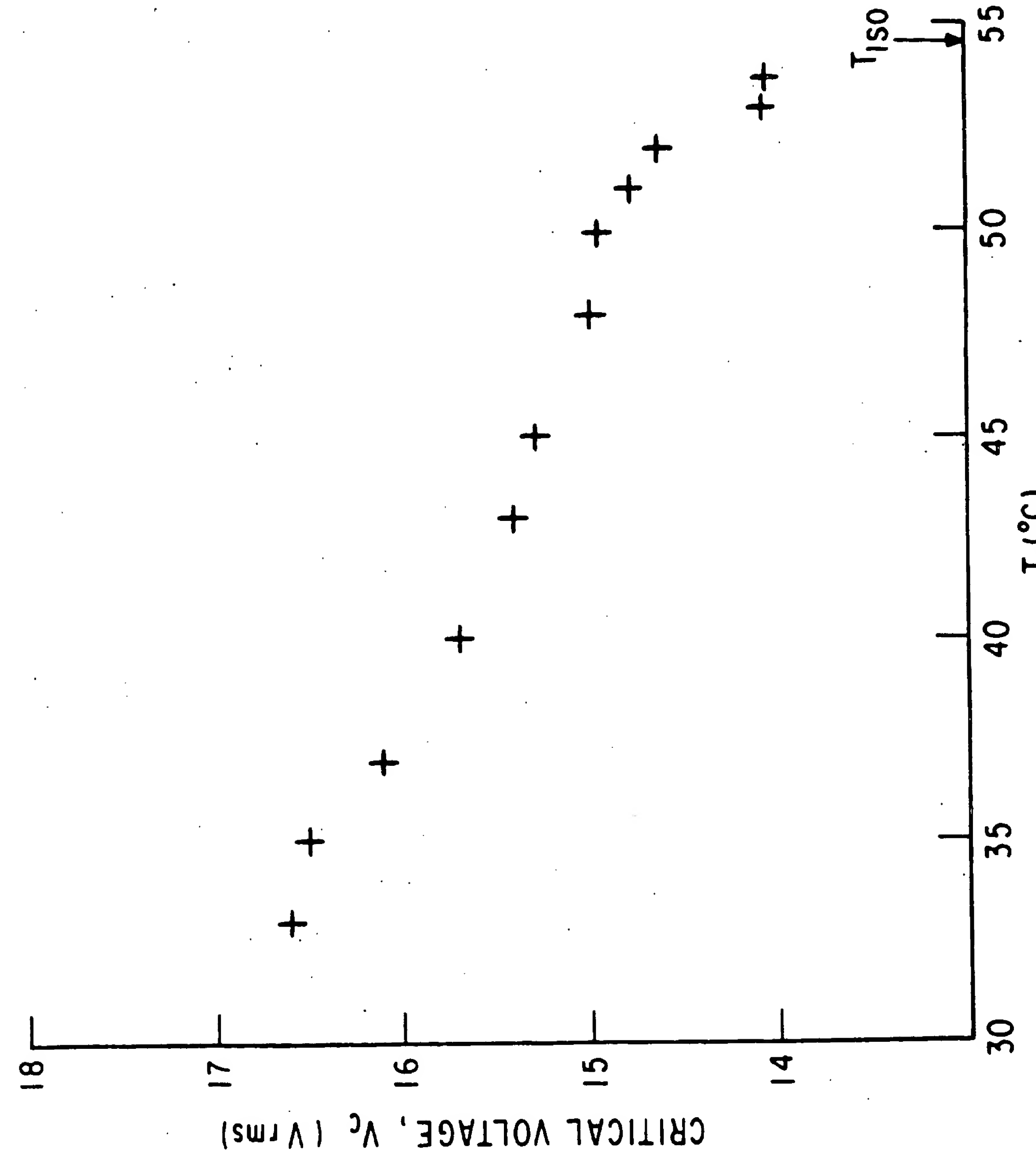

Figure 21

Temperature dependence of the threshold voltage for a sample containing 3% COC.

DVI 000277

For case (2) the dynamics are complicated by the formation of disclinations and complex transient molecular arrangements. Some observations of these transients were reported by Wysocki et al[16,17] and more recently by Ohtsuka and Tsukamoto.[18] These authors noted that a transient optical rotation occurs during relaxation, from which they inferred a Grandjean-planar-like structure, such as the conical deformation described by Meyer.[10] Whereas such a transient state may occur for the case of parallel boundary conditions, it seems less likely for samples with perpendicular (homeotropic) boundaries. We have made time-dependent optical and capacitive measurements, as well as direct microscopic observations, which indicate the dependence of the relaxation sequence on sample boundary conditions. Moreover, the structure observed in the scattering transient even without polarizing optics indicates the importance of birefringent effects rather than optical rotation.

Figure 22 shows representative relaxation transients in the form of the time-dependence of the zero-order-transmission of an unpolarized He-Ne laser beam as observed without polarizing optics for samples with homeotropic (a) and parallel (b) boundaries. Both samples contained 5 parts by weight COC, 80 parts MBBA and 20 parts PEBAB; the quiescent pitch was $p_0 \approx 8.4\ \mu m$ and cell thickness was $d \approx 15\ \mu m$. The same qualitative features - e.g., pronounced delay time (i.e. the lifetime of the aligned state) for homeotropic samples - were observed for both faster and slower samples (i.e. with shorter and longer pitches, respectively) with the following qualification: (1) For $p_0/d > 1$, the decay times increase markedly with decreasing d for fixed p_0; (2) For $p_0/d \ll 1$, the distinctions between homeotropic and parallel samples diminish, and delay times may be observed even for rubbed samples.

DVI 000278

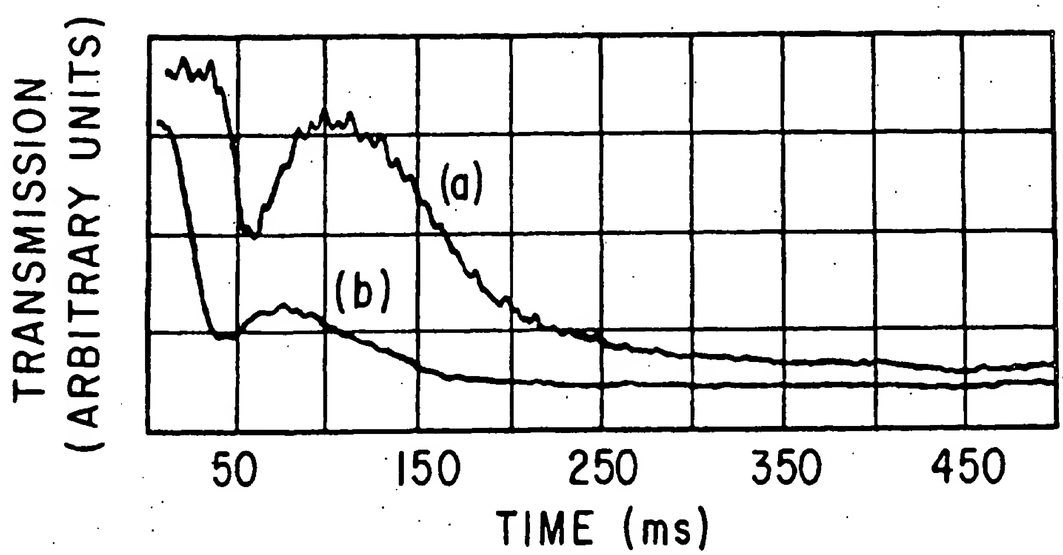

Figure 22

Oscillographs showing light scattering transients for 15μm thick,

(a) homeotropic and (b) parallel samples containing 4.8 percent COC; no polarizing optics were used; λ = 633 nm.

DVI 000279

In order to study the transient capacitance and to make direct microscopic observations during the relaxation we required a slow sample. Figure 23 shows the (unpolarized) optical trace (a) and the capacitance transient (b) for an 18 μm thick, homeotropic sample consisting of 1.25 parts COC, 80 parts MBBA, and 20 parts PEBAB. The capacitance was measured at 1 kHz (well below the relaxation frequency for the parallel component of the dielectric constant) on a laboratory-constructed capacitance meter incorporating a lock-in amplifier. Both traces exhibit a real delay time, the electric field having been completely turned off within 50 μs of t = 0. Whereas the optical trace exhibits two relative extrema, the capacitance decreases monotonically from C_i = 3.20 nf to C_f = 2.44 nf during the transition from the aligned state to the light-scattering domain texture. For this sample, if we neglect the contribution of the small COC content, we may take the parallel and transverse dielectric constants at 1 kHz to be $\varepsilon_p = 13$ and $\varepsilon_t = 6.8$, respectively, as reported for MBBA/PEBAB mixtures in Reference 19. Then, since A/d ≈ 27.8 m, and neglecting small parasitic effects (typically about 40 pf for these cells), $C_i \approx C_p = \varepsilon_p\, \varepsilon_0 A/c$, and $C_f - (\varepsilon_p + \varepsilon_t)\varepsilon_0 A/2d$.

The latter value for C_f corresponds to that expected for the domain texture in which the helical axis is assumed parallel to the substrates: i.e., if the electric field direction is y and we take the director distribution to be $n = (\cos(2\pi\, z/p_0), \sin(2\pi z/p_0), 0)$, then $\varepsilon_f = \langle n_y^2 \rangle \varepsilon_p + \langle n_x^2 \rangle \varepsilon_t = (\varepsilon_p + \varepsilon_t)/2$. Whereas the measured value of C_f is much larger than that expected for a Grandjean planar state ($C_t = \varepsilon_t\, \varepsilon_0 A/d$ = 1.67 nf), it is not inconsistent with a conical deformation for which the maximum tilt angle θ, with respect to the field direction, is 45 degrees, since for that state, $C_f = (\varepsilon_p \cos^2\theta + \varepsilon_t \sin^2\theta)\, \varepsilon_0 A/d$.

DVI 000280

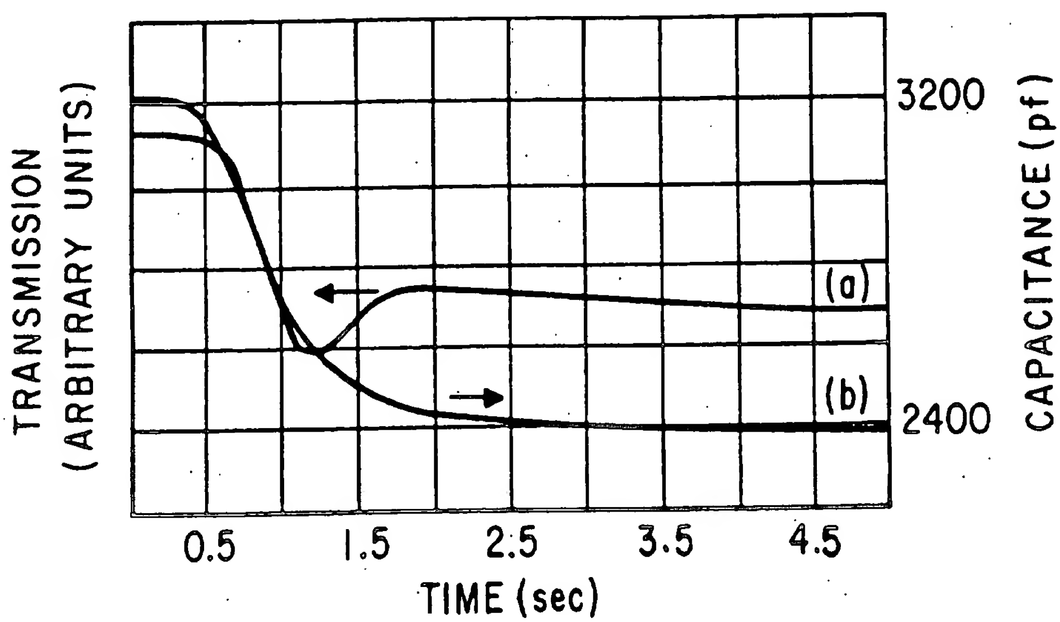

Figure 23

Optical (a) and capacitive (b) transients for a 20μm thick sample containing 1.2 percent COC.

DVI 000281

Cine-microphotography of this sample in polarized light, Figure 24, has shown that the relaxation begins with nucleation about a number of points, often defects pinned to the surfaces (24a). Birefingence about each of these sites results in a transient pattern of closed contour lines (24b); as these regions grow together (24c), the light-scattering is slightly diminished, corresponding to the "hump" in the optical decay curves. Subsequently the strongly light-scattering domain texture forms, possibly as the disclinations formed during relaxation split into λ and τ disclinations form near the surfaces.[9] Eventually, on a longer time scale this array of disclinations "anneals" to a stable, more transmissive quiescent state, in the form of a double spiral structure (Figure 14) which resembles that described by Bouligand.[20] This is in contrast to the case of parallel boundary conditions, for which the ultimate quiescent state is the planar Grandjean one; in both cases, the time scale depends upon the p_0/d ratio.

During the initial part of the decay, corresponding to the appearance of the contour lines (24b), we have measured the relaxation of zero-order-transmission as detected by a small fiber optic probe in the eyepiece of a Zeiss polarizing microscope. Figure 25 shows a trace, taken with parallel polarizers and a 546 nm filter, for the same composition as studied in Figures 23 and 24. The number of peaks corresponds to the maximum number of contour lines observed microscopically. The number N scales with the sample thickness; in fact, we note that $N = 1/2\ \Delta n\ d/\lambda$, where Δn is the optical birefringence (about 0.2) and λ is the wavelength of observation light. These observations suggest that, for the homeotropic

DVI 000282

This page is reproduced at the back of the report by a different reproduction method to provide better detail.

DVI 000283

Figure 24

Prints of microphotographic movie of relaxation sequence for sample of Figure 14; parallel polarizers, 546 nm filter. Approximate times after removal of field:
(a) 0.7 s, (b) 1.1 s, (c) 1.4 s

samples, the transient molecular arrangement resembles the spiral structure shown in Figure 14b, but a light-scattering defect structure is superimposed on it. The initial nucleation occurs about defect sites where the local boundary condition is parallel; for samples with rubbed boundaries, the entire bounding surface may act as a nucleation site.

We may define a decay time to characterize the relaxation process as the elapsed time (following sudden removal of the field) to the light-scattering domain structure. The parametric dependences of this decay time are described by[21]

$$\tau_D = \eta/k_{22}q^2 \tag{4}$$

The temperature dependence of the decay time for a particularly fast sample is shown in Figure 26, where, for definiteness, we have plotted t_h, the elapsed time to the "hump" in the decay curve.

A glance at Equations (1) and (4) indicate the nature of the trade-offs encountered in designing a liquid crystal material with both rapid response and low threshold field. These material considerations are discussed in detail below.

DVI 000284

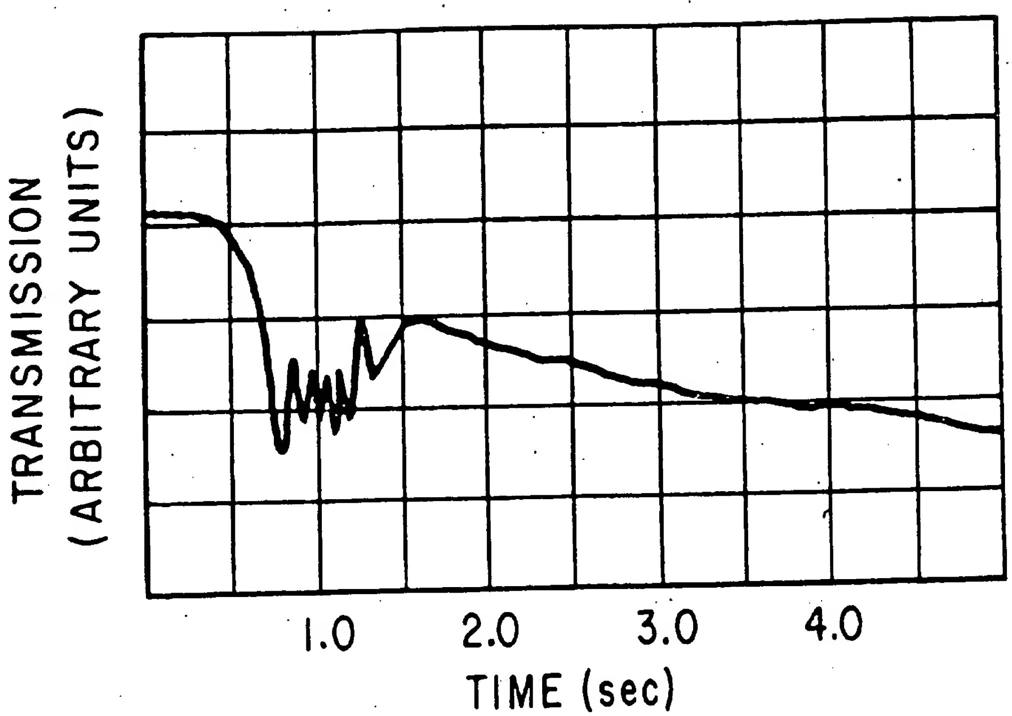

Figure 25

Optical transient, measured with parallel polarizers, 546 nm filter, and fiber optic eyepiece probe, of a 24μm thick sample containing 1.2 percent COC.

DVI 000285

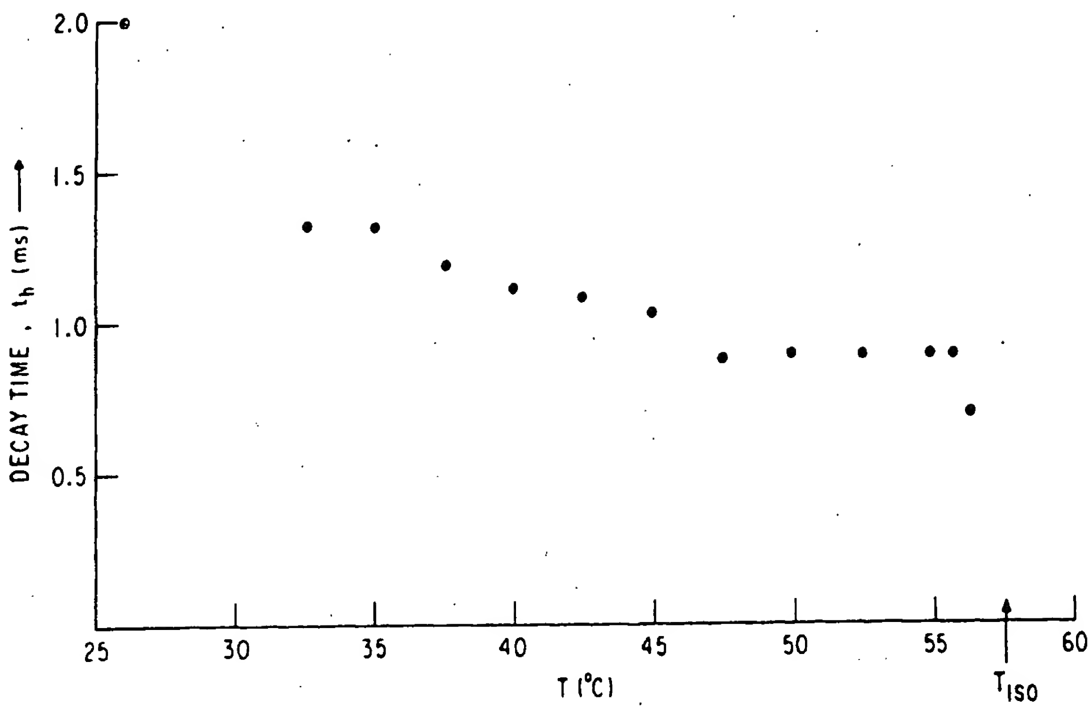

Figure 26

Temperature dependence of the decay time, measured to the "hump" (see Fig. 22a) in the scattering curve.

DVI 000286

II. DEVELOPMENT OF LIQUID CRYSTAL MATERIALS

INTRODUCTION

The purpose of this investigation was to develop a liquid crystal formulation undergoing the field-induced cholesteric-nematic transition for use in an X-Y matrix display. This application dictated the requirements of:

1. Fast relaxation time from the honeotropic nematic orientation (field "on") to the light-scattering focal conic texture (field "off").
2. Reasonably low threshold field to avoid excessively large driving voltages.
3. Room temperature mesophase.

High light transmission was also stipulated because the display is a stack of ten liquid crystal cells.

In terms of material-dependent parameters, low viscosity and small pitch promote fast relaxation time while large values of dielectric anisotropy ($\Delta\varepsilon$) and pitch lower the threshold field. Since low voltage operation and fast response put contradictory demands on the pitch, a compromise between the two had to be reached.

RESULTS

It might appear that the most obvious materials for the cholesteric-nematic transition are pure cholesteric liquid crystals of the cholestrol family. However, the use of such compounds is not practical because they have a small pitch, of the order of a few tenths of a micron, and relatively

DVI 000287

high viscosity. The threshold in layers of practical thickness (10-20 microns) is well over 100V, and the relaxation time is slow. More suitable characteristics can be obtained by diluting a cholesteric liquid crystal with a nematic liquid crystal of positive $\Delta\varepsilon$. A useful conceptual approach is to start with a nematic of positive $\Delta\varepsilon$ and to impart helical ordering by the addition of an optically active compound. The pitch of the resulting mixture is inversely proportional to the concentration of the optically active component.[14] This component may be, but need not be, a cholesterol derivative. It need not even be a liquid, but a liquid crystal is preferable because a nonliquid crystal will produce a mixture of narrower mesophase temperature range.

The technical approach in the present work was to identify a suitable nematic host of positive $\Delta\varepsilon$ and to impart it with chirality of controlled pitch by addition of an optically active compound. There is, of course, interaction between all the components so that the final properties, such as mesophase temperature range and viscosity, depend on the type and concentration of each constituent. At this time, only one pure nematic of positive $\Delta\varepsilon$ and room temperature mesophase is known. This compount,[22] dibutylazoxybenzene, has $\Delta\varepsilon$ of 0.4 and a mesophase range of 14-28^{o}C. Both $\Delta\varepsilon$ and temperature range are so small that this material is not useful for the present application. Compounds of large positive $\Delta\varepsilon$ have a strong polar group, such as CN, at one end of the liquid crystal molecule. Typical representatives and their mesophase ranges are listed in Table III. The dielectric constants parallel and perpendicular to the molecular axis are approximately 20 and 6, respectively, so that $\Delta\varepsilon$ is about 14. The mosophases of all the compounds in Table III are above room temperature, and only compounds No. 2 and 3, are commercially available.

DVI 000288

Table I

Nematic Liquid Crystals with Positive $\Delta\epsilon$

No.	Abbreviation	Chemical Name	Mesophase Temperature Range (°C)	Reference
1	PEthyBAB	N-(p-Ethylbenzylidene)-p-aminobenzonitrile		
2	MEBAB	N-(p-Methoxybenzylidene)-p-aminobenzonitrile	108-119	a)
3	PEBAB	N-(p-Ethoxybenzylidene)-p-aminobenzonitrile	105-127	a)
4	BuBAB	N-(p-Butoxybenzylidene)-p-aminobenzonitrile	60-106	21
5	PentylBAB	N-(p-Pentoxybenzylidene)-p-aminobenzonitrile	56- 85	
6	OctylBAB	N-(p-Octyloxybenzylidene)-p-aminobenzonitrile	75- 90	21
7	HexylBAB	N-(p-Hexyloxybenzylidene)-p-aminobenzonitrile		22
8	CapBAB	N-(p-Caprylo-oxybenzylidene)-p-aminobenzonitrile		22

a) Eastman Organic Chemicals

DVI 000289

Two techniques for preparing room temperature nematics of positive $\Delta\varepsilon$ are available. One of these is to prepare mixtures from two or more nematics which are solids at room temperature. Thus, a mixture of equal parts of compounds 4, 7, and 8 of Table III has a mesophase of 20 to 94°C. The other technique for producing positive nematics consists in adding a solid of positive $\Delta\varepsilon$, such as PEBAB, to a room temperature liquid crystal of negative $\Delta\varepsilon$ such as MBBA. The anisotropy of the mixture is proportional to the concentration of the positive component,[19] and the practical limit of concentration is reached when the mixture becomes solid at room temperature. An undesirable feature is that such mixtures have higher viscosity than the pure room temperature nematic component.

The performance of the formulations was evaluated by determination of threshold voltage and relaxation time. Since the cholesteric-nematic transition is a field effect, the threshold voltage is inversely proportional to sample thickness. Sample thickness ranged between 10 to 20 microns corresponding to spacer thicknesses of nominally 0.0005 and 0.00075 inch. The thickness was a compromise between a desirable small value and anticipated attainable uniformity in large cells of 10 inch diagonal dimension. Threshold voltage was measured at 60 Hz and is reported in Table IV. For comparison of different samples, a threshold is also computed in volts per micron of sample thickness, and the error is estimated at $\pm$ 10% to reflect the uncertainty in thickness.

The relaxation time was obtained from scope traces of the type shown in Fig. 22. Two relaxation times are recorded in Table IV corresponding to elapsed time to the "hump" and "flat" portion of the response curve. The latter value may not be precise but serves as a rough comparison of

TABLE II

Performance of Liquid Crystal Formulations

Formulation	Composition: % By Weight	Composition: Components	Threshold Potential: Vrms	Threshold Potential: Thickness (mils)	Threshold Potential: V/micron	Relaxation Time (millisec): To "hazy"	Relaxation Time (millisec): To "flat"
A	76	MBBA	20	0.75	1.07		180
	19	PEBAB					
	5	Cholesteryl Erucate					
B	73	MBBA	45	0.75	2.4		50
	18	PEBAB					
	9	Cholesteryl Erucate					
C	76	MBBA	33	0.75	1.8		80
	19	PEBAB					
	5	Cholesteryl Nonanoate (ChoNo)					
D	73	MBBA	65	0.75	3.5	10	16
	18	PEBAB					
	9	ChoNo					
E	63	MBBA	80	0.5	6.4	9	15
	20	PEBAB					
	17	Cholesteryl Oleyl Carbonate (COC)					
F	40	MBBA	55	0.5	4.4	9	16
	40	BuBAB					
	20	COC					
G	35	MBBA	70	0.5	5.6	5	10
	35	BuBAB					
	30	COC					
H	36	MBBA	48	0.5	3.8	6	16
	36	BuBAB					
	18	COC					
	10	Dodecane					
I	33	MBBA	70	0.5	5.6	4	7
	33	BuBAB					
	29	COC					
	5	Dodecane					
J	37.5	MBBA	60	0.4	6.0	2.5	4.5
	37.5	BuBAB					
	20	ChoNo					
	5	Dodecane					
K	36	MBBA	100	0.4	10.	1.7	3.5
	36	BuBAB					
	24	ChoNo					
	4	Dodecane					
L	45	MBBA	85	0.7	4.9	2.4	
	30	BuBAB					
	20	ChoNo					
	5	Dodecane					
M	32	BuBAB					50
	32	OctylBAB					
	32	COC					
	4	Dodecane					
N	75	BuBAB					
	25	ChoNo					
O	68	BuBAB					
	23	ChoNo					
	9	Dodecane					
P	65	PEBAB					
	35	ChoNo					
Q	30	BuBAB				2.5	
	30	OctylBAB					
	30	ChoNo					
	10	Xylene					
R	25	PEthylBAB	65	0.5	5.2	6	
	25	BuBAB					
	25	OctylBAB					
	25	ChoNo					
S	23	PEthylBAB	50	0.5	4.0	3	
	23	BuBAB					
	23	OctylBAB					
	23	ChoNo					
	8	Dodecane					
T	20	BuBAB					
	20	OctylBAB					
	20	PEthylBAB					
	25	ChoNo					
	15	Dodecane					
U	23	MBBA	75	0.7	4.3	2.1	3.5
	23	BuBAB					
	23	OctylBAB					
	23	ChoNo					
	8	Dodecane					
V	30	BuBAB					
	30	OctylBAB					
	30	Cholesteryl Propionate					
	10	MBBA					
W	30	BuBAB					50
	30	OctylBAB					
	20	Cholesteryl Propionate					
	10	MBBA					
	10	Dodecane					
X	30	BuBAB	65	0.7	3.7	10	
	30	OctylBAB					
	25	Cholesteryl Geranyl Carbonate					
	14	MBBA					
Y	27	BuBAB				5	
	27	OctylBAB					
	23	Cholesteryl Geranyl Carbonate					
	14	MBBA					
	9	Dodecane					
Z	37.5	MBBA	75	0.7	4.3		20
	37.5	BuBAB					
	25	Cinnamate, (see text)					

performance between formulations. For the samples studied, the half-pitch was smaller than the thickness, and the relaxation time is therfore independent of thickness. All measurements were done at room temperature (about 23^{o}C).

The first positive nematic host studies as a 4:1 mixture of MBBA and PEBAB with $\Delta\varepsilon$ of 6. PEBAB has a high solid-nematic transition temperature of 105^{o}. It tends to elevate the mesophase range of the mixture and cannot be used i- excess of about 25%. Three cholesterol esters were investigated in this host: erucate, nonanoate and oleyl carbonate. The formulations are designated A-E in Table IV. An increase in cholesteryl erucate concentration from about 5 to 10% (samples A and B) decreased the response time but increased the threshold voltage as expected from its effect on shortening the pitch. The same trend is seen for cholesteryl nonanoate (samples C and D). The nonanoate is more effective than the erucate at equal weight-% in shortening the pitch and therefore gives the faster response (compare samples A and C).

BuBAB has a lower solid-nematic transition temperature than PEBAB and can be used in higher concentration with MBBA for a mixture of larger $\Delta\varepsilon$. Several formulations, e.g. F-I, in which the nematic host contained 50% of BuBAB were prepared. Samples E and F have approximately the same cholesteryl oleyl carbonate content but the latter contains a higher concentration of positive nematic (BuBAB in place of PEBAB). Although both have approximately the same response time, sample F with presumably larger $\Delta\varepsilon$ has the smaller voltage threshold. The cholesterol ester content was increased from 20% in sample F to 30% in sample G. Response time became faster but the threshold increased.

DVI 000292

In a Company-sponsored program on liquid crystal materials development it was discovered that relaxation time can be shortened by lowering the viscosity with a compatible nonmesomorphic diluent such as the aliphatic hydrocarbon dodecane. Samples H and I were similar to F and G, respectively, except that a small percentage of dodecane was added. This resulted in decreased relaxation time. Cholesteryl oleyl carbonate was replaced by the nonanoate in samples J and K and this resulted in even faster response time. However the threshold voltage increased substantially in sample K. Sample J was tested for stability under voltage, and crystals of apparently BuBAB appeared after 20 hours, indicating lack of compatibility at the concentrations used. This sample is probably a supercooled mesomorph at room temperature and tends to crystallize in time. The formulation was modified by decreasing the BuBAB concentration to give sample L.

Sample M was the result of an attempt to prepare an all-positive nematic host. The formulation had a mesophase of about 20-80^{o} but had high viscosity, and the relaxation time was slow.

Other compositions with all-positive nematic hosts were formulations N-Q. Sample N had a mesophase of 55-97^{o}, sample O with mesophase of 55-70^{o} showed segregation of components after standing from some time, sample P had a mesophase of 90-105^{o} and sample Q crystallized at room temperature after standing.

An all-positive mixture of equal parts of p-ethylbenzylidene-p-aminobenzonitrile, BuBAB and OctylBAB had a mesophase of 0-80^{o}. A

DVI 000293

chiral-nematic made from this mixture with cholesteryl nonanoate (sample R) had fast response time which would be further improved by addition of 10% of dodecane (sample S). A further increase in dodecane concentration (sample T) caused segregation of components.

It appeared that formulations made with MBBA might be the best candidates because the room temperature liquid crystal has a beneficial effect on lowering the viscosity and improving compatibility. Sample U seemed to offer the best compromise between fast response and threshold field.

It was hypothesized that cholesteryl propionate, owing to its shorter ester chain, might contribute less to the viscosity than cholesteryl nonanoate, but it turned out that sample V was solid at room temperature and sample W had slow relaxation time. A lower melting chosteric liquid crystal, cholesteryl geranyl carbonate, was also tested (samples X and Y) but no dramatic improvements was noted.

In all the preceding formulations, the chirality producing constituent was an opitcally active cholesteryl ester. To test whether an optically-active liquid crystal unrelated to cholesterol might furnish materials of better response time, the compound amyl p-(4-cyanobenzy-lideneamino) cinnamate, mesophase 90-109^{o}, was synthesized. A mixture of 40% of this compound with 60% of PEBAB had a mesophase of 80-115^{o}, and a mixture of the same proportion with BuBAB had a range of 45-98^{o}. Sample Z, which also contained MBBA, was mesomorphic at room temperature but was relatively slow.

DVI 000294

Many of the samples containing BuBAB which had been recrystallized once of twice tended toward dielectric breakdown. The cholesteric-nematic transition is a field effect and does not require ionic conductivity as for dynamic scattering. Materials used for this transition may therefore have the highest possible resistivity. This is, in fact, desirable as it would make electro-chemical decomposition less likely. To increase the resistivity and prevent dielectric breakdown, BuBAB was more highly purified by multiple recrystallizations and sublimation. Further, the purfied grade of MBBA supplied by Eastman Organic Chemicals was employed after this problem had been encountered.

Formulation U is the best material so far available and will probably be used in the cells for the display. The resistivity of this formulation can probably be improved by purification of all its constituents. While the long-term stability of this formulation is not known, it is likely to be very good as judged by the results obtained on a similar formulation. Sample L, which has the same components but lacks OctylBAB, had been kept continuously at 110V-60Hz for more than three months without apparent degradation or change in conductivity. OctylBAB, the additional ingredient in formulation U, should be no less stable than the chemically related BuBAB of formulation L.

Synthesis of N(p-Alkoxybenzylidene)-p-aminobenzonitriles

These Schiff bases were prepared from equimolar quantities of p-aminobenzonitrile and the appropriate p-alkoxybenzaldehyde. The mixture of starting materials was warmed to 80°C for 15 minutes and cooled, and the product was recrystallized from absolute ethanol. The product was then purified by multiple recrystallizations until melting point and clearing point transitions were reproducible. The products were then vacuum sublimed to raise the resistivity of the formulations.

APPENDIX C

Circuit Board Schematics

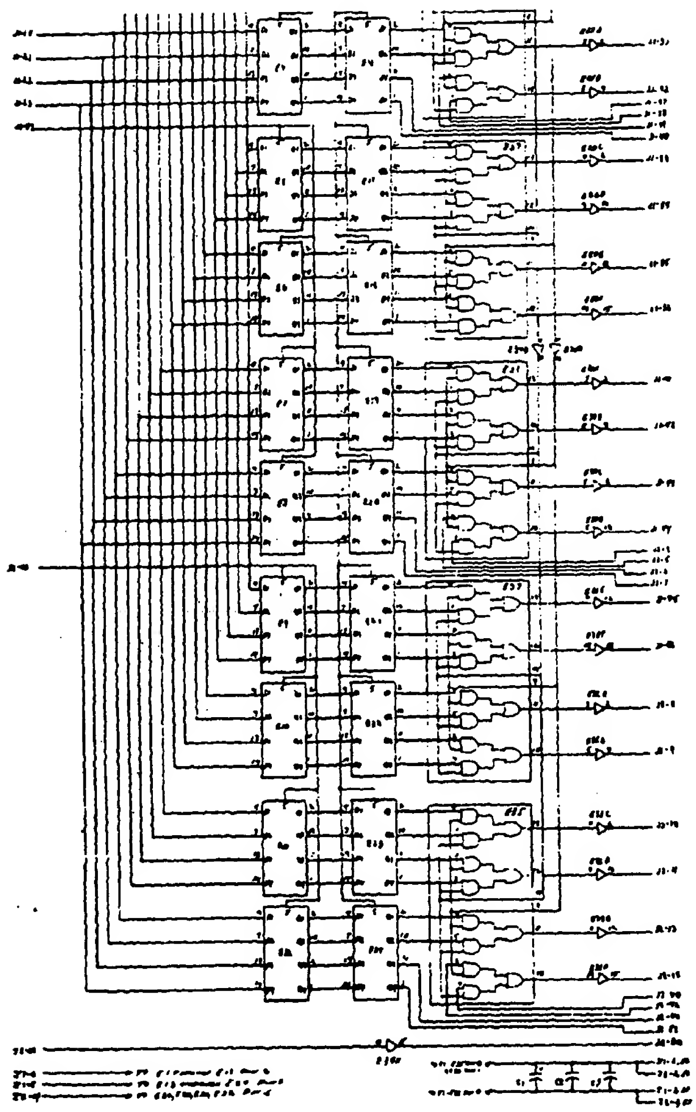

Figure 27 Logic Latch Board Schematic

DVI 000297

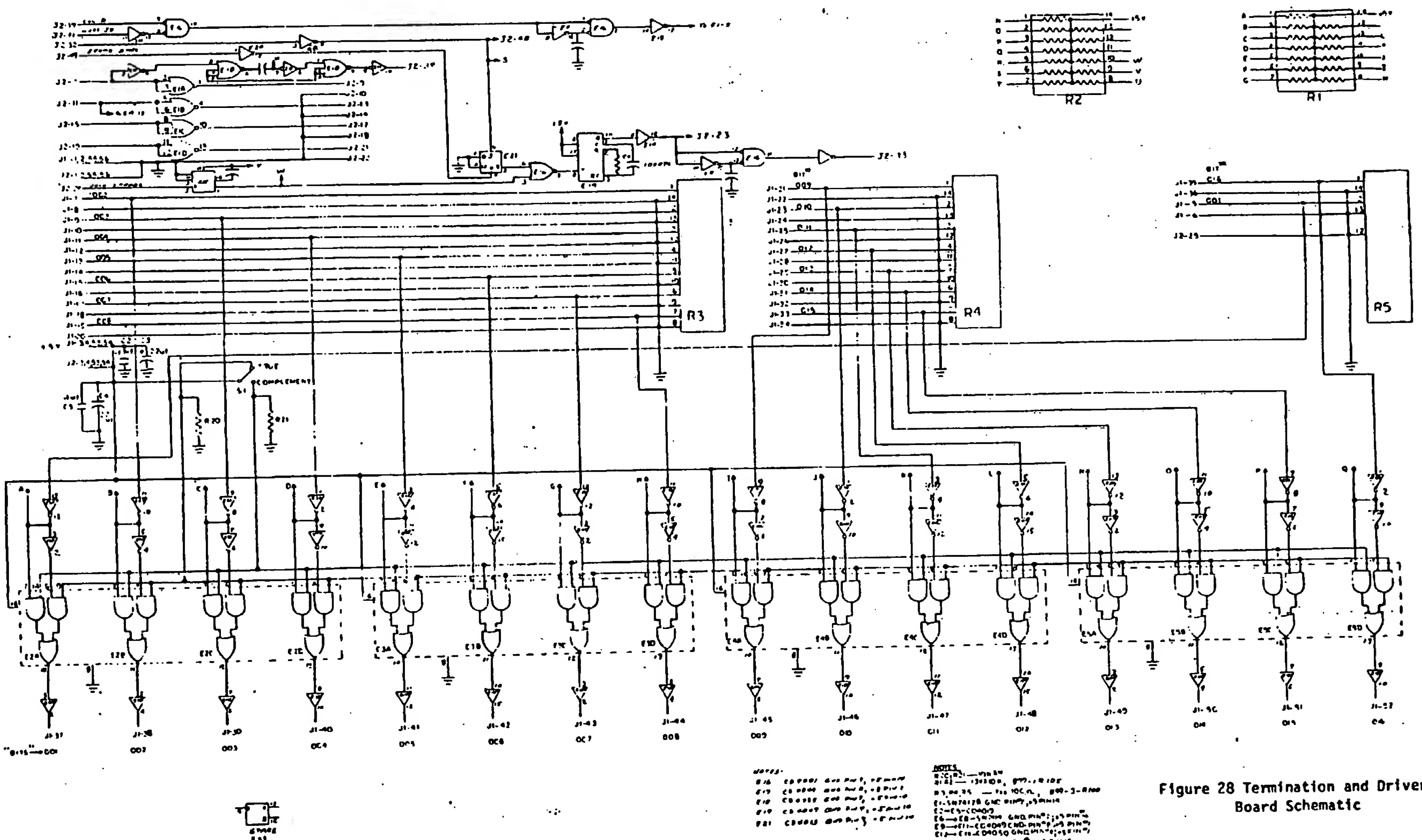

Figure 28 Termination and Driver Board Schematic

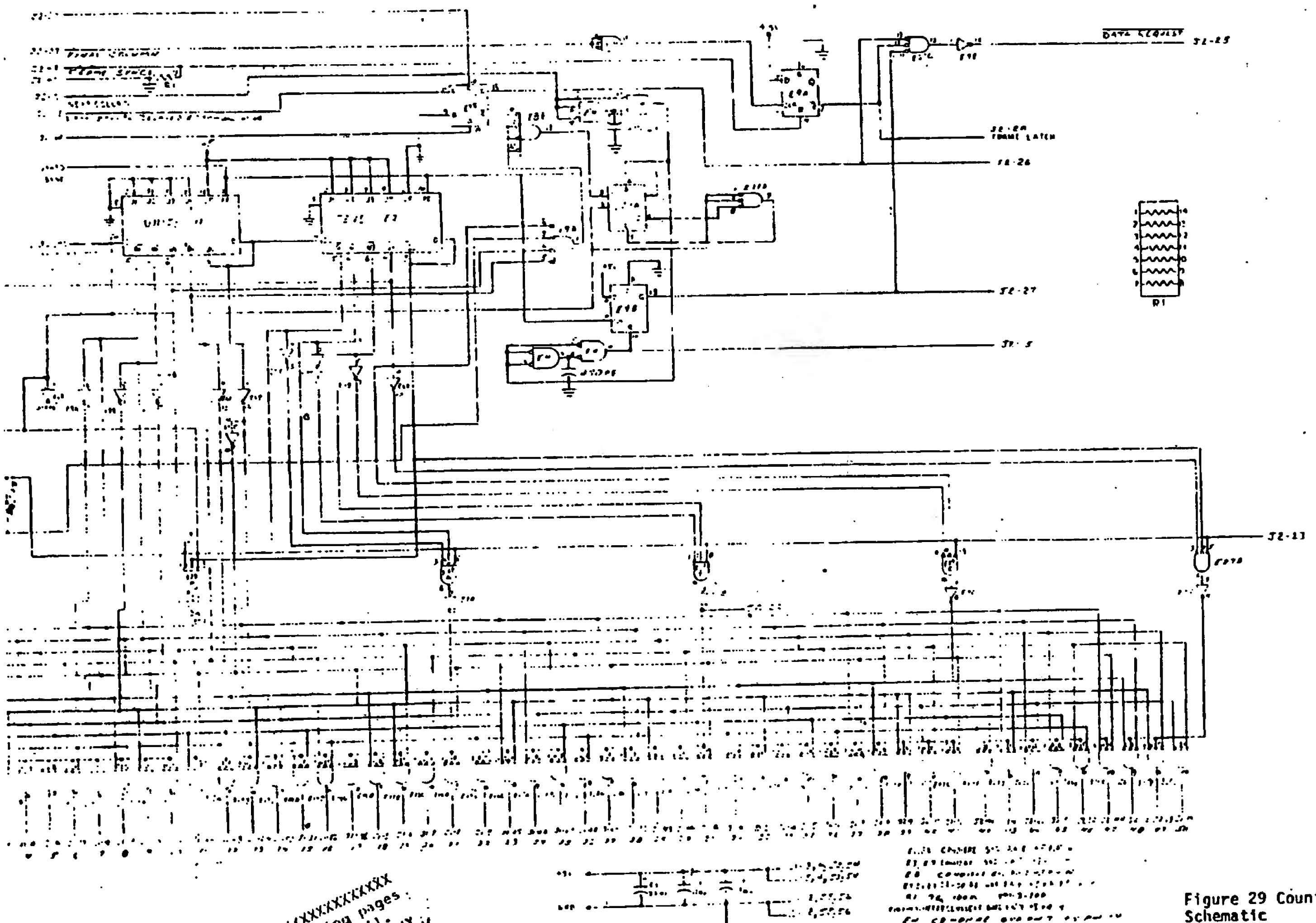

Figure 29 Counter Board Schematic

XXXXXXXXXXXXXXXXXXXXXX
See the following pages
for greater detail.
XXXXXXXXXXXXXXXXXXXXXX

A P P E N D I X   D

CIRCUIT BOARD

WIRE LISTS

DVI 000300

001	1A2/1A3/CA1
002	1A4/1A5/CB1
003	1A6/1A9/1A1/CC1
004	1A8/1A11
005	1A10/1B1
006	1B9/1H1/1H2/1H4/1H5/1E12/1F2
007	1B6/1C1/1E13/1G13
008	1C4/1J23/1K23/CX10
009	1C11/1E1/1J22/1K22/CX12
010	1C9/1E2/1J21/1K21/CX14
011	1C6/1E4/1J20/1K20/CX16
012	1B11/1E10/1F1
013	1G12/1F4
014	1F3/1F5
015	1F6/1G5/1H10/1H9
016	1G6/1H12/1H13
017	1E6/1C2/1D3
018	1D14/1G3/1K18/1K19
019	1G4/1E5/1J18/1J19/CX18
020	1E8/1G1
021	CX2/1A7/CA2/CB2/CC2/1B7/1B2/1C7/1D5/1E7/1F6/1G7/1H7/1J12/1K12
022	CX1/1A14/1B14/1C14/1D5/1D4/1D16/1E14/1F14/1G14/1H14/1J24/1K24
023	1H3/CX4
024	1H6/CX6
025	1G2/CX8
026	1H11/CX20
027	1H8/CX22
028	1J1/CX24
029	1J2/CX23
030	1J3/CX26
031	1J4/CX25
032	1J5/CX28
033	1J6/CX27
034	1J7/CX30
035	1J8/CX29
036	1J9/CX32
037	1J10/CX31
038	1J11/CX34
039	1J13/CX33
040	1J14/CX36
041	1J15/CX35
042	1J16/CX38
043	1J17/CX37
044	1K1/CX40
045	1K2/CX39
046	1K3/CX42
047	1K4/CX41
048	1K5/CX44
049	1K6/CX43
050	1K7/CX46
051	1K8/CX45
052	1K9/CX48
053	1K10/CX47
054	1K11/CX50
055	1K13/CX49
056	1K14/CX52
057	1K15/CX51

DVI 000301

TABLE III ADDRESS BOARD WIRELIST

001	CX9/RD2/2A1/2A5/2A8/2A12/2B1/2B5/2B8/2B12/2C1/2C5/2C8/
002	2C12/2D1/2D5/2D8/2D12/2E1/2E5/2E8/2F12
003	1A10/1A16/1A14/1B2
004	CX10/RC2
005	2F2/RC1
006	2G2/RD1
007	2F5/1A2
008	2G5/1A1
009	1A15/1A13/TA2
010	TA1/1A6/1A7/1B1/RA2
011	1B16/1D2/1A9/RB2
012	1A8/1B2/TB1
013	TD3/TC2
014	1B9/1B15/1B11/1B5/CX7
015	TC3/1B8
016	1B6/1C4/TE1/TG1
017	TG3/TE2
018	TE3/1C14
019	TG2/1C5/TJ1
020	1B12/1C16/TF1/TH1
021	TH3/TF2
022	TF3/1C2
023	TH2/TJ2/1C10/1B7/1C6
024	1B10/1A11
025	TA3/1A5
026	TH3/1B13
027	1B4/1B14
028	CX11/2A2
029	CX12/2A6
030	CX13/2A9
031	CX14/2A13
032	CX15/2B2
033	CX16/2B6
034	CX17/2B9
035	CX18/2B13
036	CX19/2C2
037	CX20/2C6
038	CX21/2C9
039	CX22/2C13
040	CX23/2D2
041	CX24/2D6
042	CX25/2D9
043	CX26/2D13
044	CX27/2F2
045	CX28/2F6
046	CX29/2F9
047	CX30/2F13
048	1D8/TL2/1D10/TM1
049	2A3/1D6
050	TL3/1D3/CX33
051	1D9/1D5/TM2
052	TM3/1D4
053	1E8/TN2/1E10/TP1
054	2A4/1F6
055	TN3/1F3/CX34
056	1F9/1E5/TP2
057	TP3/1F4
058	1F8/TQ2/1F10/TR1
059	2A10/1F6
060	TQ3/1F3/CX35

TABLE IV DATA BOARD WIRELIST

061	1F9/1F5/TR2
062	TR3/1F4
063	1G8/TS2/1G10/TT1
064	2A11/1G6
065	TS3/1G3/CX36
066	1G9/1G5/TT2
067	TT3/1G4
068	1H8/TU2/1H10/TV1
069	2B3/1H6
070	TU3/1H3/CX37
071	1H9/1H5/TV2
072	TV3/1H4
073	1J8/TW2/1J10/TX1
074	2B4/1J6
075	TW3/1J3/CX38
076	1J9/1J5/TX2
077	TX3/1J4
078	1K8/TY2/1K10/TZ1
079	2B10/1K6
080	TY3/1K3/CX39
081	1K9/1K5/TZ2
082	TZ3/1K4
083	1L8/QA2/1L10/QB1
084	2B11/1L6
085	QA3/1L3/CX40
086	1L9/1L5/QB2
087	QB3/1L4
088	1M8/QC2/1M10/QD1
089	2C3/1M6
090	QC3/1M3/CX41
091	1M9/1M5/QD2
092	QD3/1M4
093	1N8/QE2/1N10/QF1
094	2C4/1N6
095	QE3/1N3/CX42
096	1N9/1N5/QF2
097	QF3/1N4
098	3D8/QL2/3D10/QM1
099	2C10/3D6
100	QL3/3D3/CX43
101	3D9/3D5/QM2
102	QM3/3D4
103	3E8/QN2/3E10/QP1
104	2C11/3E6
105	QN3/3E3/CX44
106	3E9/3E5/QP2
107	QP3/3E4
108	3F8/QQ2/3F10/QR1
109	2D3/3F6
110	QQ3/3F3/CX45
111	3F9/3F5/QR2
112	QR3/3F4
113	3G8/QS2/3G10/QT1
114	2D4/3G6
115	QS3/3G3/CX46
116	3G9/3G5/QT2
117	QT3/3G4
118	3H8/QU2/3H10/QV1
119	2D10/3H6
120	QU3/3H3/CX47
121	3H9/3H5/QV2

TABLE IV (CONTINUED)

122 QV3/3H4
123 3J8/QW2/3J10/QX1
124 2D11/3J6
125 QW3/3J3/CX48
126 3J9/3J5/QX2
127 QX3/3J4
128 3K8/QY2/3K10/QZ1
129 2E3/3K6
130 QY3/3K3/CX49
131 3K9/3K5/QZ2
132 QZ3/3K4
133 3L8/VA2/3L10/VB1
134 2E4/3L6
135 VA3/3L3/CX50
136 3L9/3L5/VB2
137 VB3/3L4
138 3M8/VC2/3M10/VD1
139 2E10/3M6
140 VC3/3M3/CX51
141 3M9/3M5/VD2
142 VD3/3M4
143 3N8/VE2/3N10/VF1
144 2E11/3N6
145 VE3/3N3/CX52
146 3N9/3N5/VF2
147 VF3/3N4
148 CX4/RA1/RB1/TB1/TC1/1C13/1C12/1C11
149 CX6/TL1/1D1/TN1/1E1/TQ1/1F1/TS1/1G1/TU1/1H1/
149 QL1/3D1/QN1/3E1/QQ1/3F1/QS1/3G1/QU1/3H1/
149 TW1/1J1/TY1/1K1/QA1/1L1/QC1/1M1/QE1/1N1/
149 QW1/3J1/QY1/3K1/VA1/3L1/VC1/3M1/VE1/3N1
150 CX5/1C3/1C15/1J3
151 CX2/1A3/1A4/1D2/1E2/1F2/1G2/1H2/1J2/1K2/1L2/1M2/1N2/2A14/2B14/2C14/
151 3D2/3E2/3F2/3G2/3H2/3J2/3K2/3L2/3M2/3N2/2D14/2E14
152 CX3/1A12/1B3/1C1/1C7/2F4/2G4
153 CX1/2A7/2B7/2C7/2D7/2E7/1D7/1E7/1F7/1G7/1H7/1J7/1K7/1L7/1M7/1N7/
153 3D7/3E7/3F7/3G7/3H7/3J7/3K7/3L7/3M7/3N7

TABLE IV (CONTINUED)

1	01F4 1JB4 05F4 08E4
2	01F7 1JA5 05F7 08E7
3	01F13 1JA5 08E13 08E13
4	01F14 1JA6 08E14 08E14
5	02F4 1JB6 06F4 10E4
6	02F7 1JA7 06F7 10E7
7	02F13 1JA7 08E13 10E13
8	02F14 1JA8 08E14 10E14
9	03F4 1JB8 07F4 11E4
10	03F7 1JA9 07F7 11E7
11	03F13 1JA9 07E13 11E13
12	03F14 1JA10 07E14 11E14
13	04F4 1JB10 08E4 12E4
14	04F7 1JA11 08E7 12E7
15	04F13 1JA11 08F13 12F13
16	04F14 1JA12 08F14 12F14
17	05F5 1JB26 08E5 08F5 07E5
18	05F5 21B8 10F5 11E5 12F5
19	26F2 1JA13
20	26F4 1JB13
21	26F6 1JA14
22	26F10 1JA14
23	26F12 1JA15
24	26F15 1JA15
25	28F2 1JA16
26	28F4 1JB16
27	28F6 1JA17
28	28F10 1JA17
29	28F12 1JA18
30	28F15 1JA18
31	30F2 1JA21
32	30F4 1JB21
33	30F6 1JA22
34	30F10 1JA22
35	30F12 1JA23
36	30F15 1JA23
37	32F2 21B4
38	32F4 21B5
39	32F6 21B5
40	32F10 2JA6
41	32F12 2JA6
42	32F15 2JA7
43	27F7 1JA19
44	27F6 1JB19
45	18F11 1JA20
46	18F1 1JB20
47	31F7 21B2
48	31F6 21B3
49	20F11 2JA3
50	20F1 21B4
51	35F7 21B20
52	35F6 21B21
53	24F11 2JA25
54	24F1 21B26
55	01F5 1JA4 02F5 03E5 04F5
56	34F3 21B13
57	34F5 21B14
58	34F7 21B14
59	34F14 2JA15
60	34F15 2JA15
61	01F2 13E4
62	01F10 13F7
63	01F11 13F13
64	01F1 13E14
65	02F2 14E4
66	02F10 14F7
67	02F11 14F13
68	02F1 14E14
69	03F2 15E4
70	03F10 15F7
71	03F11 15F13
72	03F1 15E14
73	04F2 16E4
74	04F10 16F7
75	04F11 16F13
76	04F1 16E14
77	05F2 17E4
78	05F10 17F7
79	05F11 17F13
80	05F1 17E14
81	06F2 18E4
82	06F10 18F7
83	06F11 18F13
84	06F1 18E14
85	07F2 19E4
86	07F10 19F7
87	07F11 19F13
88	07F1 19E14
89	08E2 20E4
90	08F10 20F7
91	08F11 20E13
92	08F1 20E14
93	09F2 21E4
94	09E10 21E7
95	09E11 21E13
96	09F1 21E14
97	10E2 22E4
98	10E10 22E7
99	10E11 22E13
100	10E1 22E14
101	11E2 23E4
102	11E10 23E7
103	11F11 23F13
104	11F1 23F14
105	12F2 24E4
106	12F10 24F7
107	12F11 24F13
108	12F1 24E14
109	13F2 25E15
110	13F10 25F1
111	13F11 25F2
112	13F1 25E3
113	14F2 25E4
114	14F10 25F5
115	14F11 25F6
116	14F1 25E7
117	15F2 27E15
118	15F10 27F1
119	15F11 27F2
120	15F1 27E3
121	16F2 27E4
122	16F10 27F5
123	17F2 29E15
124	17F10 29F1
125	17F11 29F2
126	17F1 29E3
127	18F2 29E4
128	18F10 29F5
129	18F11 29F6
130	18F1 29E7
131	19F2 31E15
132	19F10 31F1
133	19F11 31F2
134	19F1 31E3
135	20F2 31E4
136	20F10 31F5
137	21F2 33E15
138	21F10 33F1
139	21F11 33F2
140	21F1 33E3
141	22F2 33E4
142	22F10 33F5.
143	22F11 33F6
144	22F1 33E7
145	23F2 35E15
146	23F10 35F1
147	23F11 35F2
148	23F1 35E3
149	24F2 35E4
150	24F10 35F5
151	25F13 26F3
152	25F12 26F5
153	25F11 26F7
154	25F10 26F9
155	27F13 26F11
156	27F12 26F14
157	27F11 28F3
158	27F10 28F5
159	29F13 28F7
160	29F12 28F9
161	29F11 28F11
162	29F10 28F14
163	31F13 30F3
164	31F12 30F5
165	31F11 30F7
166	31F10 30F9
167.	33F13 30F11
168	33F12 30F14
169	33F11 32F3
170	33F10 32F5
171	35F13 32F7
172	35F12 32F9
173	35F11 32F11
174	35F10 32F14
175	34F2 25E9 27F9 29E9 34F11
176	34F4 25E14 27E14 29E14 34E9
177	34F12 31F9 33E9 35F9
178	34F10 31F14 33F14 35F14
179	34F6 13E5 14F5 15E5 16F5 17E5 18F5 19E5 20E5 21E5 22E5 23E5 24E5
180	01F6 02E6 03F6 04E6 05F6 06E6 07E6 08E6 09E6 10E6 11E6 12E6 1JA3
181	13F6 14E6 15F6 16E6 17F6 18E6 19F6 20E6 21E6 22E6 23E6 24E6 1JA3
182	26F1 28E1 30F1 32E1 2JA7
183	1JA1 25E6 2G1 13F6 1G1 01E6
184	26F6 2G2 14E6 1G2 02F6
185	27F6 2G3 15E6 1G3 03F6
186	28F6 2G4 16E6 1G4 04F6
187	29F6 2G5 17E6 1G5 05F6
188	3CH 1JA26 30F6 2G6 18E6 1G6 06F6
189	31F6 2G7 19E6 1G7 07F6
190	2CH 2JA1 32E6 2G8 20F6 1G8 08E6
191	33F6 2G9 21E6 1G9 09F6
192	34F6 2G10 22F6 1G10 10F6
193	35F6 2G11 23F6 1G11 11F6
194	2JA26 1CH 2G12 24E6 1G12 12E6
195	1JA1 25E16 2P1 13E16 1P1 01E16
196	26F16 2P2 14F16 1P2 02F16
197	27F16 2P3 15F16 1P3 03F16
198	28F16 2P4 16F16 1P4 04E16
199	3CP 1JA20 29F16 2P5 17F16 1P5 05F16
200	30F16 2P6 18F16 1P6 06F16
201	2CP 2JA1 31E16 2P7 19E16 1P7 07E16
202	32E16 2P8 20F16 1P8 08F16
203	33F16 2P9 21F16 1P9 09E16
204	34E1 34E16 2P10 22F16 1P10 10E16
205	35F16 2P11 23E16 1P11 11F16
206	2JA26 1CP 2P12 24E16 1P12 12E16

TABLE V LOGIC LATCH BOARD WIRELIST

APPENDIX E

BOARD LAYOUTS

DVI 000306

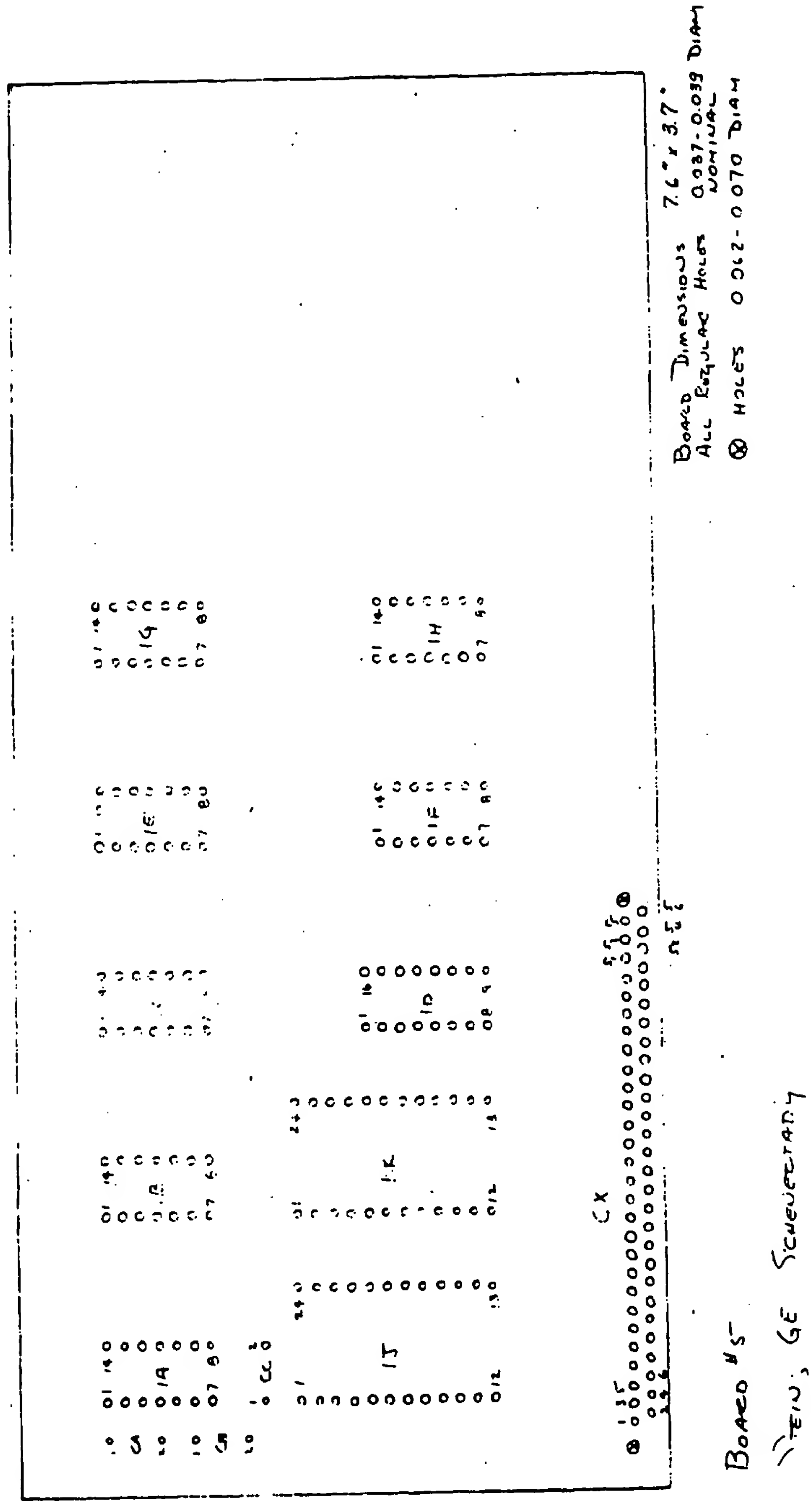

Figure 30 Address Board Layout

DVI 000307

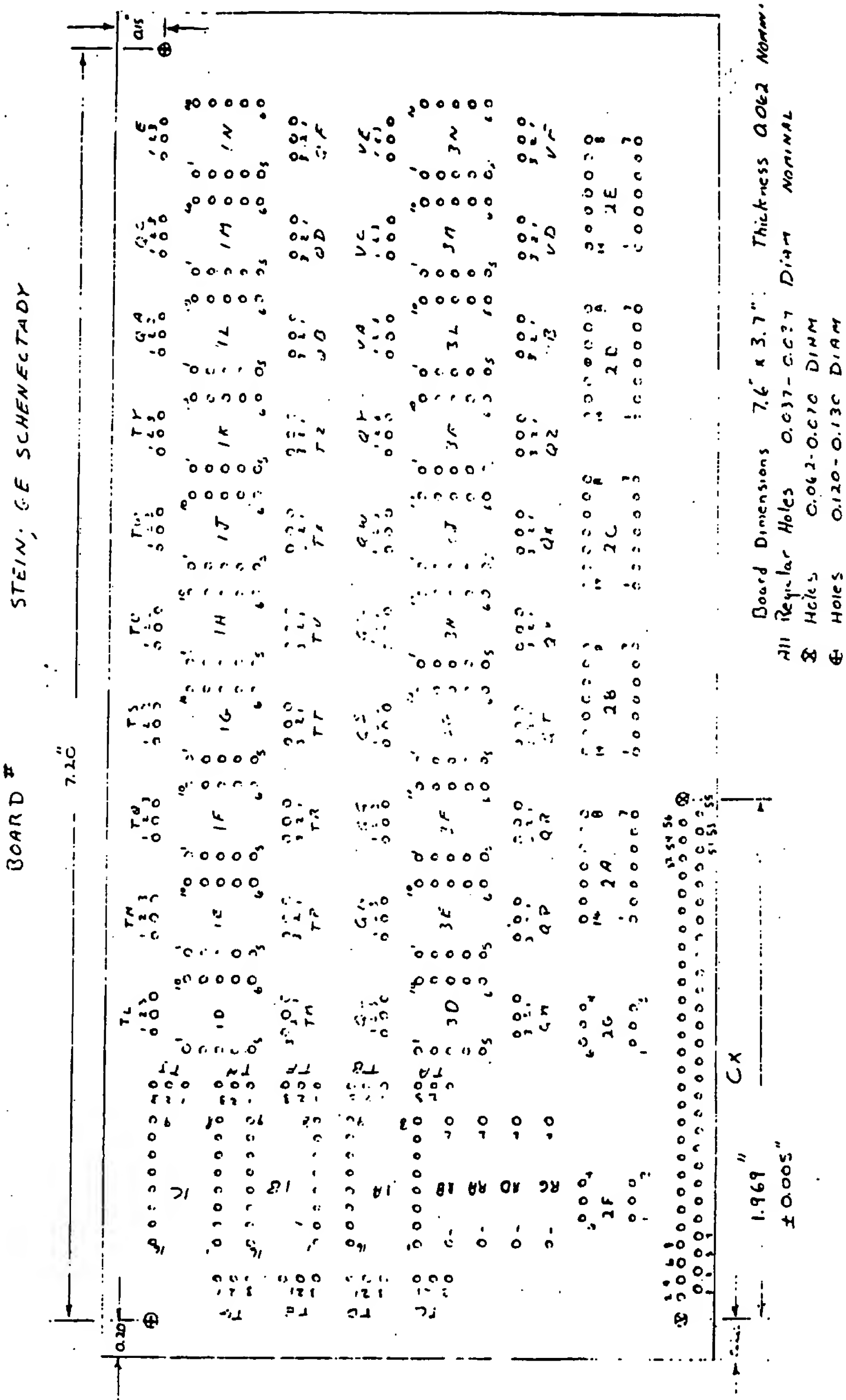

Figure 31 Data Board Layout

DVI 000308

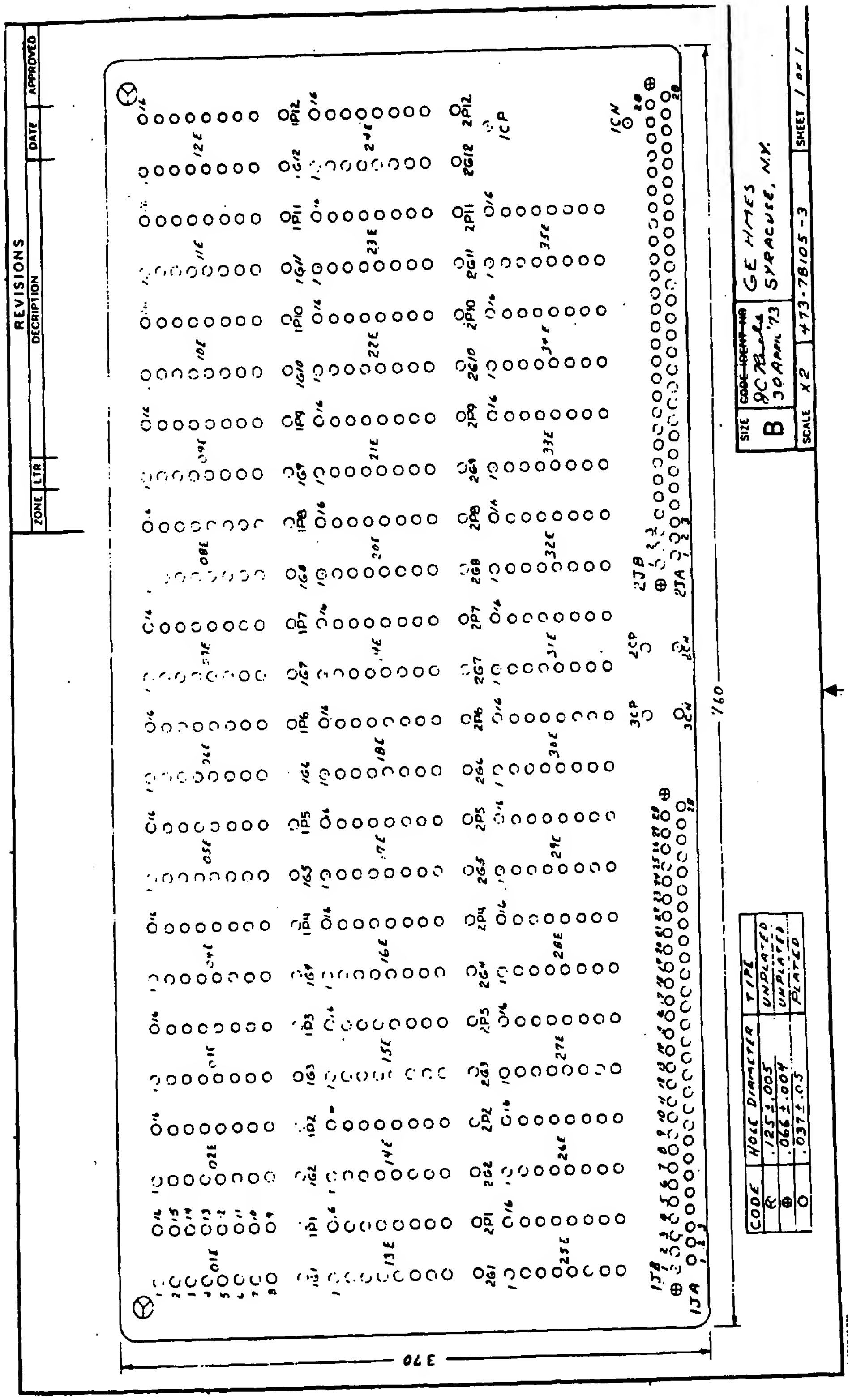

Figure 32 Logic Latch Layout

DVI 000309

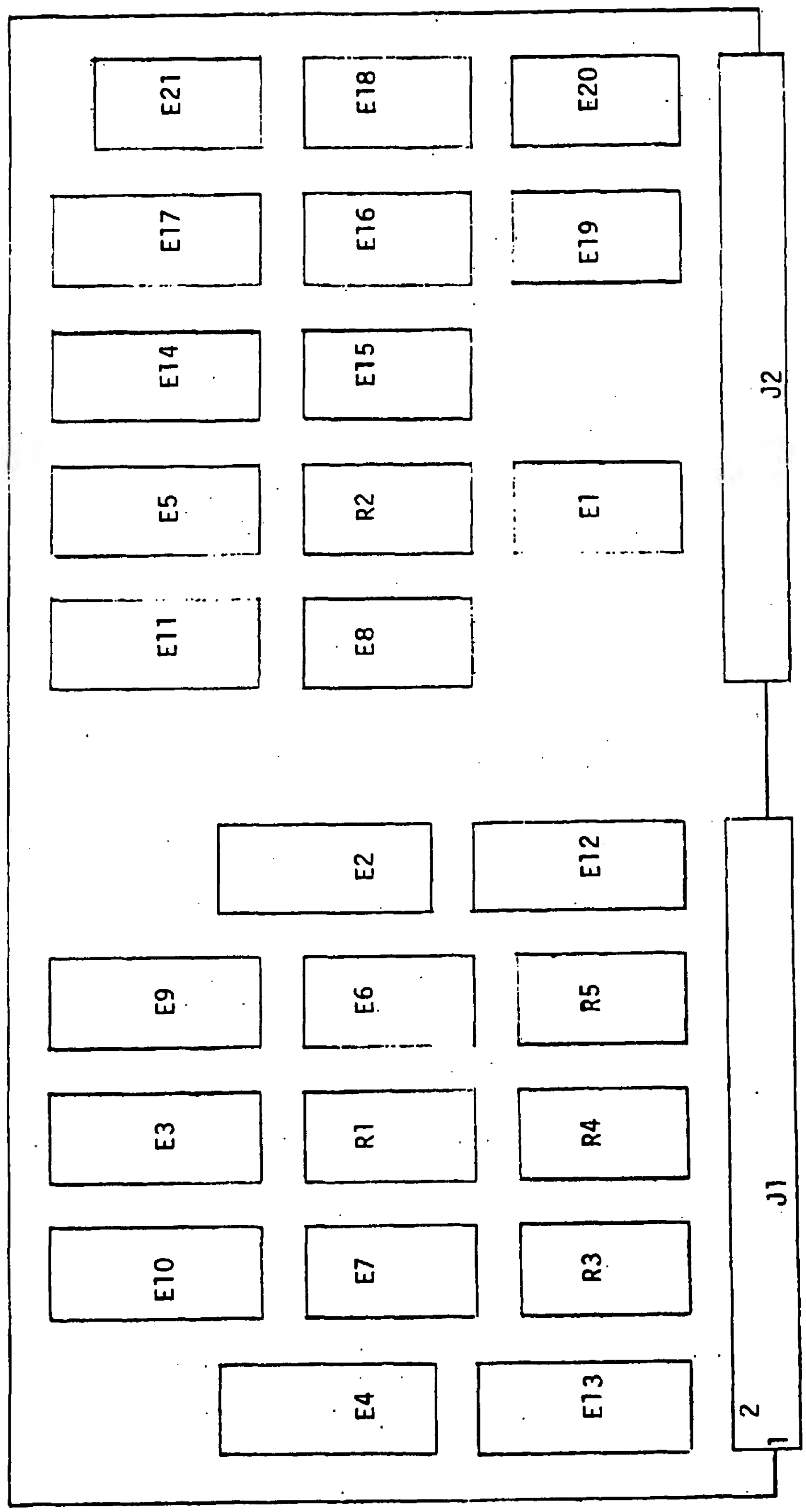

FIGURE 33 TERMINATION AND DRIVER BOARD LAYOUT
(TOP VIEW)

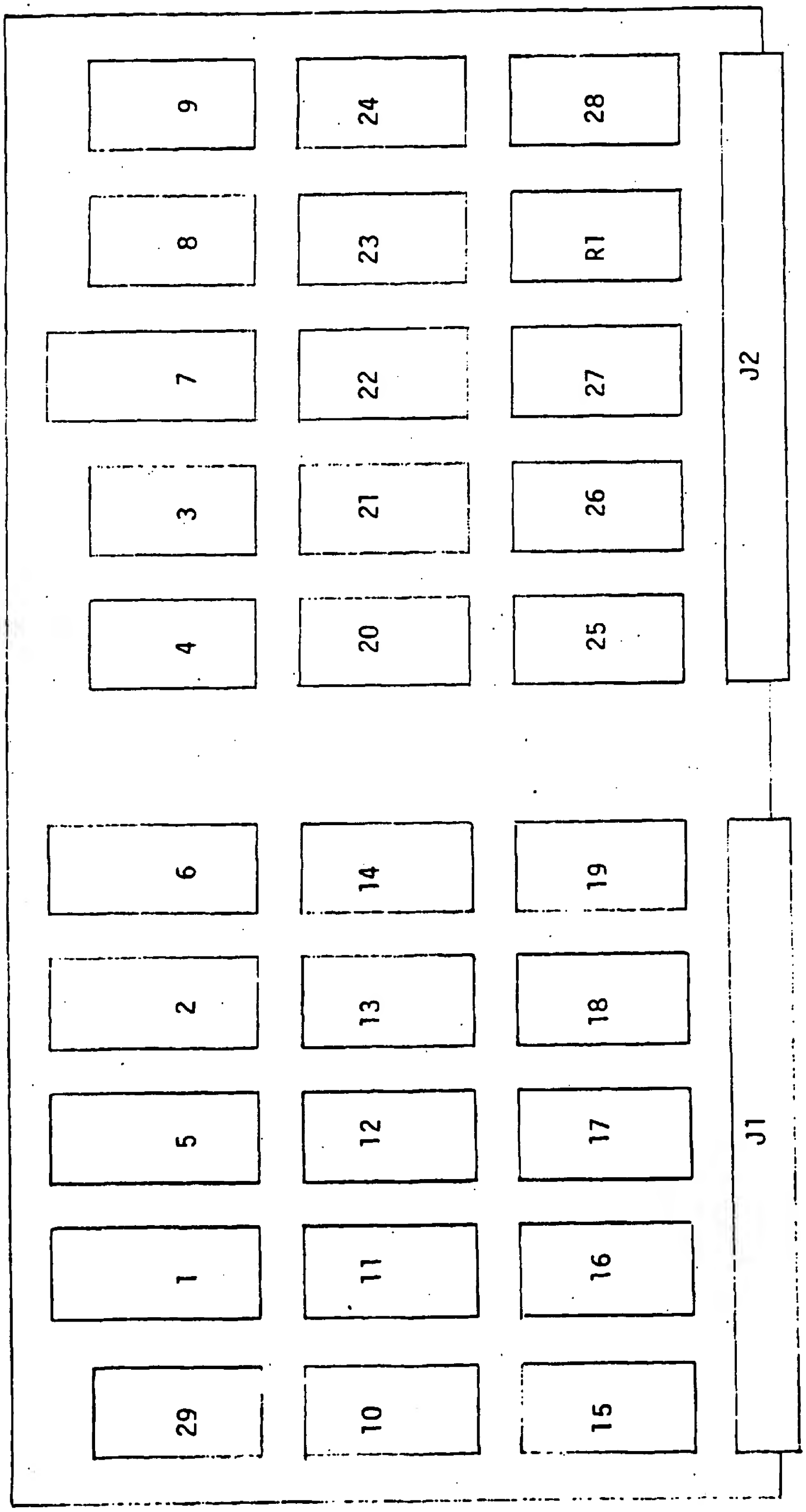

FIGURE 34 COUNTER BOARD LAYOUT
(TOP VIEW)

APPENDIX F

TIMING AND DISPLAY REFRESH SEQUENCE DIAGRAMS

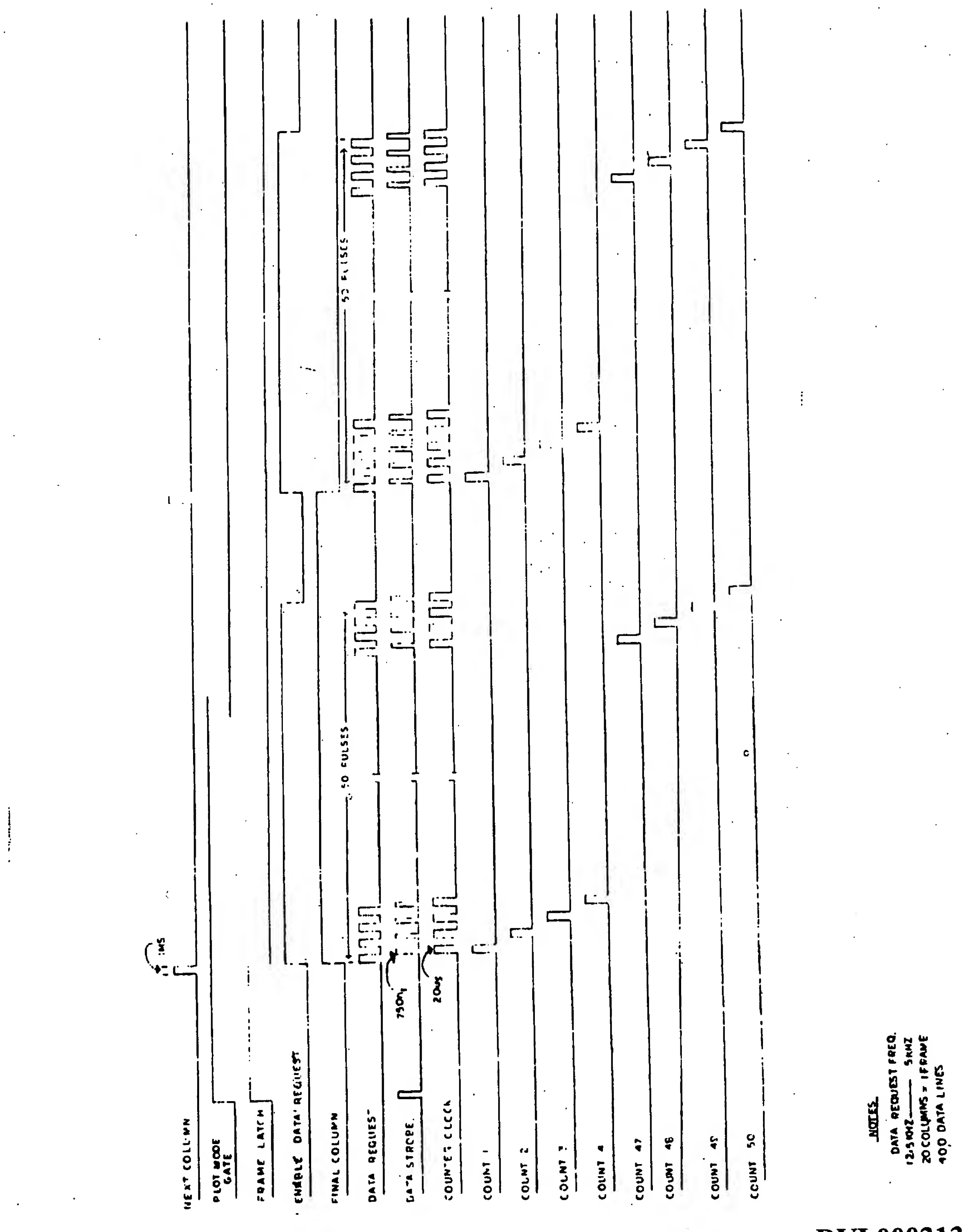

DVI 000313

Figure 35 Timing Diagram

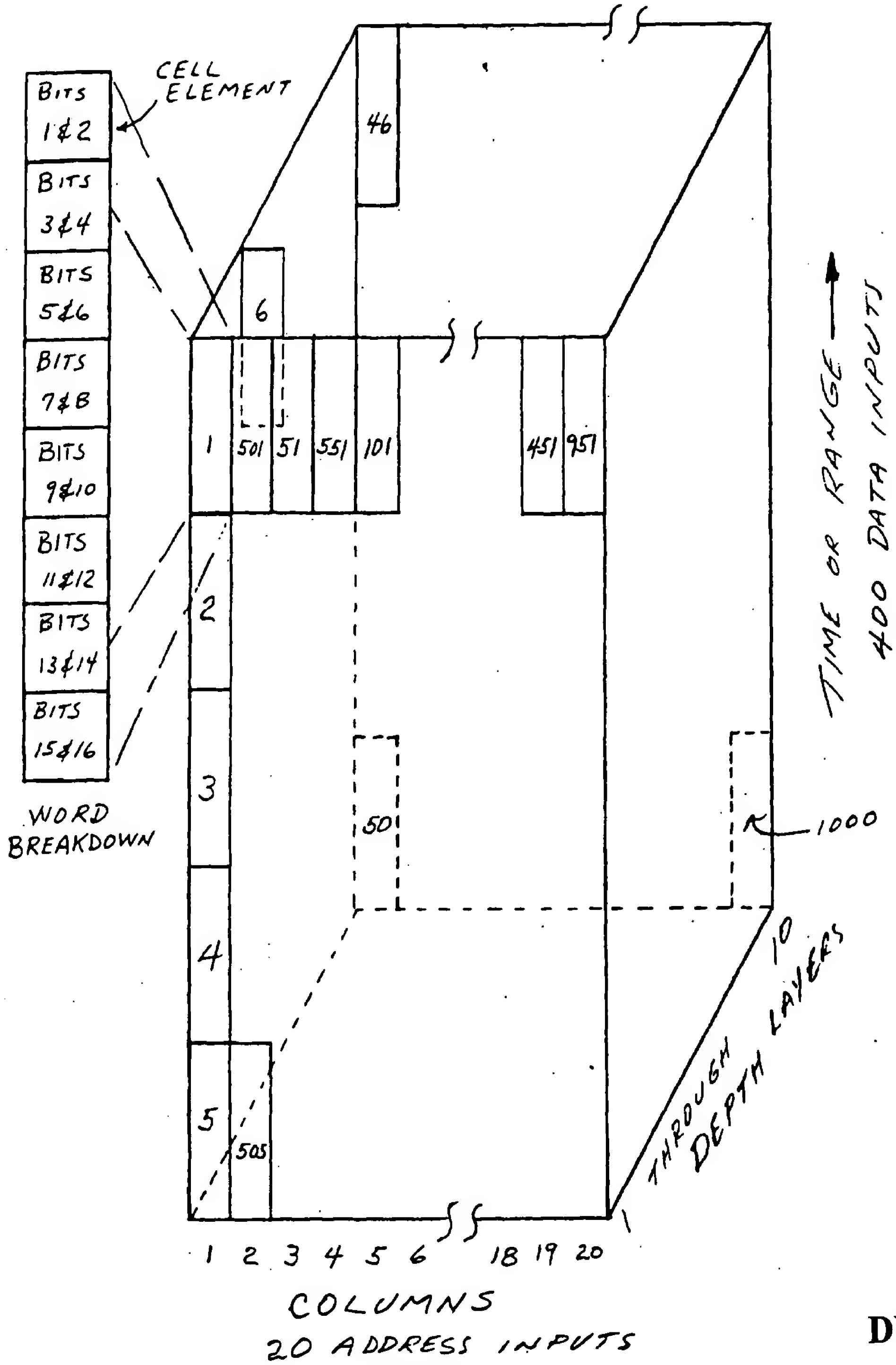

DVI 000314

FIGURE 36

Display refresh sequence showing word numbers and positions where they are steered to on the display.

THIS PAGE INTENTIONALLY BLANK

APPENDIX G

SOFTWARE PROGRAMS

DVI 000316

Preceding page blank

```
C---DEMO PATTERN GENERATOR FOR 3-D DISPLAY
        DIMENSION IBUF(2,20,120)
        EXTERNAL TOST,OTBK,RCNT,DUMPF
C---CLEAR IBUF
2       DO 1 J=1,120
        DO 1 I=1,20
        IBUF(1,I,J)=0
1       IBUF(2,I,J)=0
C---GENERATE TEST PATTERN ARRAY
C---'BRICK'
3       DO 6 J=1,40
        DO 6 I=1,20
        IF (J-20) 8,8,7
8       IF (I-5) 7,7,9
9       IF (15-I) 7,7,10
10      IBUF (1,I,J)=127
        IBUF(2,I,J)=-1024
        GO TO 6
7       IBUF (1,I,J)=0
        IBUF (2,I,J)=0
6       CONTINUE
C--- PYRAMID
4       IBUF (1,7,41)=8190
        IBUF(1,8,41)=1022
        IBUF(1,9,41)=126
        IBUF(1,10,41)=14
        IBUF(1,7,42)=1022
        IBUF(1,8,42)=126
        IBUF(1,9,42)=14
        IBUF(1,7,43)=126
        IBUF(1,8,43)=14
        IBUF(1,7,44)=14
        IBUF(2,7,41)=-16
        IBUF(2,8,41)=-16
        IBUF(2,9,11)=-16
        IBUF(2,10,41)=-16
        IBUF(2,11,41)=-16
        IBUF(2,12,41)=8176
        IBUF(2,13,41)=1008
        IBUF(2,14,41)=112
        IBUF(2,7,42)=-16
        IBUF(2,8,42)=-16
        IBUF(2,9,42)=-16
        IBUF(2,10,42)=-16
        IBUF(2,11,42)=8176
        IBUF(2,12,42)=1008
        IBUF(2,13,42)=112
        IBUF(2,7,43)=-16
        IBUF(2,8,43)=-16
        IBUF(2,9,43)=-16
        IBUF(2,10,43)=8176
        IBUF(2,11,43)=1008
        IBUF(2,12,43)=112
        IBUF(2,7,44)=-16
        IBUF(2,8,44)=-16
        IBUF(2,9,44)=8176
        IBUF(2,10,44)=1008
        IBUF(2,11,44)=112
        IBUF(2,7,45)=-16
        IBUF(2,8,45)=8176
        IBUF(2,9,45)=1008
        IBUF(2,10,45)=112
        IBUF(2,7,46)=8176
        IBUF(2,8,45)=1008
        IBUF(2,9,46)=112
        IBUF(2,7,47)=1008
        IBUF(2,8,47)=112
        IBUF(2,7,48)=112
C---SHADED PYRAMID
        IBUF(1,7,81)=7334
        IBUF(1,8,81)=166
        IBUF(1,9,81)=38
        IBUF(1,10,81)=6
        IBUF(1,7,82)=166
        IBUF(1,8,82)=38
        IBUF(1,9,82)=6
        IBUF(1,7,83)=38
        IBUF(1,8,83)=6
        IBUF(1,7,84)=6
        IBUF(2,7,81)=-26768
        IBUF(2,8,81)=-26768
        IBUF(2,9,81)=-26768
        IBUF(2,10,81)=-26768
        IBUF(2,11,81)=-26768
        IBUF(2,12,81)=6000
        IBUF(2,13,81)=880
        IBUF(2,14,81)=112
        IBUF(2,7,82)=-26768
        IBUF(2,8,82)=-26768
        IBUF(2,9,82)=-26768
        IBUF(2,10,82)=-26768
        IBUF(2,11,82)=6000
        IBUF(2,12,82)=880
        IBUF(2,13,82)=112
        IBUF(2,7,83)=-26768
        IBUF(2,8,83)=-26768
        IBUF(2,9,83)=-26768
        IBUF(2,10,83)=6000
        IBUF(2,11,83)=880
        IBUF(2,12,83)=112
        IBUF(2,7,84)=-26768
        IBUF(2,8,84)=-26768
        IBUF(2,9,84)=6000
        IBUF(2,10,84)=880
        IBUF(2,11,84)=112
        IBUF(2,7,85)=-26768
        IBUF(2,8,85)=6000
        IBUF(2,9,85)=880
        IBUF(2,10,85)=112
        IBUF(2,7,86)=6000
        IBUF(2,8,86)=880
        IBUF(2,9,86)=112
        IBUF(2,7,87)=880
        IBUF(2,8,87)=112
        IBUF(2,7,88)=112
C---CONTINUOUS LOOP TO TRANSMIT TO 620-I
        N1=22
        N2=32767
        CALL TOST (N1,N2)
41      DO 51 K=1,120
            N=121-K
        CALL OTBK (IBUF(1,1,N),40)
        CALL RCNT
51      CONTINUE
        GO TO 41
        END
```

TABLE VI

SOFTWARE PROGRAM FOR DEMONSTRATION PATTERN GENERATOR

DVI 000317

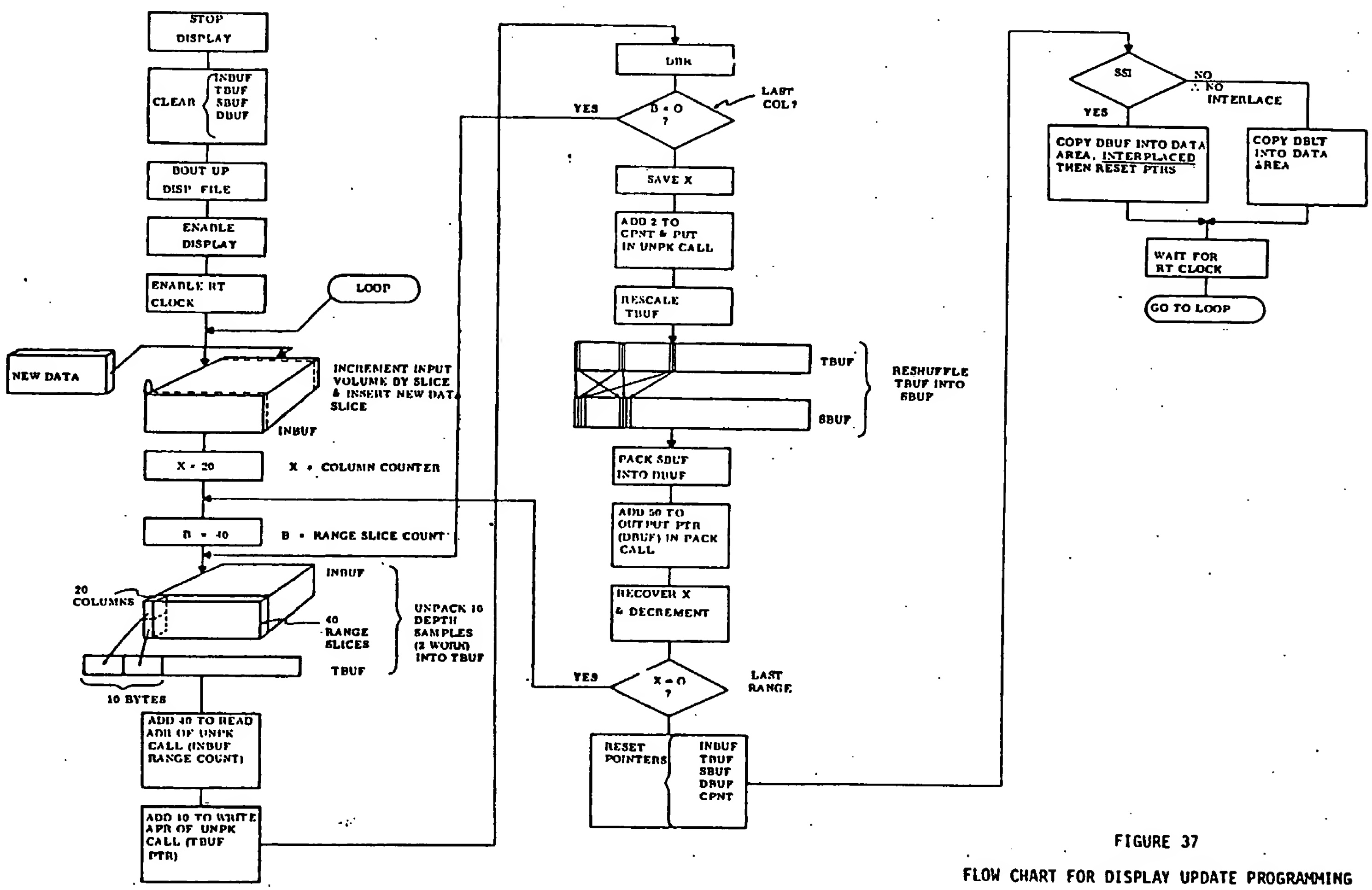

FIGURE 37

FLOW CHART FOR DISPLAY UPDATE PROGRAMMING

APPENDIX H

BACK PLANE

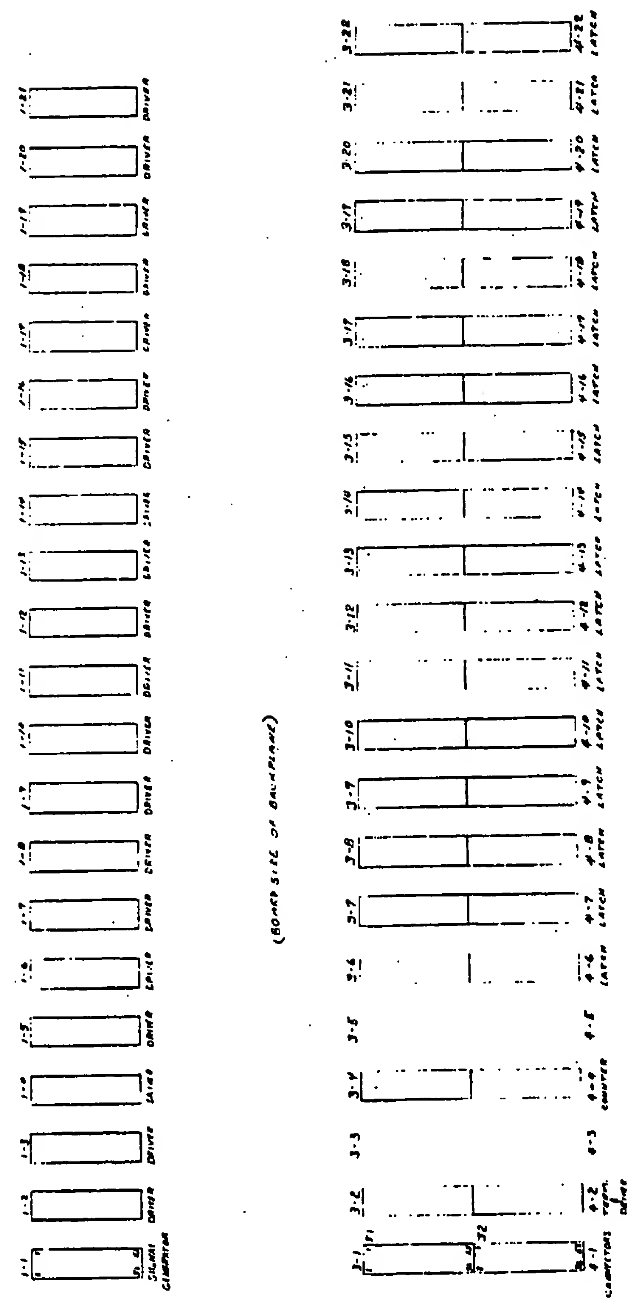

DVI 000320

Figure 38 Back Plane Board Placement (Board Side).

REFERENCE ROW-CON-PIN	DESTINATION ROW-CON-PIN	LEVEL	SIGNAL NAME	REFERENCE ROW-CON-PIN	DESTINATION ROW-CON-PIN	LEVEL	SIGNAL NAME	REFERENCE ROW-CON-PIN	DESTINATION ROW-CON-PIN	LEVEL	SIGNAL NAME	REFERENCE ROW-CON-PIN	DESTINATION ROW-CON-PIN	LEVEL	SIGNAL NAME
1- 1- 1	1- 2- 2	1	PFVL01	1- 2- 27	3- 6- 45	1	L01C17	1- 4- 5	1- 3- 5	1	DRWHVL	1- 5- 22	4- 8- 13	1	L02C32
1- 1- 2	1- 2- 1	1	DR1GND	1- 2- 28	3- 6- 46	1	L01C18	1- 4- 5	1- 5- 5	1	DRWHVL	1- 5- 23	3- 9- 25	1	L02C33
1- 1- 8	4- 4- 17	1	NXTCLM	1- 2- 29	4- 6- 8	1	L01C19	1- 4- 7	1- 4- 55	1	A1C003	1- 5- 24	3- 9- 26	1	L02C34
1- 1- 20	4- 6- 26	1	GRAY01	1- 2- 30	4- 6- 9	1	L01C20	1- 4- 10	1- 1- 26	1	A1SC04	1- 5- 25	3- 9- 27	1	L02C35
1- 1- 22	4- 6- 27	1	GRAY02	1- 2- 55	1- 2- 7	1	A1C001	1- 4- 11	3- 7- 45	1	L02C01	1- 5- 26	3- 9- 28	1	L02C36
1- 1- 23	1- 3- 10	1	A1SC01	1- 2- 55	1- 2- 56	1	A1C001	1- 4- 12	3- 7- 46	1	L02C02	1- 5- 27	3- 9- 29	1	L02C37
1- 1- 24	1- 2- 10	1	A1SC02	1- 2- 56	1- 2- 55	1	A1C001	1- 4- 13	4- 7- 8	1	L02C03	1- 5- 28	3- 9- 30	1	L02C38
1- 1- 25	1- 5- 10	1	A1SC03	1- 3- 1	1- 2- 1	1	DR1GND	1- 4- 14	4- 7- 9	1	L02C04	1- 5- 29	3- 9- 31	1	L02C39
1- 1- 26	1- 4- 10	1	A1SC04	1- 3- 1	1- 4- 1	1	DR1GND	1- 4- 15	4- 7- 10	1	L02C05	1- 5- 30	3- 9- 32	1	L02C40
1- 1- 27	1- 7- 10	1	A1SC05	1- 3- 2	1- 4- 2	1	PFVL01	1- 4- 16	4- 7- 11	1	L02C06	1- 5- 55	1- 5- 7	1	A1C004
1- 1- 28	1- 6- 10	1	A1SC06	1- 3- 2	1- 2- 2	1	PFVL01	1- 4- 17	4- 7- 12	1	L02C07	1- 5- 55	1- 5- 56	1	A1C004
1- 1- 29	1- 9- 10	1	A1SC07	1- 3- 3	1- 2- 3	1	ALTGND	1- 4- 18	4- 7- 13	1	L02C08	1- 5- 56	1- 5- 55	1	A1C004
1- 1- 30	1- 8- 10	1	A1SC08	1- 3- 3	1- 4- 3	1	ALTGND	1- 4- 19	3- 8- 25	1	L02C09	1- 6- 1	1- 5- 1	1	DR1GND
1- 1- 31	1- 11- 10	1	A1SC09	1- 3- 4	1- 2- 4	1	DR1HVL	1- 4- 20	3- 8- 26	1	L02C10	1- 6- 1	1- 7- 1	1	DR1GND
1- 1- 32	1- 10- 10	1	A1SC10	1- 3- 4	1- 4- 4	1	DR1HVL	1- 4- 21	3- 8- 27	1	L02C11	1- 6- 2	1- 5- 2	1	PFVL01
1- 1- 39	1- 13- 10	1	A1SC11	1- 3- 5	1- 2- 5	1	DRWHVL	1- 4- 22	3- 8- 28	1	L02C12	1- 6- 2	1- 7- 2	1	PFVL01
1- 1- 40	1- 12- 10	1	A1SC12	1- 3- 5	1- 4- 5	1	DRWHVL	1- 4- 23	3- 8- 29	1	L02C13	1- 6- 3	1- 5- 3	1	ALTGND
1- 1- 41	1- 15- 10	1	A1SC13	1- 3- 7	1- 3- 55	1	A1C002	1- 4- 24	3- 8- 30	1	L02C14	1- 6- 3	1- 7- 3	1	ALTGND
1- 1- 42	1- 14- 10	1	A1SC14	1- 3- 10	1- 1- 23	1	A1SC01	1- 4- 25	3- 8- 31	1	L02C15	1- 6- 4	1- 7- 4	1	DR1HVL
1- 1- 43	1- 17- 10	1	A1SC15	1- 3- 11	4- 6- 10	1	L01C21	1- 4- 26	3- 8- 32	1	L02C16	1- 6- 4	1- 5- 4	1	DR1HVL
1- 1- 44	1- 16- 10	1	A1SC16	1- 3- 12	4- 6- 11	1	L01C22	1- 4- 27	3- 8- 33	1	L02C17	1- 6- 5	1- 7- 5	1	DRWHVL
1- 1- 45	1- 19- 10	1	A1SC17	1- 3- 13	4- 6- 12	1	L01C23	1- 4- 28	3- 8- 34	1	L02C18	1- 6- 5	1- 5- 5	1	DRWHVL
1- 1- 46	1- 18- 10	1	A1SC18	1- 3- 14	4- 6- 13	1	L01C24	1- 4- 29	3- 8- 35	1	L02C19	1- 6- 7	1- 6- 55	1	A1C005
1- 1- 47	1- 21- 10	1	A1SC19	1- 3- 15	3- 7- 25	1	L01C25	1- 4- 30	3- 8- 36	1	L02C20	1- 6- 10	1- 1- 28	1	A1SC06
1- 1- 48	1- 20- 10	1	A1SC20	1- 3- 16	3- 7- 26	1	L01C26	1- 4- 55	1- 4- 7	1	A1C003	1- 6- 11	3- 9- 33	1	L03C01
1- 2- 1	1- 1- 2	1	DR1GND	1- 3- 17	3- 7- 27	1	L01C27	1- 4- 55	1- 4- 56	1	A1C003	1- 6- 12	3- 9- 34	1	L03C02
1- 2- 1	1- 3- 1	1	DR1GND	1- 3- 18	3- 7- 28	1	L01C28	1- 4- 56	1- 4- 55	1	A1C003	1- 6- 13	3- 9- 35	1	L03C03
1- 2- 2	1- 1- 1	1	PFVL01	1- 3- 19	3- 7- 29	1	L01C29	1- 5- 1	1- 4- 1	1	DR1GND	1- 6- 14	3- 9- 36	1	L03C04
1- 2- 2	1- 3- 2	1	PFVL01	1- 3- 20	3- 7- 30	1	L01C30	1- 5- 1	1- 6- 1	1	DR1GND	1- 6- 15	3- 9- 41	1	L03C05
1- 2- 3	1- 3- 3	1	ALTGND	1- 3- 21	3- 7- 31	1	L01C31	1- 5- 2	1- 4- 2	1	PFVL01	1- 6- 16	3- 9- 42	1	L03C06
1- 2- 4	1- 3- 4	1	DR1HVL	1- 3- 22	3- 7- 32	1	L01C32	1- 5- 2	1- 6- 2	1	PFVL01	1- 6- 17	3- 9- 43	1	L03C07
1- 2- 5	1- 3- 5	1	DRWHVL	1- 3- 23	3- 7- 33	1	L01C33	1- 5- 3	1- 4- 3	1	ALTGND	1- 6- 18	3- 9- 44	1	L03C08
1- 2- 7	1- 2- 55	1	A1C001	1- 3- 24	3- 7- 34	1	L01C34	1- 5- 3	1- 6- 3	1	ALTGND	1- 6- 19	3- 9- 45	1	L03C09
1- 2- 10	1- 1- 24	1	A1SC02	1- 3- 25	3- 7- 35	1	L01C35	1- 5- 4	1- 6- 4	1	DR1HVL	1- 6- 20	3- 9- 46	1	L03C10
1- 2- 11	3- 6- 25	1	L01C01	1- 3- 26	3- 7- 36	1	L01C36	1- 5- 4	1- 4- 4	1	DR1HVL	1- 6- 21	4- 9- 8	1	L03C11
1- 2- 12	3- 6- 26	1	L01C02	1- 3- 27	3- 7- 41	1	L01C37	1- 5- 5	1- 6- 5	1	DRWHVL	1- 6- 22	4- 9- 9	1	L03C12
1- 2- 13	3- 6- 27	1	L01C03	1- 3- 28	3- 7- 42	1	L01C38	1- 5- 5	1- 4- 5	1	DRWHVL	1- 6- 23	4- 9- 10	1	L03C13
1- 2- 14	3- 6- 28	1	L01C04	1- 3- 29	3- 7- 43	1	L01C39	1- 5- 7	1- 5- 55	1	A1C004	1- 6- 24	4- 9- 11	1	L03C14
1- 2- 15	3- 6- 29	1	L01C05	1- 3- 30	3- 7- 44	1	L01C40	1- 5- 10	1- 1- 25	1	A1SC03	1- 6- 25	4- 9- 12	1	L03C15
1- 2- 16	3- 6- 30	1	L01C06	1- 3- 55	1- 3- 7	1	A1C002	1- 5- 11	3- 8- 41	1	L02C21	1- 6- 26	4- 9- 13	1	L03C16
1- 2- 17	3- 6- 31	1	L01C07	1- 3- 55	1- 3- 56	1	A1C002	1- 5- 12	3- 8- 42	1	L02C22	1- 6- 27	3- 10- 25	1	L03C17
1- 2- 18	3- 6- 32	1	L01C08	1- 3- 56	1- 3- 55	1	A1C002	1- 5- 13	3- 8- 43	1	L02C23	1- 6- 28	3- 10- 26	1	L03C18
1- 2- 19	3- 6- 33	1	L01C09	1- 4- 1	1- 3- 1	1	DR1GND	1- 5- 14	3- 8- 44	1	L02C24	1- 6- 29	3- 10- 27	1	L03C19
1- 2- 20	3- 6- 34	1	L01C10	1- 4- 1	1- 5- 1	1	DR1GND	1- 5- 15	3- 8- 45	1	L02C25	1- 6- 30	3- 10- 28	1	L03C20
1- 2- 21	3- 6- 35	1	L01C11	1- 4- 2	1- 3- 2	1	PFVL01	1- 5- 16	3- 8- 46	1	L02C26	1- 6- 55	1- 6- 7	1	A1C005
1- 2- 22	3- 6- 36	1	L01C12	1- 4- 2	1- 5- 2	1	PFVL01	1- 5- 17	4- 8- 8	1	L02C27	1- 6- 55	1- 6- 56	1	A1C005
1- 2- 23	3- 6- 41	1	L01C13	1- 4- 3	1- 3- 3	1	ALTGND	1- 5- 18	4- 8- 9	1	L02C28	1- 6- 56	1- 6- 55	1	A1C005
1- 2- 24	3- 6- 42	1	L01C14	1- 4- 3	1- 5- 3	1	ALTGND	1- 5- 19	4- 8- 10	1	L02C29	1- 7- 1	1- 6- 1	1	DR1GND
1- 2- 25	3- 6- 43	1	L01C15	1- 4- 4	1- 5- 4	1	DR1HVL	1- 5- 20	4- 8- 11	1	L02C30	1- 7- 1	1- 8- 1	1	DR1GND
1- 2- 26	3- 6- 44	1	L01C16	1- 4- 4	1- 3- 4	1	DR1HVL	1- 5- 21	4- 8- 12	1	L02C31	1- 7- 2	1- 6- 2	1	PFVL01

DVI 000321

Table VII Back Plane Running List

REFERENCE ROW-CON-PIN	DESTINATION ROW-CON-PIN	LEVEL	SIGNAL NAME	REFERENCE ROW-CON-PIN	DESTINATION ROW-CON-PIN	LEVEL	SIGNAL NAME	REFERENCE ROW-CON-PIN	DESTINATION ROW-CON-PIN	LEVEL	SIGNAL NAME	REFERENCE ROW-CON-PIN	DESTINATION ROW-CON-PIN	LEVEL	SIGNAL NAME
1- 7- 2	1- 8- 2	1	PFVL01*	1- 8- 17	3- 11- 31	1	L04C07*	1- 9- 55	1- 9- 56	1	A1C008*	1- 11- 12	3- 13- 42	1	L05C22
1- 7- 3	1- 6- 3	1	ALTGND*	1- 8- 18	3- 11- 32	1	L04C08*	1- 9- 55	1- 9- 55	1	A1C008*	1- 11- 13	3- 13- 43	1	L05C23
1- 7- 3	1- 8- 3	1	ALTGND*	1- 8- 19	3- 11- 33	1	L04C09*	1- 10- 1	1- 9- 1	1	DR1GND*	1- 11- 14	3- 13- 44	1	L05C24
1- 7- 4	1- 6- 4	1	DR1HVL*	1- 8- 20	3- 11- 34	1	L04C10*	1- 10- 1	1- 11- 1	1	DR1GND*	1- 11- 15	3- 13- 45	1	L05C25
1- 7- 4	1- 8- 4	1	DR1HVL*	1- 8- 21	3- 11- 35	1	L04C11*	1- 10- 2	1- 11- 2	1	PFVL01*	1- 11- 16	3- 13- 46	1	L05C26
1- 7- 5	1- 8- 5	1	DRHHVL*	1- 8- 22	3- 11- 36	1	L04C12*	1- 10- 2	1- 9- 2	1	PFVL01*	1- 11- 17	4- 13- 8	1	L05C27
1- 7- 5	1- 6- 5	1	DRHHVL*	1- 8- 23	3- 11- 41	1	L04C13*	1- 10- 3	1- 9- 3	1	ALTGND*	1- 11- 18	4- 13- 9	1	L05C28
1- 7- 7	1- 7- 55	1	A1C006*	1- 8- 24	3- 11- 42	1	L04C14*	1- 10- 3	1- 11- 3	1	ALTGND*	1- 11- 19	4- 13- 10	1	L05C29
1- 7- 10	1- 1- 27	1	A1SC05*	1- 8- 25	3- 11- 43	1	L04C15*	1- 10- 4	1- 9- 4	1	DR1HVL*	1- 11- 20	4- 13- 11	1	L05C30
1- 7- 11	3- 10- 29	1	L03C21*	1- 8- 26	3- 11- 44	1	L04C16*	1- 10- 4	1- 11- 4	1	DR1HVL*	1- 11- 21	4- 13- 12	1	L05C31
1- 7- 12	3- 10- 30	1	L03C22*	1- 8- 27	3- 11- 45	1	L04C17*	1- 10- 5	1- 11- 5	1	DRHHVL*	1- 11- 22	4- 13- 13	1	L05C32
1- 7- 13	3- 10- 31	1	L03C23*	1- 8- 28	3- 11- 46	1	L04C18*	1- 10- 5	1- 9- 5	1	DRHHVL*	1- 11- 23	3- 14- 25	1	L05C33
1- 7- 14	3- 10- 32	1	L03C24*	1- 8- 29	4- 11- 8	1	L04C19*	1- 10- 7	1- 10- 55	1	A1C009*	1- 11- 24	3- 14- 26	1	L05C34
1- 7- 15	3- 10- 33	1	L03C25*	1- 8- 30	4- 11- 9	1	L04C20*	1- 10- 10	1- 1- 32	1	A1SC10*	1- 11- 25	3- 14- 27	1	L05C35
1- 7- 16	3- 10- 34	1	L03C26*	1- 8- 55	1- 8- 2	1	A1C007*	1- 10- 11	3- 12- 45	1	L05C01*	1- 11- 26	3- 14- 28	1	L05C36
1- 7- 17	3- 10- 35	1	L03C27*	1- 8- 55	1- 8- 56	1	A1C007*	1- 10- 12	3- 12- 46	1	L05C02*	1- 11- 27	3- 14- 29	1	L05C37
1- 7- 18	3- 10- 36	1	L03C28*	1- 8- 56	1- 8- 55	1	A1C007*	1- 10- 13	4- 12- 8	1	L05C03*	1- 11- 28	3- 14- 30	1	L05C38
1- 7- 19	3- 10- 41	1	L03C29*	1- 9- 1	1- 8- 1	1	DR1GND*	1- 10- 14	4- 12- 9	1	L05C04*	1- 11- 29	3- 14- 31	1	L05C39
1- 7- 20	3- 10- 42	1	L03C30*	1- 9- 1	1- 10- 1	1	DR1GND*	1- 10- 15	4- 12- 10	1	L05C05*	1- 11- 30	3- 14- 32	1	L05C40
1- 7- 21	3- 10- 43	1	L03C31*	1- 9- 2	1- 10- 2	1	PFVL01*	1- 10- 16	4- 12- 11	1	L05C06*	1- 11- 55	1- 11- 7	1	A1C010
1- 7- 22	3- 10- 44	1	L03C32*	1- 9- 2	1- 8- 2	1	PFVL01*	1- 10- 17	4- 12- 12	1	L05C07*	1- 11- 55	1- 11- 56	1	A1C010
1- 7- 23	3- 10- 45	1	L03C33*	1- 9- 3	1- 8- 3	1	ALTGND*	1- 10- 18	4- 12- 13	1	L05C08*	1- 11- 56	1- 11- 55	1	A1C010
1- 7- 24	3- 10- 46	1	L03C34*	1- 9- 3	1- 10- 3	1	ALTGND*	1- 10- 19	3- 13- 25	1	L05C09*	1- 12- 1	1- 11- 1	1	DR1GND
1- 7- 25	4- 10- 8	1	L03C35*	1- 9- 4	1- 8- 4	1	DR1HVL*	1- 10- 20	3- 13- 26	1	L05C10*	1- 12- 1	1- 13- 1	1	DR1GND
1- 7- 26	4- 10- 9	1	L03C36*	1- 9- 4	1- 10- 4	1	DR1HVL*	1- 10- 21	3- 13- 27	1	L05C11*	1- 12- 2	1- 13- 2	1	PFVL01
1- 7- 27	4- 10- 10	1	L03C37*	1- 9- 5	1- 8- 5	1	DRHHVL*	1- 10- 22	3- 13- 28	1	L05C12*	1- 12- 2	1- 11- 2	1	PFVL01
1- 7- 28	4- 10- 11	1	L03C38*	1- 9- 5	1- 10- 5	1	DRHHVL*	1- 10- 23	3- 13- 29	1	L05C13*	1- 12- 3	1- 11- 3	1	ALTGND
1- 7- 29	4- 10- 12	1	L03C39*	1- 9- 7	1- 9- 55	1	A1C008*	1- 10- 24	3- 13- 30	1	L05C14*	1- 12- 3	1- 13- 3	1	ALTGND
1- 7- 30	4- 10- 13	1	L03C40*	1- 9- 10	1- 1- 29	1	A1SC07*	1- 10- 25	3- 13- 31	1	L05C15*	1- 12- 4	1- 13- 4	1	DR1HVL
1- 7- 55	1- 7- 7	1	A1C006*	1- 9- 11	4- 11- 10	1	L04C21*	1- 10- 26	3- 13- 32	1	L05C16*	1- 12- 4	1- 11- 4	1	DR1HVL
1- 7- 55	1- 7- 56	1	A1C006*	1- 9- 12	4- 11- 11	1	L04C22*	1- 10- 27	3- 13- 33	1	L05C17*	1- 12- 5	1- 11- 5	1	DRHHVL
1- 7- 56	1- 7- 55	1	A1C006*	1- 9- 13	4- 11- 12	1	L04C23*	1- 10- 28	3- 13- 34	1	L05C18*	1- 12- 5	1- 13- 5	1	DRHHVL
1- 8- 1	1- 7- 1	1	DR1GND*	1- 9- 14	4- 11- 13	1	L04C24*	1- 10- 29	3- 13- 35	1	L05C19*	1- 12- 7	1- 12- 55	1	A1C011
1- 8- 1	1- 9- 1	1	DR1GND*	1- 9- 15	3- 12- 25	1	L04C25*	1- 10- 30	3- 13- 36	1	L05C20*	1- 12- 10	1- 1- 40	1	A1SC11
1- 8- 2	1- 9- 2	1	PFVL01*	1- 9- 16	3- 12- 26	1	L04C26*	1- 10- 55	1- 10- 7	1	A1C009*	1- 12- 11	3- 14- 33	1	L06C01
1- 8- 2	1- 7- 2	1	PFVL01*	1- 9- 17	3- 12- 27	1	L04C27*	1- 10- 55	1- 10- 56	1	A1C009*	1- 12- 12	3- 14- 34	1	L06C02
1- 8- 3	1- 7- 3	1	ALTGND*	1- 9- 18	3- 12- 28	1	L04C28*	1- 10- 56	1- 10- 55	1	A1C009*	1- 12- 13	3- 14- 35	1	L06C03
1- 8- 3	1- 9- 3	1	ALTGND*	1- 9- 19	3- 12- 29	1	L04C29*	1- 11- 1	1- 12- 1	1	DR1GND*	1- 12- 14	3- 14- 36	1	L06C04
1- 8- 4	1- 7- 4	1	DR1HVL*	1- 9- 20	3- 12- 30	1	L04C30*	1- 11- 1	1- 10- 1	1	DR1GND*	1- 12- 15	3- 14- 41	1	L06C05
1- 8- 4	1- 9- 4	1	DR1HVL*	1- 9- 21	3- 12- 31	1	L04C31*	1- 11- 2	1- 12- 2	1	PFVL01*	1- 12- 16	3- 14- 42	1	L06C06
1- 8- 5	1- 9- 5	1	DRHHVL*	1- 9- 22	3- 12- 32	1	L04C32*	1- 11- 2	1- 10- 2	1	PFVL01*	1- 12- 17	3- 14- 43	1	L06C07
1- 8- 5	1- 7- 5	1	DRHHVL*	1- 9- 23	3- 12- 33	1	L04C33*	1- 11- 3	1- 10- 3	1	ALTGND*	1- 12- 18	3- 14- 44	1	L06C08
1- 8- 7	1- 8- 55	1	A1C007*	1- 9- 24	3- 12- 34	1	L04C34*	1- 11- 3	1- 12- 3	1	ALTGND*	1- 12- 19	3- 14- 45	1	L06C09
1- 8- 10	1- 1- 30	1	A1SC08*	1- 9- 25	3- 12- 35	1	L04C35*	1- 11- 4	1- 12- 4	1	DR1HVL*	1- 12- 20	3- 14- 46	1	L06C10
1- 8- 11	3- 11- 25	1	L04C01*	1- 9- 26	3- 12- 36	1	L04C36*	1- 11- 4	1- 10- 4	1	DR1HVL*	1- 12- 21	4- 14- 8	1	L06C11
1- 8- 12	3- 11- 26	1	L04C02*	1- 9- 27	3- 12- 41	1	L04C37*	1- 11- 5	1- 10- 5	1	DRHHVL*	1- 12- 22	4- 14- 9	1	L06C12
1- 8- 13	3- 11- 27	1	L04C03*	1- 9- 28	3- 12- 42	1	L04C38*	1- 11- 5	1- 12- 5	1	DRHHVL*	1- 12- 23	4- 14- 10	1	L06C13
1- 8- 14	3- 11- 28	1	L04C04*	1- 9- 29	3- 12- 43	1	L04C39*	1- 11- 7	1- 11- 55	1	A1C010*	1- 12- 24	4- 14- 11	1	L06C14
1- 8- 15	3- 11- 29	1	L04C05*	1- 9- 30	3- 12- 44	1	L04C40*	1- 11- 10	1- 1- 31	1	A1SC09*	1- 12- 25	4- 14- 12	1	L06C15
1- 8- 15	3- 11- 30	1	L04C06*	1- 9- 55	1- 9- 7	1	A1C008*	1- 11- 11	3- 13- 41	1	L05C21*	1- 12- 26	4- 14- 13	1	L06C16

DVI 000322

TABLE VII (CONTINUED)

REFERENCE ROW-CON-PIN	DESTINATION ROW-CON-PIN	LEVEL	SIGNAL NAME
1- 12- 27	3- 15- 25	1	L06C17
1- 12- 28	3- 15- 26	1	L06C18
1- 12- 29	3- 15- 27	1	L06C19
1- 12- 30	3- 15- 28	1	L06C20
1- 12- 55	1- 12- 7	1	A1C011
1- 12- 55	1- 12- 56	1	A1C011
1- 12- 56	1- 12- 55	1	A1C011
1- 13- 1	1- 12- 1	1	DR1GND
1- 13- 1	1- 14- 1	1	DR1GND
1- 13- 2	1- 14- 2	1	PFVL01
1- 13- 2	1- 12- 2	1	PFVL01
1- 13- 3	1- 12- 3	1	ALTGND
1- 13- 3	1- 14- 3	1	ALTGND
1- 13- 4	1- 14- 4	1	DR1HVL
1- 13- 4	1- 12- 4	1	DR1HVL
1- 13- 5	1- 12- 5	1	DRHHVL
1- 13- 5	1- 14- 5	1	DRHHVL
1- 13- 7	1- 13- 55	1	A1C012
1- 13- 10	1- 1- 39	1	A1SC11
1- 13- 11	3- 15- 29	1	L06C21
1- 13- 12	3- 15- 30	1	L06C22
1- 13- 13	3- 15- 31	1	L06C23
1- 13- 14	3- 15- 32	1	L06C24
1- 13- 15	3- 15- 33	1	L06C25
1- 13- 16	3- 15- 34	1	L06C26
1- 13- 17	3- 15- 35	1	L06C27
1- 13- 18	3- 15- 36	1	L06C28
1- 13- 19	3- 15- 41	1	L06C29
1- 13- 20	3- 15- 42	1	L06C30
1- 13- 21	3- 15- 43	1	L06C31
1- 13- 22	3- 15- 44	1	L06C32
1- 13- 23	3- 15- 45	1	L06C33
1- 13- 24	3- 15- 46	1	L06C34
1- 13- 25	4- 15- 8	1	L06C35
1- 13- 26	4- 15- 9	1	L06C36
1- 13- 27	4- 15- 10	1	L06C37
1- 13- 28	4- 15- 11	1	L06C38
1- 13- 29	4- 15- 12	1	L06C39
1- 13- 30	4- 15- 13	1	L06C40
1- 13- 55	1- 13- 7	1	A1C012
1- 13- 55	1- 13- 56	1	A1C012
1- 13- 56	1- 13- 55	1	A1C012
1- 14- 1	1- 15- 1	1	DR1GND
1- 14- 1	1- 13- 1	1	DR1GND
1- 14- 2	1- 13- 2	1	PFVL01
1- 14- 2	1- 15- 2	1	PFVL01
1- 14- 3	1- 13- 3	1	ALTGND
1- 14- 3	1- 15- 3	1	ALTGND
1- 14- 4	1- 15- 4	1	DR1HVL
1- 14- 4	1- 13- 4	1	DR1HVL

REFERENCE ROW-CON-PIN	DESTINATION ROW-CON-PIN	LEVEL	SIGNAL NAME
1- 14- 5	1- 13- 5	1	DRHHVL
1- 14- 5	1- 15- 5	1	DRHHVL
1- 14- 7	1- 14- 55	1	A1C013
1- 14- 10	1- 1- 42	1	A1SC14
1- 14- 11	3- 16- 25	1	L07C01
1- 14- 12	3- 16- 26	1	L07C02
1- 14- 13	3- 16- 27	1	L07C03
1- 14- 14	3- 16- 28	1	L07C04
1- 14- 15	3- 16- 29	1	L07C05
1- 14- 16	3- 16- 30	1	L07C06
1- 14- 17	3- 16- 31	1	L07C07
1- 14- 18	3- 16- 32	1	L07C08
1- 14- 19	3- 16- 33	1	L07C09
1- 14- 20	3- 16- 34	1	L07C10
1- 14- 21	3- 16- 35	1	L07C11
1- 14- 22	3- 16- 36	1	L07C12
1- 14- 23	3- 16- 41	1	L07C13
1- 14- 24	3- 16- 42	1	L07C14
1- 14- 25	3- 16- 43	1	L07C15
1- 14- 26	3- 16- 44	1	L07C16
1- 14- 27	3- 16- 45	1	L07C17
1- 14- 28	3- 16- 46	1	L07C18
1- 14- 29	4- 16- 8	1	L07C19
1- 14- 30	4- 16- 9	1	L07C20
1- 14- 55	1- 14- 7	1	A1C013
1- 14- 55	1- 14- 56	1	A1C013
1- 14- 56	1- 14- 55	1	A1C013
1- 15- 1	1- 16- 1	1	DR1GND
1- 15- 1	1- 14- 1	1	DR1GND
1- 15- 2	1- 16- 2	1	PFVL01
1- 15- 2	1- 14- 2	1	PFVL01
1- 15- 3	1- 14- 3	1	ALTGND
1- 15- 3	1- 16- 3	1	ALTGND
1- 15- 4	1- 16- 4	1	DR1HVL
1- 15- 4	1- 14- 4	1	DR1HVL
1- 15- 5	1- 14- 5	1	DRHHVL
1- 15- 5	1- 16- 5	1	DRHHVL
1- 15- 7	1- 15- 55	1	A1C014
1- 15- 10	1- 1- 41	1	A1SC13
1- 15- 11	4- 16- 10	1	L07C21
1- 15- 12	4- 16- 11	1	L07C22
1- 15- 13	4- 16- 12	1	L07C23
1- 15- 14	4- 16- 13	1	L07C24
1- 15- 15	3- 17- 25	1	L07C25
1- 15- 16	3- 17- 26	1	L07C26
1- 15- 17	3- 17- 27	1	L07C27
1- 15- 18	3- 17- 28	1	L07C28
1- 15- 19	3- 17- 29	1	L07C29
1- 15- 20	3- 17- 30	1	L07C30
1- 15- 21	3- 17- 31	1	L07C31

REFERENCE ROW-CON-PIN	DESTINATION ROW-CON-PIN	LEVEL	SIGNAL NAME
1- 15- 22	3- 17- 32	1	L07C32
1- 15- 23	3- 17- 33	1	L07C33
1- 15- 24	3- 17- 34	1	L07C34
1- 15- 25	3- 17- 35	1	L07C35
1- 15- 26	3- 17- 36	1	L07C36
1- 15- 27	3- 17- 41	1	L07C37
1- 15- 28	3- 17- 42	1	L07C38
1- 15- 29	3- 17- 43	1	L07C39
1- 15- 30	3- 17- 44	1	L07C40
1- 15- 55	1- 15- 7	1	A1C014
1- 15- 55	1- 15- 56	1	A1C014
1- 15- 56	1- 15- 55	1	A1C014
1- 16- 1	1- 15- 1	1	DR1GND
1- 16- 1	1- 17- 1	1	DR1GND
1- 16- 2	1- 15- 2	1	PFVL01
1- 16- 2	1- 17- 2	1	PFVL01
1- 16- 3	1- 15- 3	1	ALTGND
1- 16- 3	1- 17- 3	1	ALTGND
1- 16- 4	1- 15- 4	1	DR1HVL
1- 16- 4	1- 17- 4	1	DR1HVL
1- 16- 5	1- 15- 5	1	DRHHVL
1- 16- 5	1- 17- 5	1	DRHHVL
1- 16- 7	1- 16- 55	1	A1C015
1- 16- 10	1- 1- 44	1	A1SC16
1- 16- 11	3- 17- 45	1	L08C01
1- 16- 12	3- 17- 46	1	L08C02
1- 16- 13	4- 17- 8	1	L08C03
1- 16- 14	4- 17- 9	1	L08C04
1- 16- 15	4- 17- 10	1	L08C05
1- 16- 16	4- 17- 11	1	L08C06
1- 16- 17	4- 17- 12	1	L08C07
1- 16- 18	4- 17- 13	1	L08C08
1- 16- 19	3- 18- 25	1	L08C09
1- 16- 20	3- 18- 26	1	L08C10
1- 16- 21	3- 18- 27	1	L08C11
1- 16- 22	3- 18- 28	1	L08C12
1- 16- 23	3- 18- 29	1	L08C13
1- 16- 24	3- 18- 30	1	L08C14
1- 16- 25	3- 18- 31	1	L08C15
1- 16- 26	3- 18- 32	1	L08C16
1- 16- 27	3- 18- 33	1	L08C17
1- 16- 28	3- 18- 34	1	L08C18
1- 16- 29	3- 18- 35	1	L08C19
1- 16- 30	3- 18- 36	1	L08C20
1- 16- 55	1- 16- 7	1	A1C015
1- 16- 55	1- 16- 56	1	A1C015
1- 16- 56	1- 16- 55	1	A1C015
1- 17- 1	1- 18- 1	1	DR1GND
1- 17- 1	1- 16- 1	1	DR1GND
1- 17- 2	1- 18- 2	1	PFVL01

REFERENCE ROW-CON-PIN	DESTINATION ROW-CON-PIN	LEVEL	SIGNAL NAME
1- 17- 2	1- 16- 2	1	PFVL01
1- 17- 3	1- 16- 3	1	ALTGND
1- 17- 3	1- 18- 3	1	ALTGND
1- 17- 4	1- 16- 4	1	DR1HVL
1- 17- 4	1- 18- 4	1	DR1HVL
1- 17- 5	1- 16- 5	1	DRHHVL
1- 17- 5	1- 18- 5	1	DRHHVL
1- 17- 7	1- 17- 55	1	A1C016
1- 17- 10	1- 1- 43	1	A1SC15
1- 17- 11	3- 18- 41	1	L08C21
1- 17- 12	3- 18- 42	1	L08C22
1- 17- 13	3- 18- 43	1	L08C23
1- 17- 14	3- 18- 44	1	L08C24
1- 17- 15	3- 18- 45	1	L08C25
1- 17- 16	3- 18- 46	1	L08C26
1- 17- 17	4- 18- 8	1	L08C27
1- 17- 18	4- 18- 9	1	L08C28
1- 17- 19	4- 18- 10	1	L08C29
1- 17- 20	4- 18- 11	1	L08C30
1- 17- 21	4- 18- 12	1	L08C31
1- 17- 22	4- 18- 13	1	L08C32
1- 17- 23	3- 19- 25	1	L08C33
1- 17- 24	3- 19- 26	1	L08C34
1- 17- 25	3- 19- 27	1	L08C35
1- 17- 26	3- 19- 28	1	L08C36
1- 17- 27	3- 19- 29	1	L08C37
1- 17- 28	3- 19- 30	1	L08C38
1- 17- 29	3- 19- 31	1	L08C39
1- 17- 30	3- 19- 32	1	L08C40
1- 17- 55	1- 17- 7	1	A1C016
1- 17- 55	1- 17- 56	1	A1C016
1- 17- 56	1- 17- 55	1	A1C016
1- 18- 1	1- 17- 1	1	DR1GND
1- 18- 1	1- 19- 1	2	DR1GND
1- 18- 2	1- 17- 2	1	PFVL01
1- 18- 2	1- 19- 2	2	PFVL01
1- 18- 3	1- 17- 3	1	ALTGND
1- 18- 3	1- 19- 3	1	ALTGND
1- 18- 4	1- 19- 4	1	DR1HVL
1- 18- 4	1- 17- 4	1	DR1HVL
1- 18- 5	1- 19- 5	1	DRHHVL
1- 18- 5	1- 17- 5	1	DRHHVL
1- 18- 7	1- 18- 55	1	A1C017
1- 18- 10	1- 1- 46	1	A1SC18
1- 18- 11	3- 19- 33	1	L09C01
1- 18- 12	3- 19- 34	1	L09C02
1- 18- 13	3- 19- 35	1	L09C03
1- 18- 14	3- 19- 36	1	L09C04
1- 18- 15	3- 19- 41	1	L09C05
1- 18- 16	3- 19- 42	1	L09C06

DVI 000323

TABLE VII (CONTINUED)

REFERENCE ROW-CON-PIN	DESTINATION ROW-CON-PIN	LEVEL	SIGNAL NAME	REFERENCE ROW-CON-PIN	DESTINATION ROW-CON-PIN	LEVEL	SIGNAL NAME	REFERENCE ROW-CON-PIN	DESTINATION ROW-CON-PIN	LEVEL	SIGNAL NAME	REFERENCE ROW-CON-PIN	DESTINATION ROW-CON-PIN	LEVEL	SIGNAL NAME
1- 18- 17	3- 19- 43	1	L09C07	1- 19- 55	1- 19- 56	1	A1C018	1- 21- 11	4- 21- 10	1	L10C21	3- 1- 32	3- 2- 32	1	GNDR14
1- 18- 18	3- 19- 44	1	L09C08	1- 19- 56	1- 19- 55	1	A1C018	1- 21- 12	4- 21- 11	1	L10C22	3- 1- 33	3- 2- 33	1	INPT15
1- 18- 19	3- 19- 45	1	L09C09	1- 20- 1	1- 19- 1	1	DR1GND	1- 21- 13	4- 21- 12	1	L10C23	3- 1- 34	3- 2- 34	1	GNDR15
1- 18- 20	3- 19- 46	1	L09C10	1- 20- 1	1- 21- 1	2	DR1GND	1- 21- 14	4- 21- 13	1	L10C24	3- 1- 35	3- 2- 35	1	INPT16
1- 18- 21	4- 19- 8	1	L09C11	1- 20- 2	1- 21- 2	2	PFVL01	1- 21- 15	3- 22- 25	1	L10C25	3- 1- 36	3- 2- 36	1	GNDR16
1- 18- 22	4- 19- 9	1	L09C12	1- 20- 2	1- 19- 2	1	PFVL01	1- 21- 16	3- 22- 26	1	L10C26	3- 1- 41	4- 4- 46	1	STROBE
1- 18- 23	4- 19- 10	1	L09C13	1- 20- 3	1- 19- 3	2	ALTGND	1- 21- 17	3- 22- 27	1	L10C27	3- 1- 42	4- 4- 45	1	STROBR
1- 18- 24	4- 19- 11	1	L09C14	1- 20- 3	1- 21- 3	1	ALTGND	1- 21- 18	3- 22- 28	1	L10C28	3- 1- 43	4- 4- 48	1	FMSYNC
1- 18- 25	4- 19- 12	1	L09C15	1- 20- 4	1- 19- 4	2	DR1HVL	1- 21- 19	3- 22- 29	1	L10C29	3- 1- 44	4- 4- 47	1	FMSYNR
1- 18- 26	4- 19- 13	1	L09C16	1- 20- 4	1- 21- 4	1	DR1HVL	1- 21- 20	3- 22- 30	1	L10C30	3- 1- 47	4- 2- 9	1	NOTRED
1- 18- 27	3- 20- 25	1	L09C17	1- 20- 5	1- 19- 5	2	DRHHVL	1- 21- 21	3- 22- 31	1	L10C31	3- 1- 48	4- 2- 10	1	GNDNDR
1- 18- 28	3- 20- 26	1	L09C18	1- 20- 5	1- 21- 5	1	DRHHVL	1- 21- 22	3- 22- 32	1	L10C32	3- 2- 1	3- 2- 2	1	GND001
1- 18- 29	3- 20- 27	1	L09C19	1- 20- 7	1- 20- 55	1	A1C019	1- 21- 23	3- 22- 33	1	L10C33	3- 2- 2	3- 2- 55	1	GND001
1- 18- 30	3- 20- 28	1	L09C20	1- 20- 10	1- 1- 48	1	A1SC20	1- 21- 24	3- 22- 34	1	L10C34	3- 2- 2	3- 2- 1	1	GND001
1- 18- 55	1- 18- 7	1	A1C017	1- 20- 11	3- 21- 25	1	L10C01	1- 21- 25	3- 22- 35	1	L10C35	3- 2- 3	3- 2- 4	1	PWR001
1- 18- 55	1- 18- 56	1	A1C017	1- 20- 12	3- 21- 26	1	L10C02	1- 21- 26	3- 22- 36	1	L10C36	3- 2- 4	3- 2- 53	1	PWR001
1- 18- 56	1- 18- 55	1	A1C017	1- 20- 13	3- 21- 27	1	L10C03	1- 21- 27	3- 22- 41	1	L10C37	3- 2- 4	3- 2- 3	1	PWR001
1- 19- 1	1- 18- 1	2	DR1GND	1- 20- 14	3- 21- 28	1	L10C04	1- 21- 28	3- 22- 42	1	L10C38	3- 2- 5	3- 1- 5	1	INPT01
1- 19- 1	1- 20- 1	1	DR1GND	1- 20- 15	3- 21- 29	1	L10C05	1- 21- 29	3- 22- 43	1	L10C39	3- 2- 6	3- 1- 6	1	GNDR01
1- 19- 2	1- 20- 2	1	PFVL01	1- 20- 16	3- 21- 30	1	L10C06	1- 21- 30	3- 22- 44	1	L10C40	3- 2- 7	3- 1- 7	1	INPT02
1- 19- 2	1- 18- 2	2	PFVL01	1- 20- 17	3- 21- 31	1	L10C07	1- 21- 55	1- 21- 7	1	A1C020	3- 2- 8	3- 1- 8	1	GNDR02
1- 19- 3	1- 18- 3	1	ALTGND	1- 20- 18	3- 21- 32	1	L10C08	1- 21- 55	1- 21- 56	1	A1C020	3- 2- 9	3- 1- 9	1	INPT03
1- 19- 3	1- 20- 3	2	ALTGND	1- 20- 19	3- 21- 33	1	L10C09	1- 21- 56	1- 21- 55	1	A1C020	3- 2- 10	3- 1- 10	1	GNDR03
1- 19- 4	1- 18- 4	1	DR1HVL	1- 20- 20	3- 21- 34	1	L10C10	3- 1- 5	3- 2- 5	1	INPT01	3- 2- 11	3- 1- 11	1	INPT04
1- 19- 4	1- 20- 4	2	DR1HVL	1- 20- 21	3- 21- 35	1	L10C11	3- 1- 6	3- 2- 6	1	GNDR01	3- 2- 12	3- 1- 12	1	GNDR04
1- 19- 5	1- 18- 5	1	DRHHVL	1- 20- 22	3- 21- 36	1	L10C12	3- 1- 7	3- 2- 7	1	INPT02	3- 2- 13	3- 1- 13	1	INPT05
1- 19- 5	1- 20- 5	2	DRHHVL	1- 20- 23	3- 21- 41	1	L10C13	3- 1- 8	3- 2- 8	1	GNDR02	3- 2- 14	3- 1- 14	1	GNDR05
1- 19- 7	1- 19- 55	1	A1C019	1- 20- 24	3- 21- 42	1	L10C14	3- 1- 9	3- 2- 9	1	INPT03	3- 2- 15	3- 1- 15	1	INPT06
1- 19- 10	1- 1- 45	1	A1SC17	1- 20- 25	3- 21- 43	1	L10C15	3- 1- 10	3- 2- 10	1	GNDR03	3- 2- 16	3- 1- 16	1	GNDR06
1- 19- 11	3- 20- 29	1	L09C21	1- 20- 26	3- 21- 44	1	L10C16	3- 1- 11	3- 2- 11	1	INPT04	3- 2- 17	3- 1- 17	1	INPT07
1- 19- 12	3- 20- 30	1	L09C22	1- 20- 27	3- 21- 45	1	L10C17	3- 1- 12	3- 2- 12	1	GNDR04	3- 2- 18	3- 1- 18	1	GNDR07
1- 19- 13	3- 20- 31	1	L09C23	1- 20- 28	3- 21- 46	1	L10C18	3- 1- 13	3- 2- 13	1	INPT05	3- 2- 19	3- 1- 19	1	INPT08
1- 19- 14	3- 20- 32	1	L09C24	1- 20- 29	4- 21- 8	1	L10C19	3- 1- 14	3- 2- 14	1	GNDR05	3- 2- 20	3- 1- 20	1	GNDR08
1- 19- 15	3- 20- 33	1	L09C25	1- 20- 30	4- 21- 9	1	L10C20	3- 1- 15	3- 2- 15	1	INPT06	3- 2- 21	3- 1- 21	1	INPT09
1- 19- 16	3- 20- 34	1	L09C26	1- 20- 55	1- 20- 7	1	A1C019	3- 1- 16	3- 2- 16	1	GNDR06	3- 2- 22	3- 1- 22	1	GNDR09
1- 19- 17	3- 20- 35	1	L09C27	1- 20- 55	1- 20- 56	1	A1C019	3- 1- 17	3- 2- 17	1	INPT07	3- 2- 23	3- 1- 23	1	INPT10
1- 19- 18	3- 20- 36	1	L09C28	1- 20- 56	1- 20- 55	1	A1C019	3- 1- 18	3- 2- 18	1	GNDR07	3- 2- 24	3- 1- 24	1	GNDR10
1- 19- 19	3- 20- 41	1	L09C29	1- 21- 1	1- 20- 1	2	DR1GND	3- 1- 19	3- 2- 19	1	INPT08	3- 2- 25	3- 1- 25	1	INPT11
1- 19- 20	3- 20- 42	1	L09C30	1- 21- 1	4- 1- 34	1	DR1GND	3- 1- 20	3- 2- 20	1	GNDR08	3- 2- 26	3- 1- 26	1	GNDR11
1- 19- 21	3- 20- 43	1	L09C31	1- 21- 2	4- 1- 42	1	PFVL01	3- 1- 21	3- 2- 21	1	INPT09	3- 2- 27	3- 1- 27	1	INPT12
1- 19- 22	3- 20- 44	1	L09C32	1- 21- 2	1- 20- 2	2	PFVL01	3- 1- 22	3- 2- 22	1	GNDR09	3- 2- 28	3- 1- 28	1	GNDR12
1- 19- 23	3- 20- 45	1	L09C33	1- 21- 3	1- 20- 3	1	ALTGND	3- 1- 23	3- 2- 23	1	INPT10	3- 2- 29	3- 1- 29	1	INPT13
1- 19- 24	3- 20- 46	1	L09C34	1- 21- 3	4- 1- 30	2	ALTGND	3- 1- 24	3- 2- 24	1	GNDR10	3- 2- 30	3- 1- 30	1	GNDR13
1- 19- 25	4- 20- 8	1	L09C35	1- 21- 4	1- 20- 4	1	DR1HVL	3- 1- 25	3- 2- 25	1	INPT11	3- 2- 31	3- 1- 31	1	INPT14
1- 19- 26	4- 20- 9	1	L09C36	1- 21- 4	4- 1- 38	2	DR1HVL	3- 1- 26	3- 2- 26	1	GNDR11	3- 2- 32	3- 1- 32	1	GNDR14
1- 19- 27	4- 20- 10	1	L09C37	1- 21- 5	4- 1- 41	2	DRHHVL	3- 1- 27	3- 2- 27	1	INPT12	3- 2- 33	3- 1- 33	1	INPT15
1- 19- 28	4- 20- 11	1	L09C38	1- 21- 5	1- 20- 5	1	DRHHVL	3- 1- 28	3- 2- 28	1	GNDR12	3- 2- 34	3- 1- 34	1	GNDR15
1- 19- 29	4- 20- 12	1	L09C39	1- 21- 7	1- 21- 55	1	A1C020	3- 1- 29	3- 2- 29	1	INPT13	3- 2- 35	3- 1- 35	1	INPT16
1- 19- 30	4- 20- 13	1	L09C40	1- 21- 10	1- 1- 47	1	A1SC19	3- 1- 30	3- 2- 30	1	GNDR13	3- 2- 36	3- 1- 36	1	GNDR16
1- 19- 55	1- 19- 7	1	A1C019	1- 21- 13	4- 4- 37	1	A1SC19	3- 1- 31	3- 2- 31	1	INPT14	3- 2- 37	3- 6- 8	1	BIT001

DVI 000324

Table VII (Continued)

REFERENCE ROW-CON-PIN	DESTINATION ROW-CON-PIN	LEVEL	SIGNAL NAME	REFERENCE ROW-CON-PIN	DESTINATION ROW-CON-PIN	LEVEL	SIGNAL NAME	REFERENCE ROW-CON-PIN	DESTINATION ROW-CON-PIN	LEVEL	SIGNAL NAME	REFERENCE ROW-CON-PIN	DESTINATION ROW-CON-PIN	LEVEL	SIGNAL NAME
3- 2- 38	3- 6- 9	1	BIT002	3- 4- 28	3- 14- 52	1	LOAB09	3- 6- 20	3- 2- 49	1	BIT013	3- 7- 11	3- 6- 11	1	BIT004
3- 2- 39	3- 6- 10	1	BIT003	3- 4- 29	4- 14- 16	1	LOAC09	3- 6- 20	3- 7- 20	1	BIT013	3- 7- 11	3- 8- 11	1	BIT004
3- 2- 40	3- 6- 11	1	BIT004	3- 4- 30	3- 15- 7	1	LOAA10	3- 6- 21	3- 2- 50	1	BIT014	3- 7- 12	3- 6- 12	1	BIT005
3- 2- 41	3- 6- 12	1	BIT005	3- 4- 45	3- 16- 7	1	LOAA11	3- 6- 21	3- 7- 21	1	BIT014	3- 7- 12	3- 8- 12	1	BIT005
3- 2- 42	3- 6- 13	1	BIT006	3- 4- 46	3- 11- 52	1	LOAB06	3- 6- 22	3- 7- 22	1	BIT015	3- 7- 13	3- 6- 13	1	BIT006
3- 2- 43	3- 6- 14	1	BIT007	3- 4- 47	3- 16- 52	1	LOAB11	3- 6- 22	3- 2- 51	1	BIT015	3- 7- 13	3- 8- 13	1	BIT006
3- 2- 44	3- 6- 15	1	BIT008	3- 4- 48	3- 15- 52	1	LOAB10	3- 6- 23	3- 2- 52	1	BIT016	3- 7- 14	3- 8- 14	1	BIT007
3- 2- 45	3- 6- 16	1	BIT009	3- 4- 49	4- 15- 16	1	LOAC10	3- 6- 23	3- 7- 23	1	BIT016	3- 7- 14	3- 6- 14	1	BIT007
3- 2- 46	3- 6- 17	1	BIT010	3- 4- 50	3- 10- 52	1	LOAB05	3- 6- 25	1- 2- 11	1	L01C01	3- 7- 15	3- 8- 15	1	BIT008
3- 2- 47	3- 6- 18	1	BIT011	3- 4- 51	4- 10- 16	1	LOAC05	3- 6- 25	1- 2- 12	1	L01C02	3- 7- 15	3- 6- 15	1	BIT008
3- 2- 48	3- 6- 19	1	BIT012	3- 4- 52	3- 11- 7	1	LOAA06	3- 6- 27	1- 2- 13	1	L01C03	3- 7- 16	3- 8- 16	1	BIT009
3- 2- 49	3- 6- 20	1	BIT013	3- 4- 53	3- 4- 54	1	PWR001	3- 6- 28	1- 2- 14	1	L01C04	3- 7- 16	3- 6- 16	1	BIT009
3- 2- 50	3- 6- 21	1	BIT014	3- 4- 53	3- 2- 54	1	PWR001	3- 6- 29	1- 2- 15	1	L01C05	3- 7- 17	3- 8- 17	1	BIT010
3- 2- 51	3- 6- 22	1	BIT015	3- 4- 54	3- 4- 53	1	PWR001	3- 6- 30	1- 2- 16	1	L01C06	3- 7- 17	3- 6- 17	1	BIT010
3- 2- 52	3- 6- 23	1	BIT016	3- 4- 54	3- 4- 4	1	PWR001	3- 6- 31	1- 2- 17	1	L01C07	3- 7- 18	3- 6- 18	1	BIT011
3- 2- 53	3- 2- 4	1	PWR001	3- 4- 55	3- 4- 2	1	GND001	3- 6- 32	1- 2- 18	1	L01C08	3- 7- 18	3- 8- 18	1	BIT011
3- 2- 53	3- 2- 54	1	PWR001	3- 4- 55	3- 4- 56	1	GND001	3- 6- 33	1- 2- 19	1	L01C09	3- 7- 19	3- 6- 19	1	BIT012
3- 2- 54	3- 4- 53	1	PWR001	3- 4- 56	3- 4- 55	1	GND001	3- 6- 34	1- 2- 20	1	L01C10	3- 7- 19	3- 8- 19	1	BIT012
3- 2- 54	3- 2- 53	1	PWR001	3- 4- 56	3- 4- 1	1	GND001	3- 6- 35	1- 2- 21	1	L01C11	3- 7- 20	3- 8- 20	1	BIT013
3- 2- 55	3- 2- 2	1	GND001	3- 6- 1	3- 6- 55	1	GND001	3- 6- 36	1- 2- 22	1	L01C12	3- 7- 20	3- 6- 20	1	BIT013
3- 2- 55	3- 2- 56	1	GND001	3- 6- 1	3- 7- 55	1	GND001	3- 6- 37	3- 6- 40	1	CONN01	3- 7- 21	3- 6- 21	1	BIT014
3- 2- 56	3- 2- 55	1	GND001	3- 6- 2	3- 4- 3	1	PWR001	3- 6- 38	3- 6- 39	1	CONN02	3- 7- 21	3- 8- 21	1	BIT014
3- 2- 56	3- 4- 2	1	GND001	3- 6- 2	3- 6- 56	1	PWR001	3- 6- 39	3- 6- 38	1	CONN02	3- 7- 22	3- 6- 22	1	BIT015
3- 4- 1	3- 4- 56	1	GND001	3- 6- 5	3- 7- 5	1	TIE001	3- 6- 40	3- 6- 37	1	CONN01	3- 7- 22	3- 8- 22	1	BIT015
3- 4- 1	3- 6- 55	1	GND001	3- 6- 6	3- 7- 6	1	TIE002	3- 6- 41	1- 2- 23	1	L01C13	3- 7- 23	3- 6- 23	1	BIT016
3- 4- 2	3- 4- 55	1	GND001	3- 6- 7	4- 4- 50	1	LOAA01	3- 6- 42	1- 2- 24	1	L01C14	3- 7- 23	3- 8- 23	1	BIT016
3- 4- 2	3- 2- 56	1	GND001	3- 6- 8	3- 2- 37	1	BIT001	3- 6- 43	1- 2- 25	1	L01C15	3- 7- 25	1- 3- 15	1	L01C25
3- 4- 3	3- 6- 2	1	PWR001	3- 6- 8	3- 7- 8	1	BIT001	3- 6- 44	1- 2- 26	1	L01C16	3- 7- 26	1- 3- 16	1	L01C26
3- 4- 3	3- 4- 4	1	PWR001	3- 6- 9	3- 2- 38	1	BIT002	3- 6- 45	1- 2- 27	1	L01C17	3- 7- 27	1- 3- 17	1	L01C27
3- 4- 4	3- 4- 3	1	PWR001	3- 6- 9	3- 7- 9	1	BIT002	3- 6- 46	1- 2- 28	1	L01C18	3- 7- 28	1- 3- 18	1	L01C28
3- 4- 4	3- 4- 54	1	PWR001	3- 6- 10	3- 2- 39	1	BIT003	3- 6- 52	4- 4- 18	1	LOAB01	3- 7- 29	1- 3- 19	1	L01C29
3- 4- 5	4- 11- 16	1	LOAC06	3- 6- 10	3- 7- 10	1	BIT003	3- 6- 55	3- 6- 1	1	GND001	3- 7- 30	1- 3- 20	1	L01C30
3- 4- 6	3- 12- 7	1	LOAA07	3- 6- 11	3- 2- 40	1	BIT004	3- 6- 55	3- 4- 1	1	GND001	3- 7- 31	1- 3- 21	1	L01C31
3- 4- 7	3- 12- 52	1	LOAB07	3- 6- 11	3- 7- 11	1	BIT004	3- 6- 55	3- 7- 2	1	PWR001	3- 7- 32	1- 3- 22	1	L01C32
3- 4- 8	4- 12- 16	1	LOAC07	3- 6- 12	3- 2- 41	1	BIT005	3- 6- 56	3- 6- 2	1	PWR001	3- 7- 33	1- 3- 23	1	L01C33
3- 4- 9	3- 13- 7	1	LOAA08	3- 6- 12	3- 7- 12	1	BIT005	3- 7- 1	3- 8- 55	1	GND001	3- 7- 34	1- 3- 24	1	L01C34
3- 4- 14	4- 6- 16	1	LOAC01	3- 6- 13	3- 2- 42	1	BIT006	3- 7- 1	3- 7- 55	1	GND001	3- 7- 35	1- 3- 25	1	L01C35
3- 4- 15	3- 7- 7	1	LOAA02	3- 6- 13	3- 7- 13	1	BIT006	3- 7- 2	3- 7- 55	1	PWR001	3- 7- 36	1- 3- 26	1	L01C36
3- 4- 16	3- 7- 52	1	LOAB02	3- 6- 14	3- 2- 43	1	BIT007	3- 7- 2	3- 6- 55	1	PWR001	3- 7- 37	3- 7- 40	1	CONN07
3- 4- 17	4- 7- 16	1	LOAC02	3- 6- 14	3- 7- 14	1	BIT007	3- 7- 5	3- 6- 5	1	TIE001	3- 7- 38	3- 7- 39	1	CONN08
3- 4- 18	3- 8- 7	1	LOAA03	3- 6- 15	3- 7- 15	1	BIT008	3- 7- 5	3- 8- 5	1	TIE001	3- 7- 39	3- 7- 38	1	CONN08
3- 4- 19	3- 8- 52	1	LOAB03	3- 6- 15	3- 2- 44	1	BIT008	3- 7- 6	3- 8- 5	1	TIE002	3- 7- 40	3- 7- 37	1	CONN07
3- 4- 20	4- 8- 16	1	LOAC03	3- 6- 16	3- 7- 16	1	BIT009	3- 7- 6	3- 8- 6	1	TIE002	3- 7- 41	1- 3- 27	1	L01C37
3- 4- 21	3- 9- 7	1	LOAA04	3- 6- 16	3- 2- 45	1	BIT009	3- 7- 7	3- 4- 15	1	LOAA02	3- 7- 42	1- 3- 28	1	L01C38
3- 4- 22	3- 9- 52	1	LOAB04	3- 6- 17	3- 2- 46	1	BIT010	3- 7- 8	3- 6- 8	1	BIT001	3- 7- 43	1- 3- 29	1	L01C39
3- 4- 23	4- 9- 16	1	LOAC04	3- 6- 17	3- 7- 17	1	BIT010	3- 7- 8	3- 8- 8	1	BIT001	3- 7- 44	1- 3- 30	1	L01C40
3- 4- 24	3- 10- 7	1	LOAA05	3- 6- 18	3- 2- 47	1	BIT011	3- 7- 9	3- 6- 9	1	BIT002	3- 7- 45	1- 4- 11	1	L02C01
3- 4- 25	3- 13- 52	1	LOAB08	3- 6- 18	3- 7- 18	1	BIT011	3- 7- 9	3- 8- 9	1	BIT002	3- 7- 46	1- 4- 12	1	L02C02
3- 4- 26	4- 13- 16	1	LOAC08	3- 6- 19	3- 7- 19	1	BIT012	3- 7- 10	3- 6- 10	1	BIT003	3- 7- 52	3- 4- 16	1	LOAB02
3- 4- 27	3- 14- 7	1	LOAA09	3- 6- 19	3- 2- 48	1	BIT012	3- 7- 10	3- 8- 10	1	BIT003	3- 7- 55	3- 6- 1	1	GND001

DVI 000325

TABLE VII (CONTINUED)

REFERENCE ROW-CON-PIN	DESTINATION ROW-CON-PIN	LEVEL	SIGNAL NAME	REFERENCE ROW-CON-PIN	DESTINATION ROW-CON-PIN	LEVEL	SIGNAL NAME	REFERENCE ROW-CON-PIN	DESTINATION ROW-CON-PIN	LEVEL	SIGNAL NAME	REFERENCE ROW-CON-PIN	DESTINATION ROW-CON-PIN	LEVEL	SIGNAL NAME
3- 7- 55	3- 7- 1	1	GND001	3- 8- 31	1- 4- 25	1	L02C15	3- 9- 18	3- 8- 18	1	BIT011	3- 10- 9	3- 9- 9	1	BIT002
3- 7- 56	3- 8- 2	1	PWR001	3- 8- 32	1- 4- 26	1	L02C16	3- 9- 18	3- 10- 18	1	BIT011	3- 10- 9	3- 11- 9	1	BIT002
3- 7- 56	3- 7- 2	1	PWR001	3- 8- 33	1- 4- 27	1	L02C17	3- 9- 19	3- 8- 19	1	BIT012	3- 10- 10	3- 9- 10	1	BIT003
3- 8- 1	3- 8- 55	1	GND001	3- 8- 34	1- 4- 28	1	L02C18	3- 9- 19	3- 10- 19	1	BIT012	3- 10- 10	3- 11- 10	1	BIT003
3- 8- 1	3- 9- 55	1	GND001	3- 8- 35	1- 4- 29	1	L02C19	3- 9- 20	3- 8- 20	1	BIT013	3- 10- 11	3- 9- 11	1	BIT004
3- 8- 2	3- 8- 56	1	PWR001	3- 8- 36	1- 4- 30	1	L02C20	3- 9- 20	3- 10- 20	1	BIT013	3- 10- 11	3- 11- 11	1	BIT004
3- 8- 2	3- 7- 56	1	PWR001	3- 8- 37	3- 8- 40	1	CONN13	3- 9- 21	3- 8- 21	1	BIT014	3- 10- 12	3- 9- 12	1	BIT005
3- 8- 5	3- 7- 5	1	TIE001	3- 8- 38	3- 8- 39	1	CONN14	3- 9- 21	3- 10- 21	1	BIT014	3- 10- 12	3- 11- 12	1	BIT005
3- 8- 5	3- 9- 5	1	TIE001	3- 8- 39	3- 8- 38	1	CONN14	3- 9- 22	3- 8- 22	1	BIT015	3- 10- 13	3- 9- 13	1	BIT006
3- 8- 6	3- 7- 6	1	TIE002	3- 8- 40	3- 8- 37	1	CONN13	3- 9- 22	3- 10- 22	1	BIT015	3- 10- 13	3- 11- 13	1	BIT006
3- 8- 6	3- 9- 6	1	TIE002	3- 8- 41	1- 5- 11	1	L02C21	3- 9- 23	3- 10- 23	1	BIT016	3- 10- 14	3- 9- 14	1	BIT007
3- 8- 7	3- 4- 18	1	LOAA03	3- 8- 42	1- 5- 12	1	L02C22	3- 9- 23	3- 8- 23	1	BIT016	3- 10- 14	3- 11- 14	1	BIT007
3- 8- 8	3- 7- 8	1	BIT001	3- 8- 43	1- 5- 13	1	L02C23	3- 9- 25	1- 5- 23	1	L02C33	3- 10- 15	3- 11- 15	1	BIT008
3- 8- 8	3- 9- 8	1	BIT001	3- 8- 44	1- 5- 14	1	L02C24	3- 9- 26	1- 5- 24	1	L02C34	3- 10- 15	3- 9- 15	1	BIT008
3- 8- 9	3- 9- 9	1	BIT002	3- 8- 45	1- 5- 15	1	L02C25	3- 9- 27	1- 5- 25	1	L02C35	3- 10- 16	3- 11- 16	1	BIT009
3- 8- 9	3- 7- 9	1	BIT002	3- 8- 46	1- 5- 16	1	L02C26	3- 9- 28	1- 5- 26	1	L02C36	3- 10- 16	3- 9- 16	1	BIT009
3- 8- 10	3- 7- 10	1	BIT003	3- 8- 52	3- 4- 19	1	LOAB03	3- 9- 29	1- 5- 27	1	L02C37	3- 10- 17	3- 9- 17	1	BIT010
3- 8- 10	3- 9- 10	1	BIT003	3- 8- 55	3- 8- 1	1	GND001	3- 9- 30	1- 5- 28	1	L02C38	3- 10- 17	3- 11- 17	1	BIT010
3- 8- 11	3- 7- 11	1	BIT004	3- 8- 55	3- 7- 1	1	GND001	3- 9- 31	1- 5- 29	1	L02C39	3- 10- 18	3- 9- 18	1	BIT011
3- 8- 11	3- 9- 11	1	BIT004	3- 8- 56	3- 9- 2	1	PWR001	3- 9- 32	1- 5- 30	1	L02C40	3- 10- 18	3- 11- 18	1	BIT011
3- 8- 12	3- 7- 12	1	BIT005	3- 8- 56	3- 8- 2	1	PWR001	3- 9- 33	1- 6- 11	1	L03C01	3- 10- 19	3- 9- 19	1	BIT012
3- 8- 12	3- 9- 12	1	BIT005	3- 9- 1	3- 9- 55	1	GND001	3- 9- 34	1- 6- 12	1	L03C02	3- 10- 19	3- 11- 19	1	BIT012
3- 8- 13	3- 7- 13	1	BIT006	3- 9- 1	3- 10- 55	1	GND001	3- 9- 35	1- 6- 13	1	L03C03	3- 10- 20	3- 9- 20	1	BIT013
3- 8- 13	3- 9- 13	1	BIT006	3- 9- 2	3- 9- 56	1	PWR001	3- 9- 36	1- 6- 14	1	L03C04	3- 10- 20	3- 11- 20	1	BIT013
3- 8- 14	3- 7- 14	1	BIT007	3- 9- 2	3- 8- 56	1	PWR001	3- 9- 37	3- 9- 40	1	CONN19	3- 10- 21	3- 9- 21	1	BIT014
3- 8- 14	3- 9- 14	1	BIT007	3- 9- 5	3- 10- 5	1	TIE001	3- 9- 38	3- 9- 39	1	CONN20	3- 10- 21	3- 11- 21	1	BIT014
3- 8- 15	3- 7- 15	1	BIT008	3- 9- 5	3- 8- 5	1	TIE001	3- 9- 39	3- 9- 38	1	CONN20	3- 10- 22	3- 11- 22	1	BIT015
3- 8- 15	3- 9- 15	1	BIT008	3- 9- 6	3- 10- 6	1	TIE002	3- 9- 40	3- 9- 37	1	CONN19	3- 10- 22	3- 9- 22	1	BIT015
3- 8- 16	3- 9- 16	1	BIT009	3- 9- 6	3- 8- 6	1	TIE002	3- 9- 41	1- 6- 15	1	L03C05	3- 10- 23	3- 11- 23	1	BIT016
3- 8- 16	3- 7- 16	1	BIT009	3- 9- 7	3- 4- 21	1	LOAA04	3- 9- 42	1- 6- 16	1	L03C06	3- 10- 23	3- 9- 23	1	BIT016
3- 8- 17	3- 9- 17	1	BIT010	3- 9- 8	3- 8- 8	1	BIT001	3- 9- 43	1- 6- 17	1	L03C07	3- 10- 25	1- 6- 27	1	L03C17
3- 8- 17	3- 7- 17	1	BIT010	3- 9- 8	3- 10- 8	1	BIT001	3- 9- 44	1- 6- 18	1	L03C08	3- 10- 26	1- 6- 28	1	L03C18
3- 8- 18	3- 9- 18	1	BIT011	3- 9- 9	3- 8- 9	1	BIT002	3- 9- 45	1- 6- 19	1	L03C09	3- 10- 27	1- 6- 29	1	L03C19
3- 8- 18	3- 7- 18	1	BIT011	3- 9- 9	3- 10- 9	1	BIT002	3- 9- 46	1- 6- 20	1	L03C10	3- 10- 28	1- 6- 30	1	L03C20
3- 8- 19	3- 7- 19	1	BIT012	3- 9- 10	3- 8- 10	1	BIT003	3- 9- 52	3- 4- 22	1	LOAB04	3- 10- 29	1- 7- 11	1	L03C21
3- 8- 19	3- 9- 19	1	BIT012	3- 9- 10	3- 10- 10	1	BIT003	3- 9- 55	3- 9- 1	1	GND001	3- 10- 30	1- 7- 12	1	L03C22
3- 8- 20	3- 9- 20	1	BIT013	3- 9- 11	3- 8- 11	1	BIT004	3- 9- 55	3- 8- 1	1	GND001	3- 10- 31	1- 7- 13	1	L03C23
3- 8- 20	3- 7- 20	1	BIT013	3- 9- 11	3- 10- 11	1	BIT004	3- 9- 56	3- 9- 2	1	PWR001	3- 10- 32	1- 7- 14	1	L03C24
3- 8- 21	3- 9- 21	1	BIT014	3- 9- 12	3- 8- 12	1	BIT005	3- 9- 56	3- 10- 2	1	PWR001	3- 10- 33	1- 7- 15	1	L03C25
3- 8- 21	3- 7- 21	1	BIT014	3- 9- 12	3- 10- 12	1	BIT005	3- 10- 1	3- 10- 55	1	GND001	3- 10- 34	1- 7- 16	1	L03C26
3- 8- 22	3- 9- 22	1	BIT015	3- 9- 13	3- 8- 13	1	BIT006	3- 10- 1	3- 11- 55	2	GND001	3- 10- 35	1- 7- 17	1	L03C27
3- 8- 22	3- 7- 22	1	BIT015	3- 9- 13	3- 10- 13	1	BIT006	3- 10- 2	3- 10- 56	1	PWR001	3- 10- 36	1- 7- 18	1	L03C28
3- 8- 23	3- 9- 23	1	BIT016	3- 9- 14	3- 8- 14	1	BIT007	3- 10- 2	3- 9- 56	1	PWR001	3- 10- 37	3- 10- 40	1	CONN25
3- 8- 23	3- 7- 23	1	BIT016	3- 9- 14	3- 10- 14	1	BIT007	3- 10- 5	3- 11- 5	1	TIE001	3- 10- 38	3- 10- 39	1	CONN26
3- 8- 25	1- 4- 19	1	L02C09	3- 9- 15	3- 8- 15	1	BIT008	3- 10- 5	3- 9- 5	1	TIE001	3- 10- 39	3- 10- 38	1	CONN26
3- 8- 26	1- 4- 20	1	L02C10	3- 9- 15	3- 10- 15	1	BIT008	3- 10- 6	3- 11- 6	1	TIE002	3- 10- 40	3- 10- 37	1	CONN25
3- 8- 27	1- 4- 21	1	L02C11	3- 9- 16	3- 10- 16	1	BIT009	3- 10- 6	3- 9- 6	1	TIE002	3- 10- 41	1- 7- 19	1	L03C29
3- 8- 28	1- 4- 22	1	L02C12	3- 9- 16	3- 8- 16	1	BIT009	3- 10- 7	3- 4- 24	1	LOAA05	3- 10- 42	1- 7- 20	1	L03C30
3- 8- 29	1- 4- 23	1	L02C13	3- 9- 17	3- 8- 17	1	BIT010	3- 10- 8	3- 9- 8	1	BIT001	3- 10- 43	1- 7- 21	1	L03C31
3- 8- 30	1- 4- 24	1	L02C14	3- 9- 17	3- 10- 17	1	BIT010	3- 10- 8	3- 11- 8	1	BIT001	3- 10- 44	1- 7- 22	1	L03C32

DVI 000326

TABLE VII (CONTINUED)

REFERENCE ROW-CON-PIN	DESTINATION ROW-CON-PIN	LEVEL	SIGNAL NAME	REFERENCE ROW-CON-PIN	DESTINATION ROW-CON-PIN	LEVEL	SIGNAL NAME	REFERENCE ROW-CON-PIN	DESTINATION ROW-CON-PIN	LEVEL	SIGNAL NAME	REFERENCE ROW-CON-PIN	DESTINATION ROW-CON-PIN	LEVEL	SIGNAL NAME
3-10-45	1-7-23	1	L03C33	3-11-27	1-8-13	1	L04C03	3-12-16	3-13-16	1	BIT009	3-13-6	3-14-6	1	TIE002
3-10-46	1-7-24	1	L03C34	3-11-28	1-8-14	1	L04C04	3-12-16	3-11-16	1	BIT009	3-13-7	3-4-9	1	L0AA08
3-10-52	3-4-50	1	L0AB05	3-11-29	1-8-15	1	L04C05	3-12-17	3-13-17	1	BIT010	3-13-8	3-12-8	1	BIT001
3-10-55	3-9-1	1	GND001	3-11-30	1-8-16	1	L04C06	3-12-17	3-11-17	1	BIT010	3-13-8	3-14-8	1	BIT001
3-10-55	3-10-1	1	GND001	3-11-31	1-8-17	1	L04C07	3-12-18	3-11-18	1	BIT011	3-13-9	3-12-9	1	BIT002
3-10-56	3-10-2	1	PWR001	3-11-32	1-8-18	1	L04C08	3-12-18	3-13-18	1	BIT011	3-13-9	3-14-9	1	BIT002
3-10-56	3-11-2	2	PWR001	3-11-33	1-8-19	1	L04C09	3-12-19	3-13-19	1	BIT012	3-13-10	3-12-10	1	BIT003
3-11-1	3-12-55	2	GND001	3-11-34	1-8-20	1	L04C10	3-12-19	3-11-19	1	BIT012	3-13-10	3-14-10	1	BIT003
3-11-1	3-11-55	1	GND001	3-11-35	1-8-21	1	L04C11	3-12-20	3-11-20	1	BIT013	3-13-11	3-12-11	1	BIT004
3-11-2	3-10-56	2	PWR001	3-11-36	1-8-22	1	L04C12	3-12-20	3-13-20	1	BIT013	3-13-11	3-14-11	1	BIT004
3-11-2	3-11-56	1	PWR001	3-11-37	3-11-40	1	CONN31	3-12-21	3-13-21	1	BIT014	3-13-12	3-12-12	1	BIT005
3-11-5	3-10-5	1	TIE001	3-11-38	3-11-39	1	CONN32	3-12-21	3-11-21	1	BIT014	3-13-12	3-14-12	1	BIT005
3-11-5	3-12-5	1	TIE001	3-11-39	3-11-38	1	CONN32	3-12-22	3-13-22	1	BIT015	3-13-13	3-12-13	1	BIT006
3-11-6	3-12-6	1	TIE002	3-11-40	3-11-37	1	CONN31	3-12-22	3-11-22	1	BIT015	3-13-13	3-14-13	1	BIT006
3-11-6	3-10-6	1	TIE002	3-11-41	1-8-23	1	L04C13	3-12-23	3-11-23	1	BIT016	3-13-14	3-14-14	1	BIT007
3-11-7	3-4-52	1	L0AA06	3-11-42	1-8-24	1	L04C14	3-12-23	3-13-23	1	BIT016	3-13-14	3-12-14	1	BIT007
3-11-8	3-10-8	1	BIT001	3-11-43	1-8-25	1	L04C15	3-12-25	1-9-15	1	L04C25	3-13-15	3-14-15	1	BIT008
3-11-8	3-12-8	1	BIT001	3-11-44	1-8-26	1	L04C16	3-12-26	1-9-16	1	L04C26	3-13-15	3-12-15	1	BIT008
3-11-9	3-10-9	1	BIT002	3-11-45	1-8-27	1	L04C17	3-12-27	1-9-17	1	L04C27	3-13-16	3-12-16	1	BIT009
3-11-9	3-12-9	1	BIT002	3-11-46	1-8-28	1	L04C18	3-12-28	1-9-18	1	L04C28	3-13-16	3-14-16	1	BIT009
3-11-10	3-10-10	1	BIT003	3-11-52	3-4-46	1	L0AB06	3-12-29	1-9-19	1	L04C29	3-13-17	3-14-17	1	BIT010
3-11-10	3-12-10	1	BIT003	3-11-55	3-11-1	1	GND001	3-12-30	1-9-20	1	L04C30	3-13-17	3-12-17	1	BIT010
3-11-11	3-10-11	1	BIT004	3-11-55	3-10-1	2	GND001	3-12-31	1-9-21	1	L04C31	3-13-18	3-14-18	1	BIT011
3-11-11	3-12-11	1	BIT004	3-11-56	3-11-2	1	PWR001	3-12-32	1-9-22	1	L04C32	3-13-18	3-12-18	1	BIT011
3-11-12	3-10-12	1	BIT005	3-11-56	3-12-2	2	PWR001	3-12-33	1-9-23	1	L04C33	3-13-19	3-14-19	1	BIT012
3-11-12	3-12-12	1	BIT005	3-12-1	3-13-55	2	GND001	3-12-34	1-9-24	1	L04C34	3-13-19	3-12-19	1	BIT012
3-11-13	3-10-13	1	BIT006	3-12-1	3-12-55	1	GND001	3-12-35	1-9-25	1	L04C35	3-13-20	3-14-20	1	BIT013
3-11-13	3-12-13	1	BIT005	3-12-2	3-12-56	1	PWR001	3-12-36	1-9-26	1	L04C36	3-13-20	3-12-20	1	BIT013
3-11-14	3-10-14	1	BIT007	3-12-2	3-11-56	2	PWR001	3-12-37	3-12-40	1	CONN37	3-13-21	3-12-21	1	BIT014
3-11-14	3-12-14	1	BIT007	3-12-5	3-11-5	1	TIE001	3-12-38	3-12-39	1	CONN38	3-13-21	3-14-21	1	BIT014
3-11-15	3-12-15	1	BIT008	3-12-5	3-13-5	1	TIE001	3-12-39	3-12-38	1	CONN38	3-13-22	3-12-22	1	BIT015
3-11-15	3-10-15	1	BIT008	3-12-6	3-13-6	1	TIE002	3-12-40	3-12-37	1	CONN37	3-13-22	3-14-22	1	BIT015
3-11-16	3-10-16	1	BIT009	3-12-6	3-11-6	1	TIE002	3-12-41	1-9-27	1	L04C37	3-13-23	3-14-23	1	BIT016
3-11-16	3-12-16	1	BIT009	3-12-7	3-4-8	1	L0AA07	3-12-42	1-9-28	1	L04C38	3-13-23	3-12-23	1	BIT016
3-11-17	3-12-17	1	BIT010	3-12-8	3-11-8	1	BIT001	3-12-43	1-9-29	1	L04C39	3-13-25	1-10-19	1	L05C09
3-11-17	3-10-17	1	BIT010	3-12-8	3-13-8	1	BIT001	3-12-44	1-9-30	1	L04C40	3-13-26	1-10-20	1	L05C10
3-11-18	3-10-18	1	BIT011	3-12-9	3-11-9	1	BIT002	3-12-45	1-10-11	1	L05C01	3-13-27	1-10-21	1	L05C11
3-11-18	3-12-18	1	BIT011	3-12-9	3-13-9	1	BIT002	3-12-46	1-10-12	1	L05C02	3-13-28	1-10-22	1	L05C12
3-11-19	3-10-19	1	BIT012	3-12-10	3-11-10	1	BIT003	3-12-52	3-4-7	1	L0AB07	3-13-29	1-10-23	1	L05C13
3-11-19	3-12-19	1	BIT012	3-12-10	3-13-10	1	BIT003	3-12-55	3-12-1	1	GND001	3-13-30	1-10-24	1	L05C14
3-11-20	3-10-20	1	BIT013	3-12-11	3-11-11	1	BIT004	3-12-55	3-11-1	2	GND001	3-13-31	1-10-25	1	L05C15
3-11-20	3-12-20	1	BIT013	3-12-11	3-13-11	1	BIT004	3-12-56	3-12-2	1	PWR001	3-13-32	1-10-26	1	L05C16
3-11-21	3-10-21	1	BIT014	3-12-12	3-11-12	1	BIT005	3-12-56	3-13-2	2	PWR001	3-13-33	1-10-27	1	L05C17
3-11-21	3-12-21	1	BIT014	3-12-12	3-13-12	1	BIT005	3-13-1	3-13-55	1	GND001	3-13-34	1-10-28	1	L05C18
3-11-22	3-12-22	1	BIT015	3-12-13	3-11-13	1	BIT006	3-13-1	3-14-55	2	GND001	3-13-35	1-10-29	1	L05C19
3-11-22	3-10-22	1	BIT015	3-12-13	3-13-13	1	BIT006	3-13-2	3-12-56	2	PWR001	3-13-36	1-10-30	1	L05C20
3-11-23	3-10-23	1	BIT016	3-12-14	3-11-14	1	BIT007	3-13-2	3-13-56	1	PWR001	3-13-37	3-13-40	1	CONN43
3-11-23	3-12-23	1	BIT016	3-12-14	3-13-14	1	BIT007	3-13-5	3-12-5	1	TIE001	3-13-38	3-13-39	1	CONN44
3-11-25	1-8-11	1	L04C01	3-12-15	3-13-15	1	BIT008	3-13-5	3-14-5	1	TIE001	3-13-39	3-13-38	1	CONN44
3-11-26	1-8-12	1	L04C02	3-12-15	3-11-15	1	BIT008	3-13-6	3-12-6	1	TIE002	3-13-40	3-13-37	1	CONN43

DVI 000327

Table VII (Continued)

REFERENCE ROW-CON-PIN	DESTINATION ROW-CON-PIN	LEVEL	SIGNAL NAME
3-13-41	1-11-11	1	L05C21
3-13-42	1-11-12	1	L05C22
3-13-43	1-11-13	1	L05C23
3-13-44	1-11-14	1	L05C24
3-13-45	1-11-15	1	L05C25
3-13-46	1-11-16	1	L05C26
3-13-52	3-4-25	1	LOAA08
3-13-55	3-13-1	1	GND001
3-13-55	3-12-1	2	GND001
3-13-56	3-14-2	2	PWR001
3-13-56	3-13-2	1	PWR001
3-14-1	3-15-55	2	GND001
3-14-1	3-14-55	1	GND001
3-14-2	3-14-56	1	PWR001
3-14-2	3-13-56	2	PWR001
3-14-5	3-13-5	1	TIE001
3-14-5	3-15-5	1	TIE001
3-14-6	3-15-6	1	TIE002
3-14-6	3-13-6	1	TIE002
3-14-7	3-4-27	1	LOAA09
3-14-8	3-13-8	1	BIT001
3-14-8	3-15-8	1	BIT001
3-14-9	3-13-9	1	BIT002
3-14-9	3-15-9	1	BIT002
3-14-10	3-13-10	1	BIT003
3-14-10	3-15-10	1	BIT003
3-14-11	3-13-11	1	BIT004
3-14-11	3-15-11	1	BIT004
3-14-12	3-13-12	1	BIT005
3-14-12	3-15-12	1	BIT005
3-14-13	3-13-13	1	BIT006
3-14-13	3-15-13	1	BIT006
3-14-14	3-13-14	1	BIT007
3-14-14	3-15-14	[illegible]	[illegible]
3-14-15	3-13-15	1	BIT008
3-14-15	3-15-15	1	BIT008
3-14-16	3-15-16	1	BIT009
3-14-16	3-13-16	1	BIT009
3-14-17	3-15-17	1	BIT010
3-14-17	3-13-17	1	BIT010
3-14-18	3-13-18	1	BIT011
3-14-18	3-15-18	1	BIT011
3-14-19	3-13-19	1	BIT012
3-14-19	3-15-19	1	BIT012
3-14-20	3-13-20	1	BIT013
3-14-20	3-15-20	1	BIT013
3-14-21	3-15-21	1	BIT014
3-14-21	3-13-21	1	BIT014
3-14-22	3-13-22	1	BIT015
3-14-22	3-15-22	1	BIT015

REFERENCE ROW-CON-PIN	DESTINATION ROW-CON-PIN	LEVEL	SIGNAL NAME
3-14-23	3-13-23	1	BIT016
3-14-23	3-15-23	1	BIT016
3-14-25	1-11-23	1	L05C33
3-14-26	1-11-24	1	L05C34
3-14-27	1-11-25	1	L05C35
3-14-28	1-11-26	1	L05C36
3-14-29	1-11-27	1	L05C37
3-14-30	1-11-28	1	L05C38
3-14-31	1-11-29	1	L05C39
3-14-32	1-11-30	1	L05C40
3-14-33	1-12-11	1	L06C01
3-14-34	1-12-12	1	L06C02
3-14-35	1-12-13	1	L06C03
3-14-36	1-12-14	1	L06C04
3-14-37	3-14-40	1	CONN49
3-14-38	3-14-39	1	CONN50
3-14-39	3-14-38	1	CONN50
3-14-40	3-14-37	1	CONN49
3-14-41	1-12-15	1	L06C05
3-14-42	1-12-16	1	L06C06
3-14-43	1-12-17	1	L06C07
3-14-44	1-12-18	1	L06C08
3-14-45	1-12-19	1	L06C09
3-14-46	1-12-20	1	L06C10
3-14-52	3-4-28	1	LOAB09
3-14-55	3-14-1	1	GND001
3-14-55	3-13-1	2	GND001
3-14-56	3-15-2	2	PWR001
3-14-56	3-14-2	1	PWR001
3-15-1	3-15-55	1	GND001
3-15-1	3-16-55	2	GND001
3-15-2	3-14-56	2	PWR001
3-15-2	3-15-56	1	PWR001
3-15-5	3-14-5	1	TIE001
3-15-5	3-16-5	1	TIE001
3-15-6	3-16-6	1	TIE002
3-15-6	3-14-6	1	TIE002
3-15-7	3-4-30	1	LOAA10
3-15-8	3-14-8	1	BIT001
3-15-8	3-16-8	1	BIT001
3-15-9	3-14-9	1	BIT002
3-15-9	3-16-9	1	BIT002
3-15-10	3-14-10	1	BIT003
3-15-10	3-16-10	1	BIT003
3-15-11	3-14-11	1	BIT004
3-15-11	3-16-11	1	BIT004
3-15-12	3-14-12	1	BIT005
3-15-12	3-16-12	1	BIT005
3-15-13	3-14-13	1	BIT006
3-15-13	3-16-13	1	BIT006

REFERENCE ROW-CON-PIN	DESTINATION ROW-CON-PIN	LEVEL	SIGNAL NAME
3-15-14	3-14-14	1	BIT007
3-15-14	3-16-14	1	BIT007
3-15-15	3-14-15	1	BIT008
3-15-15	3-16-15	1	BIT008
3-15-16	3-16-16	1	BIT009
3-15-16	3-14-16	1	BIT009
3-15-17	3-14-17	1	BIT010
3-15-17	3-16-17	1	BIT010
3-15-18	3-16-18	1	BIT011
3-15-18	3-14-18	1	BIT011
3-15-19	3-14-19	1	BIT012
3-15-19	3-16-19	1	BIT012
3-15-20	3-16-20	1	BIT013
3-15-20	3-14-20	1	BIT013
3-15-21	3-16-21	1	BIT014
3-15-21	3-14-21	1	BIT014
3-15-22	3-14-22	1	BIT015
3-15-22	3-16-22	1	BIT015
3-15-23	3-14-23	1	BIT016
3-15-23	3-16-23	1	BIT016
3-15-25	1-12-27	1	L06C17
3-15-26	1-12-28	1	L06C18
3-15-27	1-12-29	1	L06C19
3-15-28	1-12-30	1	L06C20
3-15-29	1-13-11	1	L06C21
3-15-30	1-13-12	1	L06C22
3-15-31	1-13-13	1	L06C23
3-15-32	1-13-14	1	L06C24
3-15-33	1-13-15	1	L06C25
3-15-34	1-13-16	1	L06C26
3-15-35	1-13-17	1	L06C27
3-15-36	1-13-18	1	L06C28
3-15-37	3-15-40	1	CONN55
3-15-38	3-15-39	1	CONN55
3-15-39	3-15-38	1	CONN56
3-15-40	3-15-37	1	CONN55
3-15-41	1-13-19	1	L06C29
3-15-42	1-13-20	1	L06C30
3-15-43	1-13-21	1	L06C31
3-15-44	1-13-22	1	L06C32
3-15-45	1-13-23	1	L06C33
3-15-46	1-13-24	1	L06C34
3-15-52	3-4-48	1	LOAB10
3-15-55	3-14-1	2	GND001
3-15-55	3-15-1	1	GND001
3-15-56	3-15-2	1	PWR001
3-15-56	3-16-2	2	PWR001
3-16-1	3-17-55	2	GND001
3-16-1	3-16-55	1	GND001
3-16-2	3-15-56	2	PWR001

REFERENCE ROW-CON-PIN	DESTINATION ROW-CON-PIN	LEVEL	SIGNAL NAME
3-16-2	3-16-56	1	PWR001
3-16-5	3-15-5	1	TIE001
3-16-5	3-17-5	1	TIE001
3-16-6	3-17-6	1	TIE002
3-16-6	3-15-6	1	TIE002
3-16-6	3-16-6	1	TIE002
3-16-6	3-16-6	1	TIE002
3-16-7	3-4-45	1	LOAA11
3-16-8	3-15-8	1	BIT001
3-16-8	3-17-8	1	BIT001
3-16-9	3-17-9	1	BIT002
3-16-9	3-15-9	1	BIT002
3-16-10	3-15-10	1	BIT003
3-16-10	3-17-10	1	BIT003
3-16-11	3-15-11	1	BIT004
3-16-11	3-17-11	1	BIT004
3-16-12	3-15-12	1	BIT005
3-16-12	3-17-12	1	BIT005
3-16-13	3-17-13	1	BIT006
3-16-13	3-15-13	1	BIT006
3-16-14	3-17-14	1	BIT007
3-16-14	3-15-14	1	BIT007
3-16-15	3-15-15	1	BIT008
3-16-15	3-17-15	1	BIT008
3-16-16	3-17-16	1	BIT009
3-16-16	3-15-16	1	BIT009
3-16-17	3-15-17	1	BIT010
3-16-17	3-17-17	1	BIT010
3-16-18	3-15-18	1	BIT011
3-16-18	3-17-18	1	BIT011
3-16-19	3-15-19	1	BIT012
3-16-19	3-17-19	1	BIT012
3-16-20	3-17-20	1	BIT013
3-16-20	3-15-20	1	BIT013
3-16-21	3-15-21	1	BIT014
3-16-21	3-17-21	1	BIT014
3-16-22	3-17-22	1	BIT015
3-16-22	3-15-22	1	BIT015
3-16-23	3-17-23	1	BIT016
3-16-23	3-15-23	1	BIT016
3-16-25	1-14-11	1	L07C01
3-16-26	1-14-12	1	L07C02
3-16-27	1-14-13	1	L07C03
3-16-28	1-14-14	1	L07C04
3-16-29	1-14-15	1	L07C05
3-16-30	1-14-16	1	L07C06
3-16-31	1-14-17	1	L07C07
3-16-32	1-14-18	1	L07C08
3-16-33	1-14-19	1	L07C09
3-16-34	1-14-20	1	L07C10

DVI 000328

TABLE VII (CONTINUED)

REFERENCE ROW-CON-PIN	DESTINATION ROW-CON-PIN	LEVEL	SIGNAL NAME	REFERENCE ROW-CON-PIN	DESTINATION ROW-CON-PIN	LEVEL	SIGNAL NAME
3- 16- 35	1- 14- 21	1	L07C11	3- 17- 20	3- 18- 20	1	BIT013
3- 16- 36	1- 14- 22	1	L07C12	3- 17- 20	3- 16- 20	1	BIT013
3- 16- 37	3- 16- 40	1	CONN61	3- 17- 21	3- 16- 21	1	BIT014
3- 16- 38	3- 16- 39	1	CONN62	3- 17- 21	3- 18- 21	1	BIT014
3- 16- 39	3- 16- 38	1	CONN62	3- 17- 22	3- 16- 22	1	BIT015
3- 16- 40	3- 16- 37	1	CONN61	3- 17- 22	3- 18- 22	1	BIT015
3- 16- 41	1- 14- 23	1	L07C13	3- 17- 23	3- 16- 23	1	BIT016
3- 16- 42	1- 14- 24	1	L07C14	3- 17- 23	3- 18- 23	1	BIT016
3- 16- 43	1- 14- 25	1	L07C15	3- 17- 25	1- 15- 15	1	L07C25
3- 16- 44	1- 14- 26	1	L07C16	3- 17- 26	1- 15- 16	1	L07C26
3- 16- 45	1- 14- 27	1	L07C17	3- 17- 27	1- 15- 17	1	L07C27
3- 16- 46	1- 14- 28	1	L07C18	3- 17- 28	1- 15- 18	1	L07C28
3- 16- 52	3- 4- 47	1	L0AB11	3- 17- 29	1- 15- 19	1	L07C29
3- 16- 55	3- 16- 1	1	GND001	3- 17- 30	1- 15- 20	1	L07C30
3- 16- 55	3- 15- 1	2	GND001	3- 17- 31	1- 15- 21	1	L07C31
3- 16- 56	3- 16- 2	1	PWR001	3- 17- 32	1- 15- 22	1	L07C32
3- 16- 56	3- 17- 2	2	PWR001	3- 17- 33	1- 15- 23	1	L07C33
3- 17- 1	3- 17- 55	1	GND001	3- 17- 34	1- 15- 24	1	L07C34
3- 17- 1	3- 18- 55	2	GND001	3- 17- 35	1- 15- 25	1	L07C35
3- 17- 2	3- 17- 56	1	PWR001	3- 17- 36	1- 15- 26	1	L07C36
3- 17- 2	3- 16- 56	2	PWR001	3- 17- 37	3- 17- 40	1	CONN67
3- 17- 5	3- 16- 5	1	TIE001	3- 17- 38	3- 17- 39	1	CONN68
3- 17- 5	3- 18- 5	1	TIE001	3- 17- 39	3- 17- 38	1	CONN68
3- 17- 6	3- 16- 6	1	TIE002	3- 17- 40	3- 17- 37	1	CONN67
3- 17- 6	3- 18- 6	1	TIE002	3- 17- 41	1- 15- 27	1	L07C37
3- 17- 7	4- 4- 16	1	L0AA12	3- 17- 42	1- 15- 28	1	L07C38
3- 17- 8	3- 16- 8	1	BIT001	3- 17- 43	1- 15- 29	1	L07C39
3- 17- 8	3- 18- 8	1	BIT001	3- 17- 44	1- 15- 30	1	L07C40
3- 17- 9	3- 16- 9	1	BIT002	3- 17- 45	1- 16- 11	1	L08C01
3- 17- 9	3- 18- 9	1	BIT002	3- 17- 46	1- 16- 12	1	L08C02
3- 17- 10	3- 16- 10	1	BIT003	3- 17- 52	4- 4- 9	1	L0AB12
3- 17- 10	3- 18- 10	1	BIT003	3- 17- 55	3- 16- 1	2	GND001
3- 17- 11	3- 16- 11	1	BIT004	3- 17- 55	3- 17- 1	1	GND001
3- 17- 11	3- 18- 11	1	BIT004	3- 17- 56	3- 18- 2	2	PWR001
3- 17- 12	3- 16- 12	1	BIT005	3- 17- 56	3- 17- 2	1	PWR001
3- 17- 12	3- 18- 12	1	BIT005	3- 18- 1	3- 18- 55	1	GND001
3- 17- 13	3- 16- 13	1	BIT006	3- 18- 1	3- 19- 55	2	GND001
3- 17- 13	3- 18- 13	1	BIT006	3- 18- 2	3- 17- 56	2	PWR001
3- 17- 14	3- 16- 14	1	BIT007	3- 18- 2	3- 18- 56	1	PWR001
3- 17- 14	3- 18- 14	1	BIT007	3- 18- 5	3- 17- 5	1	TIE001
3- 17- 15	3- 18- 15	1	BIT008	3- 18- 5	3- 19- 5	1	TIE001
3- 17- 15	3- 16- 15	1	BIT008	3- 18- 6	3- 17- 6	1	TIE002
3- 17- 16	3- 18- 16	1	BIT009	3- 18- 6	3- 19- 6	1	TIE002
3- 17- 16	3- 16- 16	1	BIT009	3- 18- 7	4- 4- 7	1	L0AA13
3- 17- 17	3- 16- 17	1	BIT010	3- 18- 8	3- 17- 8	1	BIT001
3- 17- 17	3- 18- 17	1	BIT010	3- 18- 8	3- 19- 8	1	BIT001
3- 17- 18	3- 18- 18	1	BIT011	3- 18- 9	3- 17- 9	1	BIT002
3- 17- 18	3- 16- 18	1	BIT011	3- 18- 9	3- 19- 9	1	BIT002
3- 17- 19	3- 18- 19	1	BIT012	3- 18- 10	3- 17- 10	1	BIT003
3- 17- 19	3- 16- 19	1	BIT012	3- 18- 10	3- 19- 10	1	BIT003

REFERENCE ROW-CON-PIN	DESTINATION ROW-CON-PIN	LEVEL	SIGNAL NAME	REFERENCE ROW-CON-PIN	DESTINATION ROW-CON-PIN	LEVEL	SIGNAL NAME
3- 18- 11	3- 17- 11	1	BIT004	3- 18- 55	3- 18- 1	1	GND001
3- 18- 11	3- 19- 11	1	BIT004	3- 18- 56	3- 18- 2	1	PWR001
3- 18- 12	3- 17- 12	1	BIT005	3- 18- 56	3- 19- 2	2	PWR001
3- 18- 12	3- 19- 12	1	BIT005	3- 19- 1	3- 20- 55	2	GND001
3- 18- 13	3- 17- 13	1	BIT006	3- 19- 1	3- 19- 55	1	GND001
3- 18- 13	3- 19- 13	1	BIT006	3- 19- 2	3- 18- 56	2	PWR001
3- 18- 14	3- 19- 14	1	BIT007	3- 19- 2	3- 19- 56	1	PWR001
3- 18- 14	3- 17- 14	1	BIT007	3- 19- 5	3- 20- 5	1	TIE001
3- 18- 15	3- 19- 15	1	BIT008	3- 19- 5	3- 18- 5	1	TIE001
3- 18- 15	3- 17- 15	1	BIT008	3- 19- 6	3- 20- 6	1	TIE002
3- 18- 16	3- 17- 16	1	BIT009	3- 19- 6	3- 18- 6	1	TIE002
3- 18- 16	3- 19- 16	1	BIT009	3- 19- 7	4- 4- 10	1	L0AA14
3- 18- 17	3- 19- 17	1	BIT010	3- 19- 8	3- 18- 8	1	BIT001
3- 18- 17	3- 17- 17	1	BIT010	3- 19- 8	3- 20- 8	1	BIT001
3- 18- 18	3- 17- 18	1	BIT011	3- 19- 9	3- 18- 9	1	BIT002
3- 18- 18	3- 19- 18	1	BIT011	3- 19- 9	3- 20- 9	1	BIT002
3- 18- 19	3- 17- 19	1	BIT012	3- 19- 10	3- 18- 10	1	BIT003
3- 18- 19	3- 19- 19	1	BIT012	3- 19- 10	3- 20- 10	1	BIT003
3- 18- 20	3- 17- 20	1	BIT013	3- 19- 11	3- 18- 11	1	BIT004
3- 18- 20	3- 19- 20	1	BIT013	3- 19- 11	3- 20- 11	1	BIT004
3- 18- 21	3- 19- 21	1	BIT014	3- 19- 12	3- 18- 12	1	BIT005
3- 18- 21	3- 17- 21	1	BIT014	3- 19- 12	3- 20- 12	1	BIT005
3- 18- 22	3- 17- 22	1	BIT015	3- 19- 13	3- 20- 13	1	BIT006
3- 18- 22	3- 19- 22	1	BIT015	3- 19- 13	3- 18- 13	1	BIT006
3- 18- 23	3- 19- 23	1	BIT016	3- 19- 14	3- 18- 14	1	BIT007
3- 18- 23	3- 17- 23	1	BIT016	3- 19- 14	3- 20- 14	1	BIT007
3- 18- 25	1- 16- 19	1	L08C09	3- 19- 15	3- 20- 15	1	BIT008
3- 18- 26	1- 16- 20	1	L08C10	3- 19- 15	3- 18- 15	1	BIT008
3- 18- 27	1- 16- 21	1	L08C11	3- 19- 16	3- 20- 16	1	BIT009
3- 18- 28	1- 16- 22	1	L08C12	3- 19- 16	3- 18- 16	1	BIT009
3- 18- 29	1- 16- 23	1	L08C13	3- 19- 17	3- 20- 17	1	BIT010
3- 18- 30	1- 16- 24	1	L08C14	3- 19- 17	3- 18- 17	1	BIT010
3- 18- 31	1- 16- 25	1	L08C15	3- 19- 18	3- 20- 18	1	BIT011
3- 18- 32	1- 16- 26	1	L08C16	3- 19- 18	3- 18- 18	1	BIT011
3- 18- 33	1- 16- 27	1	L08C17	3- 19- 19	3- 20- 19	1	BIT012
3- 18- 34	1- 16- 28	1	L08C18	3- 19- 19	3- 18- 19	1	BIT012
3- 18- 35	1- 16- 29	1	L08C19	3- 19- 20	3- 20- 20	1	BIT013
3- 18- 36	1- 16- 30	1	L08C20	3- 19- 20	3- 18- 20	1	BIT013
3- 18- 37	3- 18- 40	1	CONN73	3- 19- 21	3- 18- 21	1	BIT014
3- 18- 38	3- 18- 39	1	CONN74	3- 19- 21	3- 20- 21	1	BIT014
3- 18- 39	3- 18- 38	1	CONN74	3- 19- 22	3- 18- 22	1	BIT015
3- 18- 40	3- 18- 37	1	CONN73	3- 19- 22	3- 20- 22	1	BIT015
3- 18- 41	1- 17- 11	1	L08C21	3- 19- 23	3- 18- 23	1	BIT016
3- 18- 42	1- 17- 12	1	L08C22	3- 19- 23	3- 20- 23	1	BIT016
3- 18- 43	1- 17- 13	1	L08C23	3- 19- 25	1- 17- 23	1	L08C33
3- 18- 44	1- 17- 14	1	L08C24	3- 19- 26	1- 17- 24	1	L08C34
3- 18- 45	1- 17- 15	1	L08C25	3- 19- 27	1- 17- 25	1	L08C35
3- 18- 46	1- 17- 16	1	L08C26	3- 19- 28	1- 17- 26	1	L08C36
3- 18- 52	4- 4- 8	1	L0AB13	3- 19- 29	1- 17- 27	1	L08C37
3- 18- 55	3- 17- 1	2	GND001	3- 19- 30	1- 17- 28	1	L08C38

DVI 000329

TABLE VII (CONTINUED)

REFERENCE ROW-CON-PIN	DESTINATION ROW-CON-PIN	LEVEL	SIGNAL NAME	REFERENCE ROW-CON-PIN	DESTINATION ROW-CON-PIN	LEVEL	SIGNAL NAME	REFERENCE ROW-CON-PIN	DESTINATION ROW-CON-PIN	LEVEL	SIGNAL NAME	REFERENCE ROW-CON-PIN	DESTINATION ROW-CON-PIN	LEVEL	SIGNAL NAME
3-19-31	1-17-29	1	L08C39	3-20-18	3-19-18	1	BIT011	3-21-9	3-20-9	1	BIT002	3-21-49	1-20-27	1	L10C17
3-19-32	1-17-30	1	L08C40	3-20-18	3-21-18	1	BIT011	3-21-9	3-22-9	1	BIT002	3-21-46	1-20-28	1	L10C18
3-19-33	1-18-11	1	L09C01	3-20-19	3-21-19	1	BIT012	3-21-10	3-22-10	1	BIT003	3-21-52	4-4-44	1	L0AB16
3-19-34	1-18-12	1	L09C02	3-20-19	3-19-19	1	BIT012	3-21-10	3-20-10	1	BIT003	3-21-55	3-21-1	1	GND001
3-19-35	1-18-13	1	L09C03	3-20-20	3-21-20	1	BIT013	3-21-11	3-20-11	1	BIT004	3-21-55	3-20-1	2	GND001
3-19-36	1-18-14	1	L09C04	3-20-20	3-19-20	1	BIT013	3-21-11	3-22-11	1	BIT004	3-21-56	3-21-2	1	PWR001
3-19-37	3-19-40	1	CONN79	3-20-21	3-21-21	1	BIT014	3-21-12	3-22-12	1	BIT005	3-21-56	3-22-2	2	PWR001
3-19-38	3-19-39	1	CONN80	3-20-21	3-19-21	1	BIT014	3-21-12	3-20-12	1	BIT005	3-22-1	3-22-55	1	GND001
3-19-39	3-19-38	1	CONN80	3-20-22	3-21-22	1	BIT015	3-21-13	3-20-13	1	BIT006	3-22-1	4-22-1	2	GND001
3-19-40	3-19-37	1	CONN79	3-20-22	3-19-22	1	BIT015	3-21-13	3-22-13	1	BIT006	3-22-2	3-22-56	1	PWR001
3-19-41	1-18-15	1	L09C05	3-20-23	3-19-23	1	BIT016	3-21-14	3-22-14	1	BIT007	3-22-2	3-21-56	2	PWR001
3-19-42	1-18-16	1	L09C06	3-20-23	3-21-23	1	BIT016	3-21-14	3-20-14	1	BIT007	3-22-5	3-21-5	1	TIE001
3-19-43	1-18-17	1	L09C07	3-20-25	1-18-27	1	L09C17	3-21-15	3-20-15	1	BIT008	3-22-6	3-21-6	1	TIE002
3-19-44	1-18-18	1	L09C08	3-20-26	1-18-28	1	L09C18	3-21-15	3-22-15	1	BIT008	3-22-7	4-4-13	1	L0AA17
3-19-45	1-18-19	1	L09C09	3-20-27	1-18-29	1	L09C19	3-21-16	3-22-16	1	BIT009	3-22-8	3-21-8	1	BIT001
3-19-46	1-18-20	1	L09C10	3-20-28	1-18-30	1	L09C20	3-21-16	3-20-16	1	BIT009	3-22-9	3-21-9	1	BIT002
3-19-52	4-4-11	1	L0AB14	3-20-29	1-19-11	1	L09C21	3-21-17	3-22-17	1	BIT010	3-22-10	3-21-10	1	BIT003
3-19-55	3-19-1	1	GND001	3-20-30	1-19-12	1	L09C22	3-21-17	3-20-17	1	BIT010	3-22-11	3-21-11	1	BIT004
3-19-55	3-18-1	2	GND001	3-20-31	1-19-13	1	L09C23	3-21-18	3-20-18	1	BIT011	3-22-12	3-21-12	1	BIT005
3-19-56	3-19-2	1	PWR001	3-20-32	1-19-14	1	L09C24	3-21-18	3-22-18	1	BIT011	3-22-13	3-21-13	1	BIT006
3-19-56	3-20-2	2	PWR001	3-20-33	1-19-15	1	L09C25	3-21-19	3-22-19	1	BIT012	3-22-14	3-21-14	1	BIT007
3-20-1	3-21-55	2	GND001	3-20-34	1-19-16	1	L09C26	3-21-19	3-20-19	1	BIT012	3-22-15	3-21-15	1	BIT008
3-20-1	3-20-55	1	GND001	3-20-35	1-19-17	1	L09C27	3-21-20	3-22-20	1	BIT013	3-22-16	3-21-16	1	BIT009
3-20-2	3-19-56	2	PWR001	3-20-36	1-19-18	1	L09C28	3-21-20	3-20-20	1	BIT013	3-22-17	3-21-17	1	BIT010
3-20-2	3-20-56	1	PWR001	3-20-37	3-20-40	1	CONN85	3-21-21	3-20-21	1	BIT014	3-22-18	3-21-18	1	BIT011
3-20-5	3-19-5	1	TIE001	3-20-38	3-20-39	1	CONN86	3-21-21	3-22-21	1	BIT014	3-22-19	3-21-19	1	BIT012
3-20-5	3-21-5	1	TIE001	3-20-39	3-20-38	1	CONN86	3-21-22	3-20-22	1	BIT015	3-22-20	3-21-20	1	BIT013
3-20-6	3-21-6	1	TIE002	3-20-40	3-20-37	1	CONN85	3-21-22	3-22-22	1	BIT015	3-22-21	3-21-21	1	BIT014
3-20-6	3-19-6	1	TIE002	3-20-41	1-19-19	1	L09C29	3-21-23	3-22-23	1	BIT016	3-22-22	3-21-22	1	BIT015
3-20-7	4-4-41	1	L0AA15	3-20-42	1-19-20	1	L09C30	3-21-23	3-20-23	1	BIT016	3-22-23	3-21-23	1	BIT016
3-20-8	3-19-8	1	BIT001	3-20-43	1-19-21	1	L09C31	3-21-25	1-20-11	1	L10C01	3-22-25	1-21-15	1	L10C25
3-20-8	3-21-8	1	BIT001	3-20-44	1-19-22	1	L09C32	3-21-26	1-20-12	1	L10C02	3-22-26	1-21-16	1	L10C26
3-20-9	3-21-9	1	BIT002	3-20-45	1-19-23	1	L09C33	3-21-27	1-20-13	1	L10C03	3-22-27	1-21-17	1	L10C27
3-20-9	3-19-9	1	BIT002	3-20-46	1-19-24	1	L09C34	3-21-28	1-20-14	1	L10C04	3-22-28	1-21-18	1	L10C28
3-20-10	3-19-10	1	BIT003	3-20-52	4-4-42	1	L0AB15	3-21-29	1-20-15	1	L10C05	3-22-29	1-21-19	1	L10C29
3-20-10	3-21-10	1	BIT003	3-20-55	3-20-1	1	GND001	3-21-30	1-20-16	1	L10C06	3-22-30	1-21-20	1	L10C30
3-20-11	3-19-11	1	BIT004	3-20-55	3-19-1	2	GND001	3-21-31	1-20-17	1	L10C07	3-22-31	1-21-21	1	L10C31
3-20-11	3-21-11	1	BIT004	3-20-56	3-21-2	2	PWR001	3-21-32	1-20-18	1	L10C08	3-22-32	1-21-22	1	L10C32
3-20-12	3-19-12	1	BIT005	3-20-56	3-20-2	1	PWR001	3-21-33	1-20-19	1	L10C09	3-22-33	1-21-23	1	L10C33
3-20-12	3-21-12	1	BIT005	3-21-1	3-21-55	1	GND001	3-21-34	1-20-20	1	L10C10	3-22-34	1-21-24	1	L10C34
3-20-13	3-21-13	1	BIT006	3-21-1	3-22-55	2	GND001	3-21-35	1-20-21	1	L10C11	3-22-35	1-21-25	1	L10C35
3-20-13	3-19-13	1	BIT006	3-21-2	3-22-56	2	PWR001	3-21-36	1-20-22	1	L10C12	3-22-36	1-21-26	1	L10C36
3-20-14	3-19-14	1	BIT007	3-21-2	3-21-56	1	PWR001	3-21-37	3-21-40	1	CONN91	3-22-37	3-22-40	1	CONN97
3-20-14	3-21-14	1	BIT007	3-21-5	3-22-5	1	TIE001	3-21-38	3-21-39	1	CONN92	3-22-38	3-22-39	1	CONN98
3-20-15	3-21-15	1	BIT008	3-21-5	3-20-5	1	TIE001	3-21-39	3-21-38	1	CONN92	3-22-39	3-22-38	1	CONN98
3-20-15	3-19-15	1	BIT008	3-21-6	3-22-6	1	TIE002	3-21-40	3-21-37	1	CONN91	3-22-40	3-22-37	1	CONN97
3-20-16	3-19-16	1	BIT009	3-21-6	3-20-6	1	TIE002	3-21-41	1-20-23	1	L10C13	3-22-41	1-21-27	1	L10C37
3-20-16	3-21-16	1	BIT009	3-21-7	4-4-52	1	L0AA16	3-21-42	1-20-24	1	L10C14	3-22-42	1-21-28	1	L10C38
3-20-17	3-21-17	1	BIT010	3-21-8	3-20-8	1	BIT001	3-21-43	1-20-25	1	L10C15	3-22-43	1-21-29	1	L10C39
3-20-17	3-19-17	1	BIT010	3-21-8	3-22-8	1	BIT001	3-21-44	1-20-26	1	L10C16	3-22-44	1-21-30	1	L10C40

DVI 000330

TABLE VII (CONTINUED)

REFERENCE ROW-CON-PIN	DESTINATION ROW-CON-PIN	LEVEL	SIGNAL NAME
3-22-52	4-4-14	1	LOAB17
3-22-55	3-21-1	2	GND001
3-22-55	3-22-1	1	GND001
3-22-56	3-22-2	1	PWR001
3-22-56	4-22-2	2	PWR001
4-1-1	4-1-55	2	GND001
4-1-1	4-2-2	1	GND001
4-1-2	4-1-56	2	GND001
4-1-2	4-6-29	1	GND001
4-1-3	4-2-54	1	PWR001
4-1-3	4-1-4	2	PWR001
4-1-4	4-1-53	1	PWR001
4-1-4	4-1-3	2	PWR001
4-1-30	1-21-3	2	ALTGND
4-1-30	4-1-31	1	ALTGND
4-1-31	4-1-30	1	ALTGND
4-1-34	1-21-1	1	DR1GND
4-1-34	4-1-35	2	DR1GND
4-1-35	4-1-34	2	DR1GND
4-1-38	1-21-4	2	DR1HVL
4-1-38	4-1-39	1	DR1HVL
4-1-39	4-1-38	1	DR1HVL
4-1-41	1-21-5	2	DRHHVL
4-1-41	4-1-42	1	DRHHVL
4-1-42	4-1-41	1	DRHHVL
4-1-45	4-1-46	2	PFVL01
4-1-45	1-21-2	1	PFVL01
4-1-46	4-1-45	2	PFVL01
4-1-53	4-1-4	1	PWR001
4-1-53	4-1-54	2	PWR001
4-1-54	4-1-53	2	PWR001
4-1-55	4-1-56	1	GND001
4-1-55	4-1-1	2	GND001
4-1-56	4-1-55	1	GND001
4-1-56	4-1-2	2	GND001
4-2-1	4-4-2	1	GND001
4-2-1	4-2-55	2	GND001
4-2-2	4-1-1	1	GND001
4-2-2	4-2-56	2	GND001
4-2-3	4-4-54	1	PWR001
4-2-3	4-2-4	2	PWR001
4-2-4	4-2-3	2	PWR001
4-2-4	4-2-53	1	PWR001
4-2-7	4-4-25	1	DATRED
4-2-8	3-1-47	1	NDTRED
4-2-10	3-1-48	1	GNDNDR
4-2-53	4-2-4	1	PWR001
4-2-53	4-2-54	2	PWR001
4-2-54	4-2-53	2	PWR001
4-2-54	4-1-3	1	PWR001

REFERENCE ROW-CON-PIN	DESTINATION ROW-CON-PIN	LEVEL	SIGNAL NAME
4-2-55	4-2-56	1	GND001
4-2-55	4-2-1	2	GND001
4-2-56	4-2-2	2	GND001
4-2-56	4-2-55	1	GND001
4-4-1	4-6-55	2	GND001
4-4-1	4-4-55	1	GND001
4-4-2	4-4-56	2	GND001
4-4-2	4-2-1	1	GND001
4-4-3	4-6-56	2	PWR001
4-4-3	4-4-4	1	PWR001
4-4-4	4-4-53	1	PWR001
4-4-4	4-4-3	1	PWR001
4-4-5	3-17-52	1	LOAB12
4-4-6	4-17-16	1	LOAC12
4-4-7	3-18-7	1	LOAA13
4-4-8	3-18-52	1	LOAB13
4-4-9	4-18-16	1	LOAC13
4-4-10	3-19-7	1	LOAA14
4-4-11	3-19-52	1	LOAB14
4-4-12	4-21-16	1	LOAC16
4-4-13	3-22-7	1	LOAA17
4-4-14	3-22-52	1	LOAB17
4-4-16	3-17-7	1	LOAA12
4-4-17	1-1-8	1	NXTCLM
4-4-17	4-6-28	1	NXTCLM
4-4-18	3-6-52	1	LOAB01
4-4-21	4-16-16	1	LOAC11
4-4-25	4-2-7	1	DATRED
4-4-37	1-21-10	1	A1SC19
4-4-40	4-19-16	1	LOAC14
4-4-41	3-20-7	1	LOAA15
4-4-42	3-20-52	1	LOAB15
4-4-44	3-21-52	1	LOAB16
4-4-45	3-1-42	1	STROBR
4-4-46	3-1-41	1	STROBE
4-4-47	3-1-44	1	FMSYNR
4-4-48	3-1-43	1	FMSYNC
4-4-50	3-6-7	1	LOAA01
4-4-51	4-20-16	1	LOAC15
4-4-52	3-21-7	1	LOAA16
4-4-53	4-4-54	2	PWR001
4-4-53	4-4-4	1	PWR001
4-4-54	4-2-3	1	PWR001
4-4-54	4-4-53	2	PWR001
4-4-55	4-4-56	1	GND001
4-4-55	4-4-1	1	GND001
4-4-56	4-4-2	2	GND001
4-4-56	4-4-55	1	GND001
4-6-1	4-6-55	1	GND001
4-6-1	4-7-55	1	GND001

REFERENCE ROW-CON-PIN	DESTINATION ROW-CON-PIN	LEVEL	SIGNAL NAME
4-6-2	4-7-56	1	PWR001
4-6-2	4-6-56	1	PWR001
4-6-3	4-6-7	1	CONN03
4-6-5	4-6-6	1	CONN04
4-6-6	4-6-5	1	CONN04
4-6-7	4-6-3	1	CONN03
4-6-8	1-2-29	1	L01C19
4-6-9	1-2-30	1	L01C20
4-6-10	1-3-11	1	L01C21
4-6-11	1-3-12	1	L01C22
4-6-12	1-3-13	1	L01C23
4-6-13	1-3-14	1	L01C24
4-6-14	4-7-14	1	TIE003
4-6-16	3-4-14	1	LOAC01
4-6-25	1-1-20	1	GRAY01
4-6-25	4-7-26	1	GRAY01
4-6-27	1-1-22	1	GRAY02
4-6-27	4-7-27	1	GRAY02
4-6-28	4-4-17	1	NXTCLM
4-6-28	4-7-28	1	NXTCLM
4-6-29	4-1-2	1	GND001
4-6-29	4-7-29	2	GND001
4-6-40	4-6-52	1	CONN05
4-6-42	4-6-50	1	CONN06
4-6-50	4-6-42	1	CONN06
4-6-52	4-6-40	1	CONN05
4-6-55	4-6-1	1	GND001
4-6-55	4-4-1	2	GND001
4-6-56	4-4-3	2	PWR001
4-6-56	4-6-2	1	PWR001
4-7-1	4-7-55	1	GND001
4-7-1	4-8-55	1	GND001
4-7-2	4-8-56	1	PWR001
4-7-2	4-7-56	1	PWR001
4-7-3	4-7-7	1	CONN09
4-7-5	4-7-6	1	CONN10
4-7-6	4-7-5	1	CONN10
4-7-7	4-7-3	1	CONN09
4-7-8	1-4-13	1	L02C03
4-7-9	1-4-14	1	L02C04
4-7-10	1-4-15	1	L02C05
4-7-11	1-4-16	1	L02C06
4-7-12	1-4-17	1	L02C07
4-7-13	1-4-18	1	L02C08
4-7-14	4-8-14	1	TIE003
4-7-14	4-6-14	1	TIE003
4-7-15	3-4-17	1	LOAC02
4-7-25	4-8-26	1	GRAY01
4-7-26	4-6-26	1	GRAY01
4-7-27	4-8-27	1	GRAY02

REFERENCE ROW-CON-PIN	DESTINATION ROW-CON-PIN	LEVEL	SIGNAL NAME
4-7-27	4-6-27	1	GRAY02
4-7-28	4-6-28	1	NXTCLM
4-7-28	4-8-28	1	NXTCLM
4-7-29	4-8-29	1	GND001
4-7-29	4-6-29	2	GND001
4-7-40	4-7-52	1	CONN11
4-7-42	4-7-50	1	CONN12
4-7-50	4-7-42	1	CONN12
4-7-52	4-7-40	1	CONN11
4-7-55	4-6-1	1	GND001
4-7-55	4-7-1	1	GND001
4-7-56	4-6-2	1	PWR001
4-7-56	4-7-2	1	PWR001
4-8-1	4-8-55	1	GND001
4-8-1	4-8-55	1	GND001
4-8-2	4-8-56	1	PWR001
4-8-2	4-9-56	1	PWR001
4-8-3	4-8-7	1	CONN15
4-8-5	4-8-6	1	CONN16
4-8-6	4-8-5	1	CONN16
4-8-7	4-8-3	1	CONN15
4-8-8	1-5-17	1	L02C27
4-8-9	1-5-18	1	L02C28
4-8-10	1-5-19	1	L02C29
4-8-11	1-5-20	1	L02C30
4-8-12	1-5-21	1	L02C31
4-8-13	1-5-22	1	L02C32
4-8-14	4-9-14	1	TIE003
4-8-14	4-7-14	1	TIE003
4-8-16	3-4-20	1	LOAC03
4-8-26	4-7-26	1	GRAY01
4-8-26	4-9-26	1	GRAY01
4-8-27	4-7-27	1	GRAY02
4-8-27	4-9-27	1	GRAY02
4-8-28	4-7-28	1	NXTCLM
4-8-28	4-9-28	1	NXTCLM
4-8-29	4-9-29	2	GND001
4-8-29	4-7-29	1	GND001
4-8-40	4-8-52	1	CONN17
4-8-42	4-8-50	1	CONN18
4-8-50	4-8-42	1	CONN18
4-8-52	4-8-40	1	CONN17
4-8-55	4-7-1	1	GND001
4-8-55	4-8-1	1	GND001
4-8-56	4-8-2	1	PWR001
4-8-56	4-7-2	1	PWR001
4-9-1	4-10-55	1	GND001
4-9-1	4-9-55	1	GND001
4-9-2	4-10-56	1	PWR001
4-9-2	4-9-56	1	PWR001

DVI 000331

TABLE VII (CONTINUED)

REFERENCE ROW-CON-PIN	DESTINATION ROW-CON-PIN	LEVEL	SIGNAL NAME
4-9-3	4-9-7	1	CONN21
4-9-5	4-9-6	1	CONN22
4-9-6	4-9-5	1	CONN22
4-9-7	4-9-3	1	CONN21
4-9-8	1-6-21	1	LO3C11
4-9-9	1-6-22	1	LO3C12
4-9-10	1-6-23	1	LO3C13
4-9-11	1-6-24	1	LO3C14
4-9-12	1-6-25	1	LO3C15
4-9-13	1-6-26	1	LO3C16
4-9-14	4-10-14	1	TIE003
4-9-14	4-8-14	1	TIE003
4-9-16	3-4-23	1	LOAC04
4-9-26	4-8-26	1	GRAY01
4-9-26	4-10-26	1	GRAY01
4-9-27	4-10-27	1	GRAY02
4-9-27	4-8-27	1	GRAY02
4-9-28	4-10-28	1	NXTCLM
4-9-28	4-8-28	1	NXTCLM
4-9-29	4-10-29	1	GND001
4-9-29	4-8-29	2	GND001
4-9-40	4-9-52	1	CONN23
4-9-42	4-9-50	1	CONN24
4-9-50	4-9-42	1	CONN24
4-9-52	4-9-40	1	CONN23
4-9-55	4-8-1	1	GND001
4-9-55	4-9-1	1	GND001
4-9-56	4-8-2	1	PWR001
4-9-56	4-9-2	1	PWR001
4-10-1	4-11-55	1	GND001
4-10-1	4-10-55	1	GND001
4-10-2	4-10-56	1	PWR001
4-10-2	4-11-56	1	PWR001
4-10-3	4-10-7	1	CONN27
4-10-5	4-10-6	1	CONN25
4-10-6	4-10-5	1	CONN23
4-10-7	4-10-3	1	CONN27
4-10-8	1-7-25	1	LO3C35
4-10-9	1-7-26	1	LO3C36
4-10-10	1-7-27	1	LO3C37
4-10-11	1-7-28	1	LO3C38
4-10-12	1-7-29	1	LO3C39
4-10-13	1-7-30	1	LO3C40
4-10-14	4-11-14	1	TIE003
4-10-14	4-9-14	1	TIE003
4-10-16	3-4-51	1	LOAC05
4-10-26	4-11-26	1	GRAY01
4-10-26	4-9-26	1	GRAY01
4-10-27	4-9-27	1	GRAY02
4-10-27	4-11-27	1	GRAY02

REFERENCE ROW-CON-PIN	DESTINATION ROW-CON-PIN	LEVEL	SIGNAL NAME
4-10-28	4-9-28	1	NXTCLM
4-10-28	4-11-28	1	NXTCLM
4-10-29	4-9-29	1	GND001
4-10-29	4-11-29	2	GND001
4-10-40	4-10-52	1	CONN29
4-10-42	4-10-50	1	CONN30
4-10-50	4-10-42	1	CONN30
4-10-52	4-10-40	1	CONN29
4-10-55	4-9-1	1	GND001
4-10-55	4-10-1	1	GND001
4-10-56	4-10-2	1	PWR001
4-10-56	4-9-2	1	PWR001
4-11-1	4-12-55	1	GND001
4-11-1	4-11-55	1	GND001
4-11-2	4-12-56	1	PWR001
4-11-2	4-11-56	1	PWR001
4-11-3	4-11-7	1	CONN33
4-11-5	4-11-6	1	CONN34
4-11-6	4-11-5	1	CONN34
4-11-7	4-11-3	1	CONN33
4-11-8	1-8-29	1	LO4C19
4-11-9	1-8-30	1	LO4C20
4-11-10	1-9-11	1	LO4C21
4-11-11	1-9-12	1	LO4C22
4-11-12	1-9-13	1	LO4C23
4-11-13	1-9-14	1	LO4C24
4-11-14	4-10-14	1	TIE003
4-11-14	4-12-14	1	TIE003
4-11-16	3-4-5	1	LOAC06
4-11-26	4-12-26	1	GRAY01
4-11-26	4-10-26	1	GRAY01
4-11-27	4-12-27	1	GRAY02
4-11-27	4-10-27	1	GRAY02
4-11-28	4-12-28	1	NXTCLM
4-11-28	4-10-28	1	NXTCLM
4-11-29	4-10-29	2	GND001
4-11-29	4-12-29	1	GND001
4-11-40	4-11-52	1	CONN35
4-11-42	4-11-50	1	CONN36
4-11-50	4-11-42	1	CONN36
4-11-52	4-11-40	1	CONN35
4-11-55	4-10-1	1	GND001
4-11-55	4-11-1	1	GND001
4-11-56	4-10-2	1	PWR001
4-11-56	4-11-2	1	PWR001
4-12-1	4-12-55	1	GND001
4-12-1	4-13-55	1	GND001
4-12-2	4-12-56	1	PWR001
4-12-2	4-13-56	1	PWR001
4-12-3	4-12-7	1	CONN39

REFERENCE ROW-CON-PIN	DESTINATION ROW-CON-PIN	LEVEL	SIGNAL NAME
4-12-5	4-12-6	1	CONN40
4-12-6	4-12-5	1	CONN40
4-12-7	4-12-3	1	CONN39
4-12-8	1-10-13	1	LO5C03
4-12-9	1-10-14	1	LO5C04
4-12-10	1-10-15	1	LO5C05
4-12-11	1-10-16	1	LO5C06
4-12-12	1-10-17	1	LO5C07
4-12-13	1-10-18	1	LO5C08
4-12-14	4-11-14	1	TIE003
4-12-14	4-13-14	1	TIE003
4-12-16	3-4-8	1	LOAC07
4-12-26	4-13-26	1	GRAY01
4-12-26	4-11-26	1	GRAY01
4-12-27	4-11-27	1	GRAY02
4-12-27	4-13-27	1	GRAY02
4-12-28	4-11-28	1	NXTCLM
4-12-28	4-13-28	1	NXTCLM
4-12-29	4-13-29	2	GND001
4-12-29	4-11-29	1	GND001
4-12-40	4-12-52	1	CONN41
4-12-42	4-12-50	1	CONN42
4-12-50	4-12-42	1	CONN42
4-12-52	4-12-40	1	CONN41
4-12-55	4-11-1	1	GND001
4-12-55	4-12-1	1	GND001
4-12-56	4-12-2	1	PWR001
4-12-56	4-11-2	1	PWR001
4-13-1	4-13-55	1	GND001
4-13-1	4-14-55	1	GND001
4-13-2	4-13-56	1	PWR001
4-13-2	4-14-56	1	PWR001
4-13-3	4-13-7	1	CONN45
4-13-5	4-13-6	1	CONN46
4-13-6	4-13-5	1	CONN46
4-13-7	4-13-3	1	CONN45
4-13-8	1-11-17	1	LO5C27
4-13-9	1-11-18	1	LO5C28
4-13-10	1-11-19	1	LO5C29
4-13-11	1-11-20	1	LO5C30
4-13-12	1-11-21	1	LO5C31
4-13-13	1-11-22	1	LO5C32
4-13-14	4-14-14	1	TIE003
4-13-14	4-12-14	1	TIE003
4-13-16	3-4-26	1	LOAC08
4-13-26	4-12-26	1	GRAY01
4-13-26	4-14-26	1	GRAY01
4-13-27	4-14-27	1	GRAY02
4-13-27	4-12-27	1	GRAY02
4-13-28	4-14-28	1	NXTCLM

REFERENCE ROW-CON-PIN	DESTINATION ROW-CON-PIN	LEVEL	SIGNAL NAME
4-13-28	4-12-28	1	NXTCLM
4-13-29	4-14-29	1	GND001
4-13-29	4-12-29	2	GND001
4-13-40	4-13-52	1	CONN47
4-13-42	4-13-50	1	CONN48
4-13-50	4-13-42	1	CONN48
4-13-52	4-13-40	1	CONN47
4-13-55	4-13-1	1	GND001
4-13-55	4-12-1	1	GND001
4-13-56	4-13-2	1	PWR001
4-13-56	4-12-2	1	PWR001
4-14-1	4-15-55	1	GND001
4-14-1	4-14-55	1	GND001
4-14-2	4-14-56	1	PWR001
4-14-2	4-15-56	1	PWR001
4-14-3	4-14-7	1	CONN51
4-14-5	4-14-6	1	CONN52
4-14-6	4-14-5	1	CONN52
4-14-7	4-14-3	1	CONN51
4-14-8	1-12-21	1	LO6C11
4-14-9	1-12-22	1	LO6C12
4-14-10	1-12-23	1	LO6C13
4-14-11	1-12-24	1	LO6C14
4-14-12	1-12-25	1	LO6C15
4-14-13	1-12-26	1	LO6C16
4-14-14	4-15-14	1	TIE003
4-14-14	4-13-14	1	TIE003
4-14-16	3-4-29	1	LOAC09
4-14-26	4-13-26	1	GRAY01
4-14-26	4-15-26	1	GRAY01
4-14-27	4-13-27	1	GRAY02
4-14-27	4-15-27	1	GRAY02
4-14-28	4-13-28	1	NXTCLM
4-14-28	4-15-28	1	NXTCLM
4-14-29	4-15-29	2	GND001
4-14-29	4-13-29	1	GND001
4-14-40	4-14-52	1	CONN53
4-14-42	4-14-50	1	CONN54
4-14-50	4-14-42	1	CONN54
4-14-52	4-14-40	1	CONN53
4-14-55	4-13-1	1	GND001
4-14-55	4-14-1	1	GND001
4-14-56	4-14-2	1	PWR001
4-14-56	4-13-2	1	PWR001
4-15-1	4-16-55	2	GND001
4-15-1	4-15-55	1	GND001
4-15-2	4-15-56	1	PWR001
4-15-2	4-16-56	2	PWR001
4-15-3	4-15-7	1	CONN57
4-15-5	4-15-6	1	CONN58

DVI 000332

TABLE VII (CONTINUED)

REFERENCE ROW-CON-PIN	DESTINATION ROW-CON-PIN	LEVEL	SIGNAL NAME	REFERENCE ROW-CON-PIN	DESTINATION ROW-CON-PIN	LEVEL	SIGNAL NAME	REFERENCE ROW-CON-PIN	DESTINATION ROW-CON-PIN	LEVEL	SIGNAL NAME	REFERENCE ROW-CON-PIN	DESTINATION ROW-CON-PIN	LEVEL	SIGNAL NAME
4- 15- 6	4- 15- 5	1	CONN98	4- 16- 29	4- 15- 29	1	GND001	4- 18- 7	4- 18- 3	1	CONN75	4- 19- 29	4- 20- 29	2	GND001
4- 15- 7	4- 15- 3	1	CONN97	4- 16- 29	4- 17- 29	1	GND001	4- 18- 8	1- 17- 17	1	L08C27	4- 19- 40	4- 19- 52	1	CONN83
4- 15- 8	1- 13- 25	1	L06C35	4- 16- 40	4- 16- 52	1	CONN65	4- 18- 9	1- 17- 18	1	L08C28	4- 19- 42	4- 19- 50	1	CONN84
4- 15- 9	1- 13- 26	1	L06C36	4- 16- 42	4- 16- 50	1	CONN66	4- 18- 10	1- 17- 19	1	L08C29	4- 19- 50	4- 19- 42	1	CONN84
4- 15- 10	1- 13- 27	1	L06C37	4- 16- 50	4- 16- 42	1	CONN66	4- 18- 11	1- 17- 20	1	L08C30	4- 19- 52	4- 19- 40	1	CONN83
4- 15- 11	1- 13- 28	1	L06C38	4- 16- 52	4- 16- 40	1	CONN65	4- 18- 12	1- 17- 21	1	L08C31	4- 19- 55	4- 18- 1	2	GND001
4- 15- 12	1- 13- 29	1	L06C39	4- 16- 55	4- 16- 1	1	GND001	4- 18- 13	1- 17- 22	1	L08C32	4- 19- 55	4- 19- 1	1	GND001
4- 15- 13	1- 13- 30	1	L06C40	4- 16- 55	4- 15- 1	2	GND001	4- 18- 14	4- 17- 14	1	TIE003	4- 19- 56	4- 18- 2	2	PWR001
4- 15- 14	4- 14- 14	1	TIE003	4- 16- 56	4- 16- 2	1	PWR001	4- 18- 14	4- 19- 14	1	TIE003	4- 19- 56	4- 19- 2	1	PWR001
4- 15- 14	4- 16- 14	1	TIE003	4- 16- 56	4- 15- 2	2	PWR001	4- 18- 16	4- 4- 9	1	LOAC13	4- 20- 1	4- 20- 55	1	GND001
4- 15- 16	3- 4- 49	1	LOAC10	4- 17- 1	4- 18- 55	2	GND001	4- 18- 26	4- 19- 26	1	GRAY01	4- 20- 1	4- 21- 55	2	GND001
4- 15- 26	4- 14- 26	1	GRAY01	4- 17- 1	4- 17- 55	1	GND001	4- 18- 26	4- 17- 26	1	GRAY01	4- 20- 2	4- 20- 56	1	PWR001
4- 15- 26	4- 16- 26	1	GRAY01	4- 17- 2	4- 17- 56	1	PWR001	4- 18- 27	4- 19- 27	1	GRAY02	4- 20- 2	4- 21- 56	2	PWR001
4- 15- 27	4- 14- 27	1	GRAY02	4- 17- 2	4- 18- 56	2	PWR001	4- 18- 27	4- 17- 27	1	GRAY02	4- 20- 3	4- 20- 7	1	CONN87
4- 15- 27	4- 16- 27	1	GRAY02	4- 17- 3	4- 17- 7	1	CONN69	4- 18- 28	4- 19- 28	1	NXTCLM	4- 20- 5	4- 20- 6	1	CONN88
4- 15- 28	4- 16- 28	1	NXTCLM	4- 17- 5	4- 17- 6	1	CONN70	4- 18- 28	4- 17- 28	1	NXTCLM	4- 20- 6	4- 20- 5	1	CONN88
4- 15- 28	4- 14- 28	1	NXTCLM	4- 17- 6	4- 17- 5	1	CONN70	4- 18- 29	4- 17- 29	2	GND001	4- 20- 7	4- 20- 3	1	CONN87
4- 15- 29	4- 16- 29	1	GND001	4- 17- 7	4- 17- 3	1	CONN69	4- 18- 29	4- 19- 29	1	GND001	4- 20- 8	1- 19- 25	1	L09C35
4- 15- 29	4- 14- 29	2	GND001	4- 17- 8	1- 16- 13	1	L08C03	4- 18- 40	4- 18- 52	1	CONN77	4- 20- 9	1- 19- 26	1	L09C36
4- 15- 40	4- 15- 52	1	CONN59	4- 17- 9	1- 16- 14	1	L08C04	4- 18- 42	4- 18- 50	1	CONN78	4- 20- 10	1- 19- 27	1	L09C37
4- 15- 42	4- 15- 50	1	CONN60	4- 17- 10	1- 16- 15	1	L08C05	4- 18- 50	4- 18- 42	1	CONN78	4- 20- 11	1- 19- 28	1	L09C38
4- 15- 50	4- 15- 42	1	CONN60	4- 17- 11	1- 16- 16	1	L08C06	4- 18- 52	4- 18- 40	1	CONN77	4- 20- 12	1- 19- 29	1	L09C39
4- 15- 52	4- 15- 40	1	CONN59	4- 17- 12	1- 16- 17	1	L08C07	4- 18- 55	4- 17- 1	2	GND001	4- 20- 13	1- 19- 30	1	L09C40
4- 15- 55	4- 14- 1	1	GND001	4- 17- 13	1- 16- 18	1	L08C08	4- 18- 55	4- 18- 1	1	GND001	4- 20- 14	4- 21- 14	1	TIE003
4- 15- 55	4- 15- 1	1	GND001	4- 17- 14	4- 18- 14	1	TIE003	4- 18- 56	4- 18- 2	1	PWR001	4- 20- 14	4- 19- 14	1	TIE003
4- 15- 56	4- 14- 2	1	PWR001	4- 17- 14	4- 16- 14	1	TIE003	4- 18- 56	4- 17- 2	2	PWR001	4- 20- 16	4- 4- 51	1	LOAC15
4- 15- 55	4- 15- 2	1	PWR001	4- 17- 16	4- 4- 6	1	LOAC12	4- 19- 1	4- 20- 55	2	GND001	4- 20- 26	4- 19- 26	1	GRAY01
4- 16- 1	4- 16- 55	1	GND001	4- 17- 26	4- 18- 26	1	GRAY01	4- 19- 1	4- 19- 55	1	GND001	4- 20- 26	4- 21- 26	1	GRAY01
4- 16- 1	4- 17- 55	1	GND001	4- 17- 26	4- 16- 26	1	GRAY01	4- 19- 2	4- 20- 56	2	PWR001	4- 20- 27	4- 19- 27	1	GRAY02
4- 16- 2	4- 17- 56	2	PWR001	4- 17- 27	4- 16- 27	1	GRAY02	4- 19- 2	4- 19- 56	1	PWR001	4- 20- 27	4- 21- 27	1	GRAY02
4- 16- 2	4- 16- 56	1	PWR001	4- 17- 27	4- 18- 27	1	GRAY02	4- 19- 3	4- 19- 7	1	CONN81	4- 20- 28	4- 21- 28	1	NXTCLM
4- 16- 3	4- 16- 7	1	CONN63	4- 17- 28	4- 18- 28	1	NXTCLM	4- 19- 5	4- 19- 6	1	CONN82	4- 20- 28	4- 19- 28	1	NXTCLM
4- 16- 5	4- 16- 6	1	CONN64	4- 17- 28	4- 16- 28	1	NXTCLM	4- 19- 6	4- 19- 5	1	CONN82	4- 20- 29	4- 19- 29	2	GND001
4- 16- 6	4- 16- 5	1	CONN64	4- 17- 29	4- 16- 29	1	GND001	4- 19- 7	4- 19- 3	1	CONN81	4- 20- 29	4- 21- 29	1	GND001
4- 16- 7	4- 16- 3	1	CONN63	4- 17- 29	4- 18- 29	2	GND001	4- 19- 8	1- 18- 21	1	L09C11	4- 20- 40	4- 20- 52	1	CONN89
4- 16- 8	1- 14- 29	1	L07C19	4- 17- 40	4- 17- 52	1	CONN71	4- 19- 9	1- 18- 22	1	L09C12	4- 20- 42	4- 20- 50	1	CONN90
4- 16- 9	1- 14- 30	1	L07C20	4- 17- 42	4- 17- 50	1	CONN72	4- 19- 10	1- 18- 23	1	L09C13	4- 20- 50	4- 20- 42	1	CONN90
4- 16- 10	1- 15- 11	1	L07C21	4- 17- 50	4- 17- 42	1	CONN72	4- 19- 11	1- 18- 24	1	L09C14	4- 20- 52	4- 20- 40	1	CONN89
4- 16- 11	1- 15- 12	1	L07C22	4- 17- 52	4- 17- 40	1	CONN71	4- 19- 12	1- 18- 25	1	L09C15	4- 20- 55	4- 19- 1	2	GND001
4- 16- 12	1- 15- 13	1	L07C23	4- 17- 55	4- 16- 1	2	GND001	4- 19- 13	1- 18- 26	1	L09C16	4- 20- 55	4- 20- 1	1	GND001
4- 16- 13	1- 15- 14	1	L07C24	4- 17- 55	4- 17- 1	1	GND001	4- 19- 14	4- 20- 14	1	TIE003	4- 20- 56	4- 20- 2	1	PWR001
4- 16- 14	4- 17- 14	1	TIE003	4- 17- 56	4- 17- 2	1	PWR001	4- 19- 14	4- 18- 14	1	TIE003	4- 20- 56	4- 19- 2	2	PWR001
4- 16- 14	4- 15- 14	1	TIE003	4- 17- 56	4- 16- 2	2	PWR001	4- 19- 16	4- 4- 40	1	LOAC14	4- 21- 1	4- 22- 55	2	GND001
4- 16- 16	4- 4- 21	1	LOAC11	4- 18- 1	4- 18- 55	1	GND001	4- 19- 26	4- 20- 25	1	GRAY01	4- 21- 1	4- 21- 55	1	GND001
4- 16- 26	4- 17- 26	1	GRAY01	4- 18- 1	4- 19- 55	2	GND001	4- 19- 26	4- 18- 26	1	GRAY01	4- 21- 2	4- 21- 56	1	PWR001
4- 16- 26	4- 15- 26	1	GRAY01	4- 18- 2	4- 19- 56	2	PWR001	4- 19- 27	4- 20- 27	1	GRAY02	4- 21- 2	4- 22- 56	2	PWR001
4- 16- 27	4- 15- 27	1	GRAY02	4- 18- 2	4- 18- 56	1	PWR001	4- 19- 27	4- 18- 27	1	GRAY02	4- 21- 3	4- 21- 7	1	CONN93
4- 16- 27	4- 17- 27	1	GRAY02	4- 18- 3	4- 18- 7	1	CONN75	4- 19- 28	4- 20- 28	1	NXTCLM	4- 21- 5	4- 21- 6	1	CONN94
4- 16- 28	4- 15- 28	1	NXTCLM	4- 18- 5	4- 18- 6	1	CONN76	4- 19- 28	4- 18- 28	1	NXTCLM	4- 21- 6	4- 21- 5	1	CONN94
4- 16- 28	4- 17- 28	1	NXTCLM	4- 18- 6	4- 18- 5	1	CONN76	4- 19- 29	4- 18- 29	1	GND001	4- 21- 7	4- 21- 3	1	CONN93

DVI 000333

TABLE VII (CONTINUED)

REFERENCE ROW-CON-PIN	DESTINATION ROW-CON-PIN	LEVEL	SIGNAL NAME	REFERENCE ROW-CON-PIN	DESTINATION ROW-CON-PIN	LEVEL	SIGNAL NAME
4- 21- 8	1- 20- 29	1	L10C19				
4- 21- 9	1- 20- 30	1	L10C20				
4- 21- 10	1- 21- 11	1	L10C21				
4- 21- 11	1- 21- 12	1	L10C22				
4- 21- 12	1- 21- 13	1	L10C23				
4- 21- 13	1- 21- 14	1	L10C24				
4- 21- 14	4- 22- 14	1	TIE003				
4- 21- 14	4- 20- 14	1	TIE003				
4- 21- 16	4- 4- 12	1	L04C16				
4- 21- 26	4- 20- 26	1	GRAY01				
4- 21- 26	4- 22- 26	1	GRAY01				
4- 21- 27	4- 20- 27	1	GRAY02				
4- 21- 27	4- 22- 27	1	GRAY02				
4- 21- 28	4- 20- 28	1	NETCLM				
4- 21- 28	4- 22- 28	2	NETCLM				
4- 21- 29	4- 22- 29	2	GND001				
4- 21- 29	4- 20- 29	1	GND001				
4- 21- 40	4- 21- 52	1	CONN95				
4- 21- 42	4- 21- 50	1	CONN96				
4- 21- 50	4- 21- 42	1	CONN96				
4- 21- 52	4- 21- 40	1	CONN95				
4- 21- 55	4- 21- 1	1	GND001				
4- 21- 55	4- 20- 1	2	GND001				
4- 21- 56	4- 20- 2	2	PWR001				
4- 21- 56	4- 21- 2	1	PWR001				
4- 22- 1	3- 22- 1	2	GND001				
4- 22- 1	4- 22- 55	1	GND001				
4- 22- 2	4- 22- 56	1	PWR001				
4- 22- 2	3- 22- 56	2	PWR001				
4- 22- 3	4- 22- 7	1	CONN99				
4- 22- 5	4- 22- 6	1	CON100				
4- 22- 6	4- 22- 5	1	CON100				
4- 22- 7	4- 22- 3	1	CONN99				
4- 22- 14	4- 21- 14	1	TIE003				
4- 22- 26	4- 21- 26	1	GRAY01				
4- 22- 27	4- 21- 27	1	GRAY02				
4- 22- 28	4- 21- 28	2	NETCLM				
4- 22- 29	4- 21- 29	2	GND001				
4- 22- 40	4- 22- 52	1	CON101				
4- 22- 42	4- 22- 50	1	CON102				
4- 22- 50	4- 22- 42	1	CON102				
4- 22- 52	4- 22- 40	1	CON101				
4- 22- 55	4- 21- 1	2	GND001				
4- 22- 55	4- 22- 1	1	GND001				
4- 22- 56	4- 22- 2	1	PWR001				
4- 22- 56	4- 21- 2	2	PWR001				

DVI 000334

TABLE VII (CONTINUED)

A P P E N D I X   I

DISPLAY ASSEMBLY
LAYOUTS

DVI 000335

RIBBON CABLE CONNECTION INSTRUCTIONS

There are twenty ribbon sockets, from the liquid crystal display, that connect to the top row of back plane connectors. The back plane connectors are labeled #1 thru #21 right to left. Back plane connector #1 does not have a ribbon socket connector. Each of the ribbon sockets connects to pins #33 thru #56 on each of the twenty back plane connectors. The bottom row of pins on the ribbon sockets have no connections.

The opposite ends of the ribbon sockets connect to the twenty connectors on the liquid crystal display that are labeled.

DVI 000336

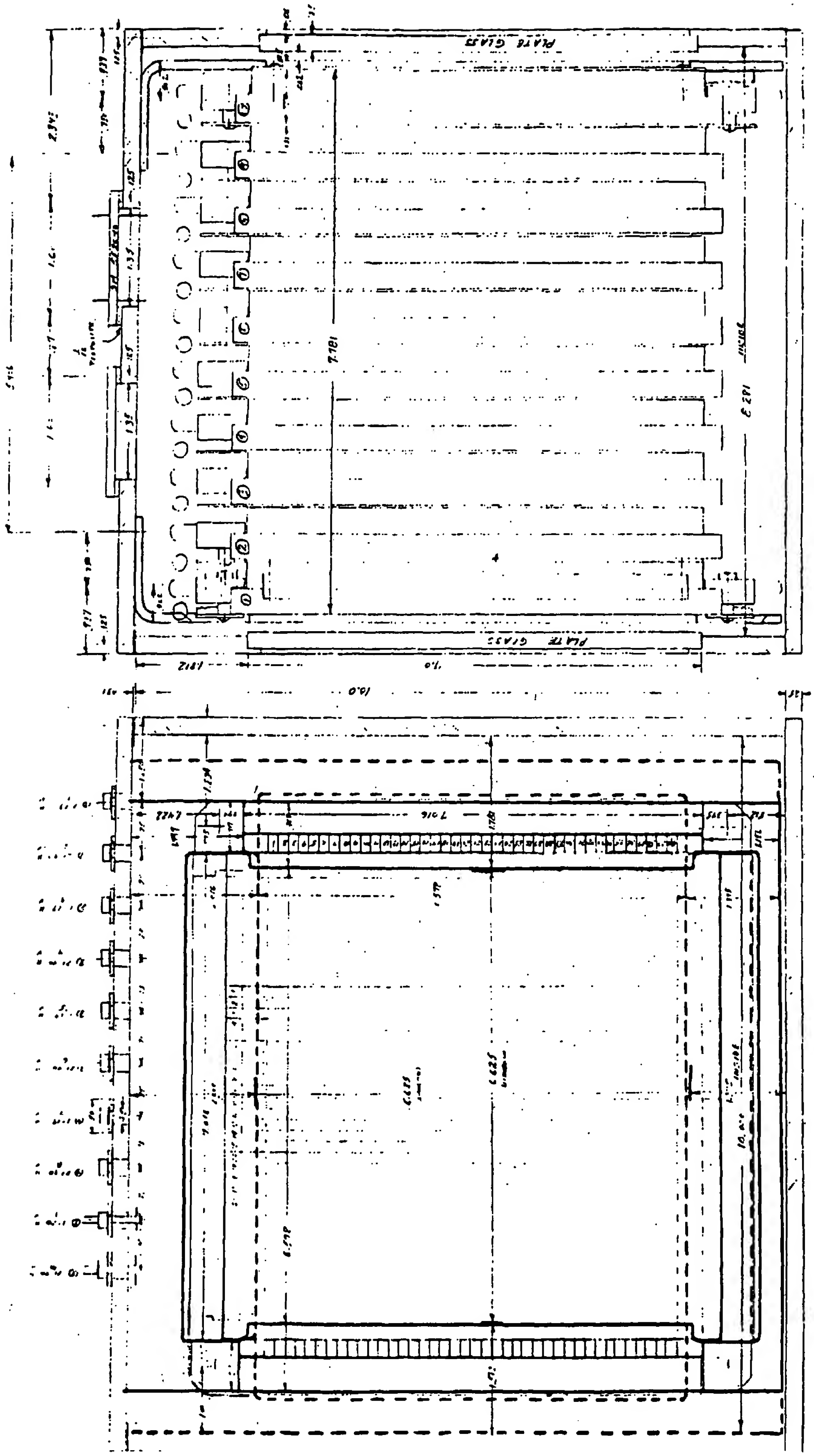

Figure 39 Display Assembly Layout

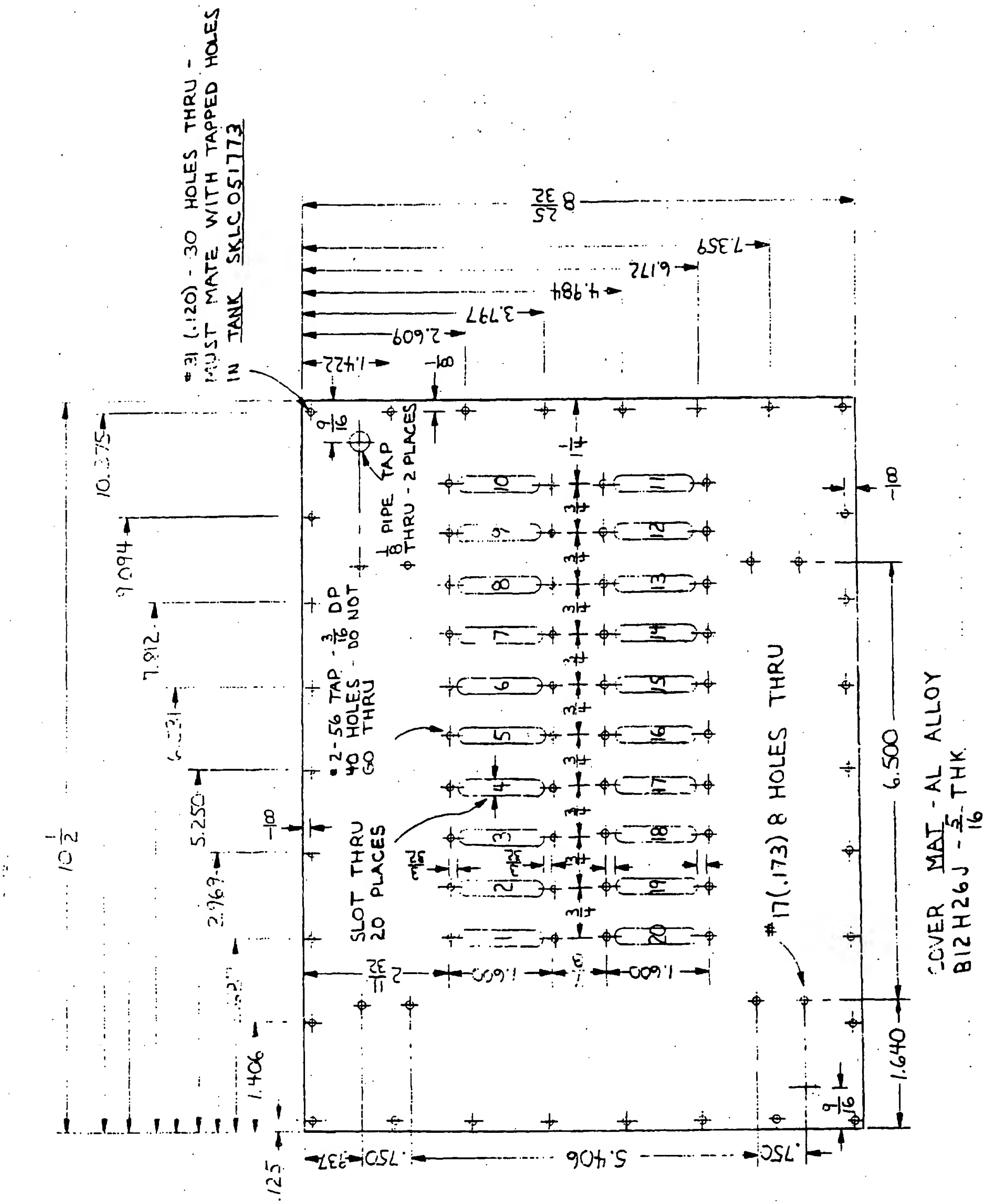

Figure 40 Display Assembly Connector Placement

DVI 000338

FOOTNOTES

1. C. R. Stein, R. A. Kashnow, A Two-Frequency Coincidence Addressing Scheme for Nematic-Liquid-Crystal Displays, Applied Physics Letters, Vol. 19, NO. 9, 1971 Nov 1.

2. C. R. Stein, A Remote Access Data Entry Terminal with Liquid Crystal Display, presented to SID, 1973 May.

3. G. W. Gray, "Molecular Structure and the Properties of Liquid Crystals," New York, Academic Press (1962).

4. J. L. Fergason, Appl. Optics 7, 1733 (1968).

5. J. Adams, W. Haas, J. Wysocki, Mol. Cryst. Liq. Cryst. 8, 9 (1969).

6. E. Sackmann, S. Meiboom, and L. C. Snyder, J. Am. Chem. Soc. 89, 5981 (1967).

7. J. J. Wysocki, J. Adams, and W. Haas, Phys. Rev. Lett. 20, 1024 (1968).

8. G. H. Heilmeier and J. Goldmacher, Proc. IEEE 57, 34 (1969).

9. P. E. Cladis and M. Kleman, Mol. Cryst. Liq. Cryst. 16, 1 (1972).

10. R. B. Meyer, Appl. Phys. Lett. 14, 281 (1968).

11. P. G. de Gennes, Sol. State Comm. 6, 163 (1968).

12. R. B. Meyer, Appl. Phys. Lett. 14, 208 (1969).

13. F. J. Kahn, Phys. Rev. Lett. 24, 209 (1970).

14. T. Nakagiri, Phys. Lett. 36A, 427 (1971).

15. R. B. Meyer, Thesis, Harvard Univ., 1969, unpublished.

16. J. J. Wysocki, J. Adams, and D. J. Olechna, "Liquid Crystals and Ordered Fluids," ed. J. F. Johnson and R. S. Porter, (Plenum Press, Inc., New York, 1970), p. 419.

17. J. J. Wysocki, Mol. Cryst. Liq. Cryst. 14, 71 (1971).

18. T. Ohtsuka and M. Tsukamoto, Japanese J. Appl. Phys. 12, 22 (1973).

19. R. A. Kashnow and H. S. Cole, Mol Cryst. Liq. Cryst. to be published.

20. Y. Bouligand, J. de Phys. 33, 525 (1972).

21. The total decay time scales with pitch as discussed by E. Jakeman and E. P. Raynes, Phys. Lett. 39A, 69 (1972), but we believe the short times they report (of order 60μs) characterize only the initial change in the light transmission, rather than the entire relaxation process.

22. W. H. deJeu and C. J. Gerritsma, J. Chem. Phys. 56, 4752 (1972).

23. U. S. Pat. 3, 499, 702.

24. M. Schadt and W. Helfrich, Appl. Phys. Lett. 18, 127 (1971).

DVI 000340

U.S. DEPARTMENT OF COMMERCE
Technology Administration
National Technical Information Service
Springfield, VA 22161 (703) 605-6000